THE ASTROPHYSICAL JOURNAL SUPPLEMENT SERIES, 129:159–227, 2000 July

INTERSTELLAR HYDROXYL MASERS IN THE GALAXY. I. THE VLA SURVEY

A. L. ARGON,[1] M. J. REID,[1,2] AND KARL M. MENTEN[2]

Received 1999 October 25; accepted 2000 February 15

ABSTRACT

Interstellar OH masers are bright signposts for recently formed massive stars, and the maser emission can be used to study the kinematic and physical conditions of dense molecular material surrounding these stars. We present interferometric maps of 91 interstellar OH maser sources in one or both of the ground-state, main-line, $^2\Pi_{3/2}\,J = 3/2$ OH transitions near 18 cm wavelength. The maps comprising this large, uniformly processed, survey have a spectral resolution of 0.14 km s^{-1} and an angular resolution of $\approx 1\farcs5$. We measured the absolute positions of the masers to an accuracy of $\approx 0\farcs3$ in the E-W direction and $\approx 0\farcs5$ in the N-S direction, except for those sources with declinations below about $-30°$, and *relative* positions of isolated OH maser spots within each source and OH transition to an accuracy of $\approx$ $0\farcs01$. This survey forms a nearly complete sample of interstellar OH masers that are stronger than 1 Jy in both right- and left-circular polarization in at least one of the ground-state OH transitions.

Subject headings: H II regions — ISM: clouds — masers — radio lines: ISM

1. INTRODUCTION

Regions of massive star formation often contain interstellar hydroxyl (OH) masers. When mapped with radio interferometers the maser emission is often found to arise from the molecular envelope surrounding an ultracompact H II (UCH II) region. Thus, OH masers are signposts for newly formed O- and early B-type stars that are still deeply embedded in their dense placental material. Typically, OH emission from a single UCH II region appears to arise from many bright "spots," which are spread over an area of sky with a characteristic size of 10^3–10^4 AU. At a representative distance of ~ 3 kpc, this corresponds to a few arcseconds. After correcting for the Zeeman splitting, induced by the magnetic field in the maser region (e.g., 3 km s^{-1} at 1665 MHz for a typical magnetic field of 5 mG), the maser emission usually covers a radial velocity range of several km s^{-1}, centered near the LSR velocity of the region in question.

To date about 300 interstellar OH masers have been found and a sizeable number have been mapped with Very Long Baseline Interferometric (VLBI) arrays or with connected element interferometers. VLBI observations generally achieve an angular resolution of $\lesssim 0\farcs01$ at 18 cm, the wavelength of the ground-state OH transitions. High-resolution VLBI maps of one or more of the four 18 cm hyperfine transitions have been published for a small number of sources including W3 OH (Reid et al. 1980; Masheder et al. 1994), W75 N (Haschick et al. 1981), W49 N (Kent & Mutel 1982), G351.78−0.54 (Fix et al. 1982), W51 M (Benson, Mutel, & Gaume 1984), NGC 6334 F (Zheng 1989), and G45.07+0.13 (Zheng 1997). While connected element interferometers, such as the Very Large Array (VLA) and the Multi-Element Radio Linked Interferometer Network (MERLIN), generally have insufficient resolution to resolve individual maser spots, they can be used to determine the relative positions of the centroids of spots accurately enough to study their distribution (e.g., Norris, Booth, & Diamond 1982a; Norris et al. 1982b; Baart & Cohen 1985; Baart et al. 1986; Gaume & Mutel 1987; Forster & Caswell 1999). The relative positions of maser spots for about a hundred sources have been measured with these interferometers. A large-scale survey has been carried out by Caswell (1998) using the Australian Telescope Compact Array (ATCA), which gives the absolute positions of over 200 southern sky OH masers to an accuracy of $\approx 1''$, but little relative positional information.

In order to better study the properties of interstellar OH masers, we conducted extensive observations with the VLA in its most extended A configuration. We mapped 91 sources in one or both of the ground-state, main-line, $^2\Pi_{3/2}\,J = 3/2$ OH transitions. All maps were sensitive to both right- and left-circular polarization (RCP and LCP, respectively). This survey represents the vast majority of interstellar OH masers that are visible from the latitude of the VLA and that are stronger than 1 Jy in both RCP and LCP. Our interferometric survey has better spectral and angular resolution than any previous survey of this magnitude.

Since our data comprise a nearly complete, flux-density limited, sample of interstellar OH masers, observed with the same instrument and analyzed in a consistent manner, further analysis should allow statistically meaningful estimates of many characteristics of interstellar OH masers, such as their luminosity function and line width versus intensity relation. In addition, the identification of Zeeman pairs within individual sources allows one to estimate the full magnitude and line-of-sight direction of the magnetic field in the dense gas near newly formed stars. Such studies using this large database will be published later. In this paper we document our observations and present interferometric spectra and maps of all sources observed.

2. SAMPLE SELECTION

Our sample of interstellar OH masers was chosen in the following manner. First, we compiled a list of all sources showing maser emission in OH and/or water vapor (H_2O) above a declination of $-45°$ that are listed in the catalog of Braz & Epchtein (1983). We then added all known interstellar H_2O maser sources from the Cesaroni et al. (1988) catalog of sources north of $-30°$ declination that are not in the Braz & Epchtein catalog. Finally, we observed all of

[1] Harvard-Smithsonian Center for Astrophysics, 60 Garden Street, Cambridge, MA 02138; aargon@cfa.harvard.edu, mreid@cfa.harvard.edu.

[2] Max-Planck-Institut für Radioastronomie, Auf dem Hügel 69, Bonn, D-53121 Germany; kmenten@mpifr-bonn.mpg.de.

these 396 candidate sources with the NRAO 43 m telescope in Green Bank, WV, between 1992 February 1 and 3. The main-line $F = 1$–1 and $F = 2$–2 hyperfine transitions at 1665.4018 and 1667.3590 MHz were observed in both RCP and LCP. Observations in each transition and polarization covered a total bandwidth of 156 kHz, centered on the expected LSR velocity of the source. The observing band was sampled with 256 spectral channels, and, after discarding a total of 38 spectral channels from the band edges, we obtained spectra covering a velocity range of 24 km s^{-1} with a velocity resolution of 0.11 km s^{-1}.

After integrating for 45 s, we achieved a typical minimum noise of about 0.2 K antenna temperature, T_A, corresponding to a single polarization flux density (i.e., multiplying T_A by $k/A_{\rm eff}$, where k is Boltzmann's constant and $A_{\rm eff}$ is the effective collecting area of the antenna) of about 0.3 Jy. For some regions in the plane of the Milky Way, strong emission from H II regions increased the total system temperature by a factor of up to about 3 from the nominal value of $\approx$25 K. Thus, our 3 σ, single-channel, detection limit ranged from about 0.9 to 2.7 Jy. Fortunately, the higher noise levels were almost always associated with prominent H II regions (e.g., Sgr B2, W49, and W51) where the strongest masers are usually found. Also, since interstellar OH masers have typical line widths of about 0.4 km s^{-1}, and often many spots blend together to further increase the frequency extent of the maser emission, we could almost always detect sources as weak as 1 Jy.

We used our Green Bank 43 m telescope survey to provide a large sample of interstellar OH masers whose declinations were above $-45°$ and peak flux densities were stronger than 1 Jy in *both* circular polarizations in at least one OH main-line transition. This criterion was motivated by our desire to seek Zeeman pairs for magnetic field measurement. We note that the selection criteria were used to determine "pointing positions" for the VLA. In some cases more than one source was found within a search region of 17′ centered on the pointing position and contained within the $\approx$30′ FWHM primary beam of a single VLA antenna at this wavelength. An example of this is the source pair G28.199−0.048 and G28.147−0.005. The first source was the one we intended to observe and satisfies the selection criteria. The second source was a "bonus" and does not meet the criterion that it is stronger than 1 Jy in *both* circular polarizations. In addition, the outer Galaxy ($90° < \ell < 270°$) is less populated with strong interstellar OH masers than the inner Galaxy. This resulted in some extra observing time for outer Galaxy sources, and we chose to include five sources whose flux density fell slightly below the 1 Jy selection criteria: G97.527+3.184, G126.715−0.822, G133.715+1.215, G173.481+2.445, and G188.946+0.886. Finally, observing time permitted the inclusion of one extra source, G337.707−0.051, which is below our Green Bank survey declination $-45°$. In total, we mapped 91 sources with the VLA in the 1665 and 1667 MHz lines. (The 1612 and 1720 satellite lines are usually much weaker than the main lines in interstellar OH masers and were observed only in a few of the strongest sources.)

To obtain a rough idea of the completeness of our sample, we compared our survey to that of Caswell & Haynes (1983a, 1983b, hereafter CH83). The CH83 survey includes 49 OH maser sources between $340° < \ell \leq 3°$ and 55 between $3° < \ell \leq 60°$ in a complete sampling of the Galactic plane in the range of $\pm 0\overset{\circ}{.}3$ of latitude. This totals 104 sources compared to our 70 in the same longitude range. The greater number of sources in the Caswell & Haynes survey can be attributed mostly to their higher sensitivity ($\approx$0.1 Jy noise level). The overlap is not perfect; they are missing 14 of our sources and we are missing 48 of theirs. The sources found in our survey, but missing in the CH83 sample, can be explained by three factors: (1) four sources are outside of their $\pm 0\overset{\circ}{.}3$ of latitude coverage, (2) their 12′ beam blends 8 sources with other sources, and (3) two sources seem to have increased in strength from less than 0.3 Jy to more than 4 Jy in the decade between the surveys. On the other hand, the sources in the CH83 sample that are not found in our survey, can be explained by three factors: (1) four sources appear to be stellar (not interstellar) masers, (2) 26 sources were weaker than 1 Jy in one polarization, and (3) 18 sources had flux densities of typically a few Jy in the early 1980's and weakened sufficiently to fall below our selection criterion.

Since we can account for all of the differences between our survey and the deeper one of Caswell & Haynes, our survey should be essentially complete for the latitude range $|\ell| < 0\overset{\circ}{.}3$. There are perhaps some undiscovered interstellar OH masers at higher Galactic latitudes. However, since interstellar OH masers are usually associated with massive star forming regions only a small number are likely to have been missed. Also there are some sources which are hard to classify. For example, we have not included the Orion KL (IRc2) OH masers in our survey because this source may be an unusual stellar-like OH maser. Overall, the evidence suggests that we are nearly complete (probably above the 80% level) at the epoch of the Green Bank observations.

3. VLA OBSERVATIONS

Observations of the 91 interstellar OH maser sources were conducted in five sessions between 1991 and 1998 (see Table 1) with the National Radio Astronomy Observatory's[3] VLA near Socorro, NM, using all 27 antennas in the A configuration. All sources were observed in spectral-line mode in at least one of the two OH main-line transitions (1665.4018 and 1667.3590 MHz) and a few in one or both of the OH satellite-line transitions (1612.2310 and 1720.5300 MHz) as well. Observations were made using 256 uniformly weighted channels, covering an observing bandwidth of 0.1953 MHz. The channel separation was 0.763 kHz, corresponding to about 0.14 km s^{-1} for the main-line OH transitions. For most sources, we retained only the inner 128 channels, covering 18 km s^{-1}, which included all of the OH maser emission.

Each source was observed simultaneously in RCP and LCP to ensure accurate registration of maps. When more than one transition was observed, they were observed consecutively in time to minimize the differences of the absolute positions owing to the effects of atmospheric and ionospheric fluctuations. In order to maximize observational efficiency, a single calibrator observation at 1665 MHz was used for both main-lines and usually for several sources nearby in angle on the sky. Typical angular differences between maser sources and a calibrator were $\approx$15°. Satellite-line transitions required independent calibrations

[3] The National Radio Astronomy Observatory is operated by Associated Universities, Inc., under cooperative agreement with the National Science Foundation.

TABLE 1

ABSOLUTE POSITION OF MAP CENTERS

Source	Alias	Epoch[a]	α^{b}_{B1950}	δ^{b}_{B1950}	α^{b}_{J2000}	δ^{b}_{J2000}
G0.375+0.041	...	2b	17 43 11.28	−28 34 32.7	17 46 21.40	−28 35 39.3
G0.547−0.852	RCW 142 ...	2c	17 47 03.91	−28 53 41.2	17 50 14.53	−28 54 30.8
G0.658−0.043	Sgr B2S ...	1	17 44 10.65	−28 22 43.3	17 47 20.48	−28 23 45.6
G0.666−0.034	Sgr B2M ...	1	17 44 10.32	−28 22 03.8	17 47 20.13	−28 23 06.1
G0.670−0.058	Sgr B2 ...	1	17 44 15.79	−28 22 35.7	17 47 25.61	−28 23 37.6
G0.672−0.031	Sgr B2N ...	1	17 44 10.23	−28 21 39.2	17 47 20.03	−28 22 41.5
G0.678−0.027	Sgr B2 ...	1	17 44 10.12	−28 21 14.5	17 47 19.90	−28 22 16.8
G2.143+0.010	...	2c	17 47 28.18	−27 04 58.5	17 50 36.10	−27 05 46.5
G5.886−0.393	...	2b	17 57 27.00	−24 03 56.4	18 00 30.63	−24 04 00.9
G6.049−1.447	...	2b	18 01 48.99	−24 26 56.2	18 04 53.15	−24 26 41.5
G9.622+0.195	...	1	18 03 15.90	−20 31 52.1	18 06 14.70	−20 31 31.3
G10.624−0.385	...	1	18 07 30.61	−19 56 29.0	18 10 28.61	−19 55 49.7
G12.210−0.102	...	2b	18 09 43.89	−18 25 06.2	18 12 39.89	−18 24 17.3
G12.216−0.117	...	2b	18 09 48.43	−18 25 13.2	18 12 44.43	−18 24 23.9
G12.680−0.181	W33 B ...	1	18 10 59.24	−18 02 40.8	18 13 54.75	−18 01 46.4
G12.890+0.488	...	2c	18 08 56.57	−17 32 14.6	18 11 51.44	−17 31 29.2
G12.908−0.259	W33 A ...	1	18 11 44.17	−17 52 57.9	18 14 39.47	−17 52 00.2
G17.639+0.155	...	2c	18 19 36.56	−13 31 43.9	18 22 26.34	−13 30 12.1
G20.081−0.135	...	2c	18 25 22.99	−11 30 45.3	18 28 10.28	−11 28 48.4
G28.147−0.005	...	2b	18 40 03.86	−04 18 35.5	18 42 42.57	−04 15 35.5
G28.199−0.048	...	2b	18 40 19.36	−04 16 59.1	18 42 58.04	−04 13 58.0
G30.589−0.044	...	2b	18 44 42.58	−02 09 36.8	18 47 18.81	−02 06 16.9
G30.703−0.069	...	2c	18 45 00.63	−02 04 15.7	18 47 36.76	−02 00 54.5
G31.412+0.307	...	1	18 44 59.05	−01 16 07.2	18 47 34.25	−01 12 46.1
G32.744−0.076	...	2c	18 48 47.80	−00 15 43.7	18 51 21.85	−00 12 06.4
G34.257+0.154	...	1	18 50 46.27	+01 11 12.8	18 53 18.67	+01 14 58.5
G35.024+0.350	...	2c	18 51 29.12	+01 57 30.0	18 54 00.64	+02 01 18.7
G35.197−0.743	...	2b	18 55 41.09	+01 36 28.7	18 58 13.02	+01 40 35.2
G35.200−1.736	...	1	18 59 13.09	+01 09 11.1	19 01 45.54	+01 13 32.6
G35.577−0.029	...	2b	18 53 51.33	+02 16 28.4	18 56 22.50	+02 20 27.1
G40.622−0.137	...	2c	19 03 35.40	+06 41 56.1	19 06 01.61	+06 46 35.8
G43.148+0.015	W49 ...	1	19 07 47.41	+09 00 23.1	19 10 11.04	+09 05 20.2
G43.165−0.028	W49 S ...	1	19 07 58.02	+09 00 04.7	19 10 21.65	+09 05 02.6
G43.167+0.010	W49 N ...	1	19 07 49.56	+09 01 14.9	19 10 13.18	+09 06 12.2
G43.796−0.127	...	2c	19 09 30.93	+09 30 45.6	19 11 54.01	+09 35 50.0
G45.071+0.134	...	1	19 11 00.42	+10 45 43.5	19 13 22.08	+10 50 54.0
G45.122+0.133	...	1	19 11 06.19	+10 48 26.2	19 13 27.81	+10 53 37.0
G45.455+0.060	...	2b	19 11 59.93	+11 04 00.8	19 14 21.26	+11 09 15.4
G45.465+0.047	...	2b	19 12 04.35	+11 04 10.2	19 14 25.68	+11 09 25.1
G45.472+0.134	...	2b	19 11 46.09	+11 07 01.9	19 14 07.36	+11 12 15.6
G49.469−0.370	W51 ...	1	19 21 20.20	+14 24 05.9	19 23 37.87	+14 29 58.9
G49.488−0.387	W51 M/S ...	1,3	19 21 26.31	+14 24 34.6	19 23 43.98	+14 30 27.9
G49.489−0.368	W51 N ...	1	19 21 22.37	+14 25 11.1	19 23 40.03	+14 31 04.2
G49.491−0.376	W51 ...	3	19 21 24.30	+14 25 06.2	19 23 41.96	+14 30 59.4
G69.540−0.976	ON 1 ...	2b	20 08 09.81	+31 22 39.9	20 10 09.05	+31 31 35.2
G70.293+1.601	K3−50 ...	2b	19 59 50.13	+33 24 21.3	20 01 45.73	+33 32 45.3
G70.329+1.590	ON 3 ...	2b	19 59 58.48	+33 25 49.3	20 01 54.07	+33 34 13.9
G75.761+0.340	ON 2 S ...	2c	20 19 48.98	+37 15 51.9	20 21 41.10	+37 25 29.3
G75.782+0.343	ON 2 N ...	2c	20 19 51.86	+37 17 00.5	20 21 43.97	+37 26 38.1
G80.864+0.421	...	1	20 35 04.34	+41 25 54.0	20 36 52.16	+41 36 24.5
G81.721+0.571	W75 S ...	1	20 37 14.05	+42 12 10.5	20 39 00.97	+42 22 48.2
G81.745+0.590	W75 ...	1	20 37 13.51	+42 13 59.4	20 39 00.38	+42 24 37.1
G81.871+0.781	W75 N ...	3	20 36 49.95	+42 26 57.9	20 38 36.39	+42 37 34.3
G97.527+3.184	...	2c	21 30 36.82	+55 40 21.5	21 32 11.28	+55 53 40.1
G109.871+2.114......	Cep A ...	1	22 54 18.93	+61 45 46.4	22 56 17.87	+62 01 48.6
G111.533+0.757......	NGC 7538 ...	1	23 11 36.27	+61 10 28.8	23 13 45.02	+61 26 49.3
G111.543+0.777......	NGC 7538 ...	1	23 11 36.60	+61 11 49.5	23 13 45.34	+61 28 10.1
G126.715−0.822......	...	2a	01 20 16.03	+61 33 10.6	01 23 33.17	+61 48 49.2
G133.715+1.215......	W3 ...	2a	02 21 53.13	+61 52 19.5	02 25 40.59	+62 05 50.5
G133.946+1.064......	W3 OH ...	2a	02 23 16.33	+61 38 57.9	02 27 03.70	+61 52 25.4
G173.481+2.445......	S231 ...	2a	05 35 51.46	+35 44 13.3	05 39 13.06	+35 45 51.4
G188.946+0.886......	S252 ...	1	06 05 53.09	+21 39 01.3	06 08 53.33	+21 38 29.0
G196.454−1.677......	S269 ...	1	06 11 46.90	+13 50 33.9	06 14 37.07	+13 49 36.3
G213.706−12.60......	Mon R2 ...	2a	06 05 21.56	−06 22 27.9	06 07 47.84	−06 22 56.7
G337.707−0.051......	...	1	16 34 48.89	−46 54 30.4	16 38 29.55	−47 00 27.0

TABLE 1—*Continued*

Source	Alias	Epoch[a]	α^{b}_{B1950}	δ^{b}_{B1950}	α^{b}_{J2000}	δ^{b}_{J2000}
G340.785−0.095......	...	2b	16 46 38.22	−44 37 15.4	16 50 14.85	−44 42 23.3
G341.219−0.212......	...	1	16 48 41.64	−44 21 50.6	16 52 17.89	−44 26 50.0
G343.128−0.063......	...	2b	16 54 43.80	−42 47 31.3	16 58 17.16	−42 52 05.4
G344.227−0.568......	...	1	17 00 35.19	−42 14 28.9	17 04 07.81	−42 18 38.4
G344.581−0.022......	...	2c	16 59 26.47	−41 37 37.3	17 02 57.76	−41 41 51.6
G345.003−0.224......	...	3	17 01 40.24	−41 25 01.1	17 05 11.25	−41 29 06.0
G345.011+1.792......	...	1	16 53 19.61	−40 09 44.1	16 56 47.61	−40 14 24.3
G345.488+0.313......	...	2c	17 00 58.58	−40 42 17.6	17 04 28.13	−40 46 25.5
G345.505+0.347......	...	2c	17 00 53.50	−40 40 15.0	17 04 22.98	−40 44 23.3
G345.699−0.090......	...	2b	17 03 20.80	−40 47 00.4	17 06 50.64	−40 50 58.3
G347.628+0.149......	...	1	17 08 24.17	−39 05 51.8	17 11 51.03	−39 09 28.2
G348.549−0.978......	...	3	17 15 53.37	−39 00 46.7	17 19 20.41	−39 03 51.1
G348.698−1.027......	...	3	17 16 32.02	−38 55 11.7	17 19 58.92	−38 58 13.2
G350.011−1.341......	...	2b	17 21 41.10	−38 01 20.6	17 25 06.51	−38 04 00.0
G350.113+0.095......	...	2b	17 16 02.15	−37 07 00.2	17 19 25.69	−37 10 04.0
G351.161+0.697......	NGC 6334 B ...	2c	17 16 35.99	−35 54 50.5	17 19 57.41	−35 57 52.0
G351.232+0.682......	NGC 6334 ...	2c	17 16 51.94	−35 51 51.5	17 20 13.29	−35 54 51.9
G351.416+0.646......	NGC 6334 F ...	2c,3	17 17 32.30	−35 44 04.2	17 20 53.44	−35 47 01.6
G351.582−0.352......	...	2b	17 22 03.45	−36 10 03.9	17 25 25.51	−36 12 41.8
G351.775−0.538......	...	1	17 23 20.55	−36 06 45.2	17 26 42.55	−36 09 17.6
G353.410−0.361......	...	2b	17 27 06.65	−34 39 29.6	17 30 26.23	−34 41 45.8
G355.345+0.146......	...	1	17 30 12.57	−32 45 55.3	17 33 29.07	−32 47 58.1
G358.235+0.116......	...	1	17 37 41.39	−30 21 07.7	17 40 54.16	−30 22 38.1
G359.138+0.032......	...	2b	17 40 13.99	−29 37 57.3	17 43 25.68	−29 39 16.7
G359.436−0.103......	...	1	17 41 29.16	−29 27 01.5	17 44 40.58	−29 28 15.4
G359.969−0.457......	...	2b	17 44 09.15	−29 10 56.2	17 47 20.19	−29 11 58.5

NOTE.—Units of right ascension are hours, minutes, and seconds, and units of declination are degrees, arcminutes, and arcseconds.

[a] Epoch of observation: (1) 1991 August 10−11, (2a) 1992 December 27, (2b) 1993 January 10, (2c) 1993 January 12, and (3) 1998 March 26.

[b] E-W ($\Delta\alpha$ cos δ) position errors are independent of declination and are estimated to be $\approx 0\farcs3$. N-S ($\Delta\delta$) position errors show a strong dependence on source declination, with errors increasing as source declination decreases. For sources with $\delta \lesssim -35°$, declination errors can exceed 1″ and for sources with $\delta \lesssim -40°$, they can be several times higher. See text and Fig. 1 for details.

because of the larger frequency shifts. Most sources were observed with *three* 2 to 4 minute scans, which were as widely spaced in time as possible during the period available between rise and set. Sources with low declinations, which were not above the VLA's 8° elevation limit for a long time, were observed with either two scans (for sources with $-44° < \delta < -38°$) or only one scan ($\delta \leq -44°$).

4. CALIBRATIONS AND IMAGING

Quasi-continuum data obtained by averaging the central 75% of the observing band were used to calibrate the complex instrumental gain of each antenna. All data were analyzed with the NRAO Astronomical Image Processing System (AIPS). We employed the standard method of determining the flux density of the (variable) secondary calibrators based on the primary calibrator, 3C 286, whose flux density was assumed to be 13.6 Jy at 1665 MHz. We then determined complex gains for the secondary calibrator using the task CALIB, interpolated these gains to the observation times of the maser source with the task CLCAL, and applied them to the spectral-line data with the tasks TACOP and SPLIT. Absolute positions for the strongest maser spots ("reference features," see below) were determined from maps made with these data.

For each maser source and transition, we first searched for emission over a large area of sky (1024″ × 1024″) using only data with projected baseline lengths less than 40 kλ, and then imaged identified sites of maser emission at full angular resolution (covering 32″ × 32″) using all the data. Before the final imaging step, we "self-calibrated" the data in order to remove the residual effects of atmospheric and ionospheric phase corruption. This was accomplished by selecting a strong unresolved feature in one of the polarizations for each transition (i.e., a "reference feature"), shifting the phase center to the position of that feature with the task UVFIX, determining residual phases using a point source model with the task ASCAL, and subtracting these residual phases from the data in all channels for *both* polarizations using the task ASCOR. Following this "phase-only" self-calibration procedure, we created a map for each spectral channel with the task MX.

5. OH MASER SPECTRA

We constructed spectra for all sources by plotting for each spectral channel its extreme brightness (as flux density per beam) within a 10″ × 10″ region centered on the centroid of the emission. In three cases (W49, W51, and G9.622+0.195) emission was detected outside of this region, and for these sources we used a 16″ × 16″ region. Our spectra are displayed in the left-hand panels of Figures 2–38. The OH transition is indicated in the upper left-hand corner of the spectra, and the heavy and light lines indicate RCP and LCP emission, respectively. The "noise" in these spectra is quantized and does *not* follow Gaussian random statistics. This occurs as the plotted image extrema are usually close to ± 2.5 times the rms noise level ($\sim$0.05 Jy,

TABLE 2

Beam and Image Specifications

Source	Alias	δ (deg)	OH Maser Maps: Major[a] (arcsec)	Minor[a] (arcsec)	P.A.[a] (deg)	σ[b] (Jy)	8.4 GHz Continuum Maps: Major[a] (arcsec)	Minor[a] (arcsec)	P.A.[a] (deg)	σ[b] (mJy)
G0.375+0.041	…	−28	3.06	1.49	−19.8	0.22	0.63	0.25	−16.2	…
G0.547−0.852	RCW 142	−28	2.99	1.70	−13.4	0.20	0.66	0.24	−21.5	0.14
G0.658−0.043	Sgr B2S	−28	2.64	1.49	11.3	0.09	0.56	0.24	−4.4	2.00
G0.666−0.034	Sgr B2M	−28	2.64	1.49	11.3	0.09	0.56	0.24	−4.4	3.48
G0.670−0.058	Sgr B2	−28	2.64	1.49	11.3	0.09	0.56	0.24	−4.4	…
G0.672−0.031	Sgr B2N	−28	2.64	1.49	11.3	0.09	0.56	0.24	−4.4	…
G0.678−0.027	Sgr B2	−28	2.64	1.49	11.3	0.09	0.56	0.24	−4.4	…
G2.143+0.010	…	−27	2.82	1.75	−13.2	0.04	0.61	0.24	−20.9	0.06
G5.886−0.393	…	−24	2.35	1.73	0.6	0.13	0.55	0.25	−19.0	0.10
G6.049−1.447	…	−24	2.33	1.81	0.8	0.07	0.56	0.25	−19.7	0.08
G9.622+0.195	…	−20	2.59	1.50	−33.1	0.07	0.45	0.24	−7.3	0.15
G10.624−0.385	…	−19	2.32	1.70	24.0	0.06	0.44	0.24	−7.7	1.61
G12.210−0.102	…	−18	2.17	1.73	−14.3	0.12	0.48	0.25	−21.3	0.11
G12.216−0.117	…	−18	2.17	1.73	−14.3	0.12	0.48	0.25	−21.3	0.11
G12.680−0.181	W33 B	−18	2.17	1.62	27.9	0.07	0.43	0.24	−7.9	…
G12.890+0.488	…	−17	2.63	1.52	−33.8	0.04	0.48	0.24	−25.7	…
G12.908−0.259	W33 A	−17	2.57	1.53	38.3	0.06	0.42	0.24	−7.4	0.03
G17.639+0.155	…	−13	2.27	1.52	−22.7	0.03	0.45	0.25	−28.3	…
G20.081−0.135	…	−11	2.22	1.29	14.1	0.12	0.43	0.25	−28.9	1.26
G28.147−0.005	…	−4	1.90	1.54	−41.9	0.03	0.38	0.25	−28.9	…
G28.199−0.048	…	−4	1.90	1.54	−41.9	0.03	0.38	0.25	−28.9	0.24
G30.589−0.044	…	−2	4.01	1.33	−51.6	0.04	0.37	0.25	−29.9	0.05
G30.703−0.069	…	−2	2.57	1.43	−45.8	0.04	0.37	0.24	−33.5	…
G31.412+0.307	…	−1	2.34	1.29	49.4	0.06	0.34	0.25	25.4	0.25
G32.744−0.076	…	−0	2.32	1.46	−46.5	0.03	0.36	0.25	−35.0	0.07
G34.257+0.154	…	1	1.99	1.41	47.3	0.05	0.33	0.25	25.4	2.30
G35.024+0.350	…	1	2.28	1.46	−47.7	0.03	0.36	0.25	−35.9	0.05
G35.197−0.743	…	1	2.30	1.41	−53.3	0.03	0.36	0.25	−33.0	0.07
G35.200−1.736	…	1	2.63	1.72	−57.0	0.06	0.33	0.25	24.0	1.33
G35.577−0.029	…	2	2.25	1.45	−48.1	0.09	0.35	0.25	−32.4	0.11
G40.622−0.137	…	6	2.59	1.36	−49.4	0.06	0.34	0.25	−40.3	0.08
G43.148+0.015	W49	9	2.11	1.67	83.5	0.37	0.30	0.25	26.0	2.72
G43.165−0.028	W49 S	9	2.11	1.67	83.5	0.37	0.30	0.25	26.0	1.71
G43.167+0.010	W49 N	9	2.11	1.67	83.5	0.37	0.30	0.25	26.0	2.03
G43.796−0.127	…	9	2.19	1.41	−52.8	0.03	0.33	0.25	−43.6	0.04
G45.071+0.134	…	10	2.03	1.56	71.8	0.05	0.29	0.25	26.2	1.13
G45.122+0.133	…	10	2.03	1.56	71.8	0.05	0.29	0.25	26.2	1.61
G45.455+0.060	…	11	2.26	1.38	−52.2	0.08	0.33	0.26	−39.5	…
G45.465+0.047	…	11	2.26	1.38	−52.2	0.08	0.33	0.26	−39.5	…
G45.472+0.134	…	11	2.26	1.38	−52.2	0.08	0.33	0.26	−39.5	…
G49.469−0.370	W51	14	2.01	1.48	72.2	0.06	0.28	0.25	25.1	…
G49.488−0.387	W51 M/S	14	2.01	1.48	72.2	0.06	0.28	0.25	25.1	0.63
G49.489−0.368	W51 N	14	2.01	1.48	72.2	0.06	0.28	0.25	25.1	2.05
G49.491−0.376	W51	14	2.01	1.48	72.2	0.06	0.28	0.25	25.1	0.78
G69.540−0.976	ON 1	31	2.39	1.25	−54.9	0.03	0.33	0.26	−81.0	0.19
G70.293+1.601	K3−50	33	2.30	1.26	−54.9	0.03	0.32	0.26	−85.3	1.37
G70.329+1.590	ON 3	33	2.30	1.26	−54.9	0.03	0.32	0.26	−85.3	1.38
G75.761+0.340	ON 2 S	37	1.72	1.30	−53.6	0.03	0.35	0.25	−84.2	…
G75.782+0.343	ON 2 N	37	1.72	1.30	−53.6	0.03	0.35	0.25	−84.2	0.15
G80.864+0.421	…	41	1.60	1.28	88.2	0.05	0.27	0.25	−56.6	0.05
G81.721+0.571	W75 S	42	1.79	1.29	−69.5	0.05	0.27	0.25	−56.0	0.08
G81.745+0.590	W75	42	1.79	1.29	−69.5	0.05	0.27	0.25	−56.0	…
G81.871+0.781	W75 N	42	1.79	1.29	−69.5	0.05	0.27	0.25	−56.0	0.04
G97.527+3.184	…	55	2.63	1.25	−43.9	0.03	0.42	0.24	−84.8	0.05
G109.871+2.114	Cep A	61	1.98	1.17	−33.3	0.05	0.29	0.24	2.1	0.11
G111.533+0.757	NGC 7538	61	1.81	1.21	−29.3	0.04	0.29	0.24	6.8	…
G111.543+0.777	NGC 7538	61	1.81	1.21	−29.3	0.04	0.29	0.24	6.8	0.26
G126.715−0.822	…	61	1.82	1.30	−79.9	0.10	0.34	0.25	−61.2	0.08
G133.715+1.215	W3	61	1.63	1.29	−60.4	0.13	0.31	0.24	−39.8	0.22
G133.946+1.064	W3 OH	61	1.66	1.29	−62.6	0.30	0.31	0.24	−39.7	0.19
G173.481+2.445	S231	35	1.33	1.26	−5.4	0.06	0.26	0.25	−10.5	…
G188.946+0.886	S252	21	2.17	1.36	−63.6	0.04	0.50	0.26	−62.8	…
G196.454−1.677	S269	13	2.74	1.37	−58.1	0.05	0.58	0.26	−58.7	…

TABLE 2—*Continued*

			OH Maser Maps				8.4 GHz Continuum Maps			
Source	Alias	δ (deg)	Major[a] (arcsec)	Minor[a] (arcsec)	P.A.[a] (deg)	σ[b] (Jy)	Major[a] (arcsec)	Minor[a] (arcsec)	P.A.[a] (deg)	σ[b] (mJy)
G213.706−12.60......	Mon R2 ...	−6	1.76	1.27	−2.9	0.03	0.35	0.25	0.5	...
G337.707−0.051......	...	−46	8.24	1.19	0.3	0.07	1.67	0.24	3.8	0.31
G340.785−0.095......	...	−44	5.99	1.27	−4.6	0.16	1.42	0.25	−9.0	0.09
G341.219−0.212......	...	−44	5.67	1.24	4.7	0.06	1.30	0.24	1.7	...
G343.128−0.063......	...	−42	5.44	1.31	−2.2	0.04	1.23	0.25	−10.1	0.10
G344.227−0.568......	...	−42	4.81	1.27	−4.9	0.06	1.10	0.24	−0.1	...
G344.581−0.022......	...	−41	5.38	1.26	−9.0	0.04	1.21	0.25	−14.3	0.08
G345.003−0.224......	...	−41	5.32	1.22	−8.3	0.06	1.01	0.23	−4.8	0.16
G345.011+1.792......	...	−40	4.47	1.31	0.6	0.06	0.95	0.24	2.4	0.37
G345.488+0.313......	...	−40	4.91	1.27	−6.8	0.04	1.13	0.25	−14.1	0.48
G345.505+0.347......	...	−40	4.91	1.27	−6.8	0.04	1.13	0.25	−14.1	...
G345.699−0.090......	...	−40	4.83	1.32	−0.2	0.06	1.08	0.24	−11.4	...
G347.628+0.149......	...	−39	4.25	1.31	−2.0	0.06	0.90	0.24	0.0	0.13
G348.549−0.978......	...	−39	4.63	1.22	−8.6	0.05	0.88	0.23	−7.2	0.11
G348.698−1.027......	...	−39	4.63	1.22	−8.6	0.05	0.88	0.23	−7.2	...
G350.011−1.341......	...	−38	3.64	1.55	6.2	0.04	0.95	0.25	−13.9	...
G350.113+0.095......	...	−37	3.55	1.56	9.9	0.03	0.88	0.25	−12.6	1.02
G351.161+0.697......	NGC 6334 B ...	−35	3.62	1.54	−4.4	0.13	0.86	0.25	−16.1	0.11
G351.232+0.682......	NGC 6334 ...	−35	3.60	1.54	7.1	0.17	0.85	0.25	−15.8	...
G351.416+0.646......	NGC 6334 F ...	−35	3.60	1.54	7.1	0.17	0.85	0.25	−15.8	0.73
G351.582−0.353......	...	−36	3.42	1.59	11.0	0.04	0.85	0.25	−13.4	0.32
G351.775−0.538......	...	−36	3.47	1.45	7.3	0.05	0.77	0.24	−2.5	0.27
G353.410−0.361......	...	−34	3.15	1.73	5.5	0.04	0.77	0.24	−14.2	0.32
G355.345+0.146......	...	−32	3.11	1.49	7.8	0.05	0.66	0.24	−3.0	0.32
G358.235+0.116......	...	−30	2.81	1.48	0.8	0.06	0.60	0.24	−3.9	...
G359.138+0.032......	...	−29	2.81	1.65	9.2	0.06	0.66	0.25	−16.8	...
G359.436−0.103......	...	−29	2.67	1.46	10.2	0.08	0.58	0.24	−4.0	...
G359.969−0.457......	...	−29	2.79	1.65	10.7	0.13	0.64	0.25	−16.7	...

[a] Restoring beam specifications: major axis, minor axis, and position angle. Position angles are measured east of north.
[b] σ is rms noise level in single channel of image.

see Table 2) in individual channel maps. We note that because our sources can be 100% circularly polarized, we divided the maps produced by the task MX by a factor of 2 so that Stokes I is obtained by summing (rather than averaging) the RCP and LCP maps.

6. PARAMETERS OF MASER FEATURES

A two-dimensional Gaussian brightness distribution was fitted to selected peaks in the maps in order to determine flux densities and position offsets relative to the reference feature. The initial selection criteria required that the peak flux density in a channel map be more than 1.3 times the absolute value of the largest negative, roughly corresponding to a 4 σ detection. Channel peaks were then grouped into possible features (2–3 adjacent channels per feature) and carefully inspected. Final selection required that the following criteria be met: (1) The emission had to persist at approximately the same position (within about a synthesized beam) over adjacent channels. (2) The emission was *not* caused by spectral "ringing" from another, much stronger, feature. (3) The emission was *not* caused by spatial sidelobes in the synthesized (dirty) beam from another, much stronger, feature. Such "artifacts" tend to occur at the LSR velocity of extremely strong features when multiple OH regions occur within the primary beam of a single VLA antenna. For example, strong features in Sgr B2, W49, and W51 were found to cause numerous artifacts. (4) Two-channel "features" had to come from an unblended spectral region.

A Gaussian spectral profile was then fitted to the peak flux densities of three adjacent spectral channels to determine the flux density (S), the LSR velocity of the line center ($v_{\rm LSR}$), and the FWHM line width (Δv) of a maser feature. See Tables 3–93 for a complete list of maser features. In some sources, a number of spots were spatially and spectrally blended (e.g., in G0.670−0.058) and the weaker spots could not be fitted reliably by this method. For these cases, position offsets from the reference feature are given as the unweighted average of the three spectral channels.

The formal uncertainty in estimating the position, σ_θ, of a spectrally isolated and spatially unresolved peak in a single channel is given by $\sigma_\theta \approx 0.5\theta_b\,\sigma_S/S$, where θ_b, σ_S, and S are the synthesized beam size, and the rms and peak flux density, respectively (cf. Reid et al. 1988, eq. [1]). Table 2 gives the synthesized FWHM beam size and rms noise levels in maps for all sources. Note that the synthesized beams become very elongated at low declination because of poor projected N-S (u, v)-coverage. Taking typical values for the beam size in the N-S direction and channel noise levels, e.g., 2".5 and 0.05 Jy, respectively, one obtains a formal fitting error of 0".01 for a 6 Jy single channel peak. Averaging the positions of the three channels reduces this error somewhat further. The position error in the E-W direction is usually significantly smaller than in the N-S direction. Thus, typical position accuracies for spatially isolated, three-channel detections are $\approx$0".01. Some features are probably spectrally and spatially blended with undetected, weaker maser emission; for such sources the relative position error could be considerably greater. For the small number of features with detections in only two adjacent channels, we estimated the peak flux density and LSR velocity as that of the strongest channel. No line widths are estimated for two channel features.

7. MAPS

The OH maser features found by spatial and spectral fitting are plotted in the right-hand panels of Figures 2–38, superposed on the 8.4 GHz continuum emission indicated by the contour plots. The 1612, 1665, 1667, and 1720 MHz maser features are represented by "triangles," "stars," "squares," and "circles," respectively. Open symbols refer to RCP features and filled symbols to LCP features. The position of the strongest OH maser feature was taken to be the origin (0,0) of each map. The absolute coordinates for the origin of the maps are given in Table 1 in both B1950 and J2000 coordinates.

Supplementary continuum observations were made for all sources at 8.4 GHz. Most of the 8.4 GHz maps came from a single ≈ 3 minute "snapshot" observation. In a few cases we recalibrated and reimaged archival VLA data in order to obtain better maps as noted in the figure captions. Since radio continuum emission from massive star forming regions often shows complex structure on many angular scales, and these maps were made with minimal (u, v)-coverage, some of the continuum maps are of poor quality. We present these maps only as a rough indication of the environment in which OH maser emission occurs. The 8.4 GHz continuum contours start at 4 times the rms noise level (see Table 2) and increase in steps of powers of 2. The peak 8.4 GHz brightness is given in the figure caption, and the restoring beam is shown in the lower right-hand corner of the maps as a shaded ellipse.

8. POSITIONS

The *absolute* positions came from images made from data calibrated in the standard manner (i.e., not self-calibrated). We compared our source positions to those of Forster & Caswell (1989) and Caswell (1998) in order to estimate uncertainties of the absolute positions. Forster & Caswell observed with the VLA in the A-B hybrid configuration and Caswell with the Australia Telescope Compact Array (ATCA). Figure 1 shows a plot of these differences with "stars" denoting our VLA minus Forster & Caswell's VLA position and "squares" denoting our VLA minus Caswell's ATCA positions. The E-W position differences appear largely independent of source declination, δ, and imply an rms error of $\approx 0\farcs3$ for each measurement, assuming equal uncertainties for positions measured with the different telescopes or configurations. No large differences in measurement accuracy are apparent between the telescopes or epochs.

The N-S position differences, on the other hand, vary significantly with source declination. While N-S position differences appear largely independent of source declination for $\delta > -30°$ (with an implied rms error of $\approx 0\farcs5$ for each measurement, assuming equal uncertainties for the positions measured with different telescopes or configurations), they show a strong dependence on source declination for $\delta \lesssim -30°$, with differences (and errors) rapidly increasing as source declination decreases. This is in part caused by the decrease in the N-S projection of the interferometer spac-

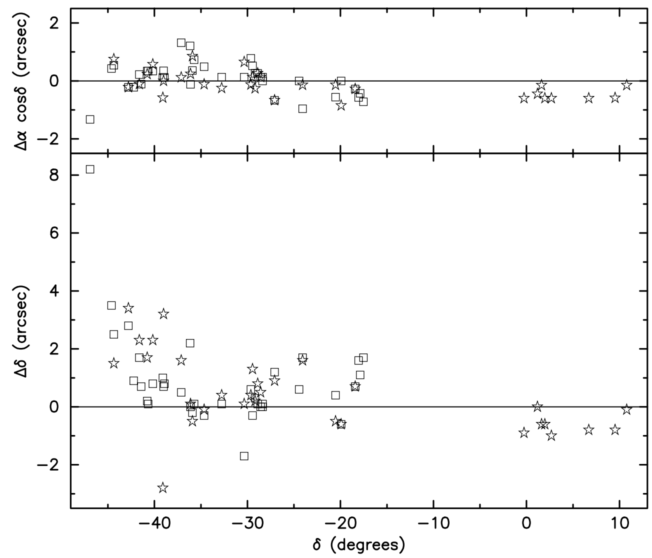

FIG. 1.—Differences in absolute position, R.A. (α) and decl. (δ), plotted as a function of source declination δ. Differences are our estimates minus those of Forster & Caswell (1989), denoted by "stars," or our estimates minus those of Caswell (1998), denoted by "squares." *Upper panel*: The E-W differences ($\Delta\alpha \cos \delta$) show no strong variation with source declination. Assuming equal measurement errors for the different telescopes implies that individual measurements have 1 σ uncertainties of $\approx 0\farcs3$. *Lower panel*: The N-S differences ($\Delta\delta$) grow rapidly with decreasing declination, probably owing to uncompensated ionospheric propagation delays at the VLA.

ings (and a corresponding increase in the synthesized beam) for the VLA when observing low declination sources. We note, however, that more than 80% of the declination differences for the VLA minus ATCA positions are positive, in the sense that the VLA declinations tend to be higher than those obtained with the ATCA. Such a systematic effect cannot be simply a result of the change in the synthesized beam size with declination. More likely it is the result of ionospheric bending, which is not compensated for in the interferometer model used when the raw data are correlated. Thus, for sources with $\delta \lesssim -35°$, our declination position errors can exceed $1''$, and for $\delta \lesssim -40°$ they can be several times greater still. For example, the southern most source in the sample, G337.707$-$0.051, has a declination position error of $8''$ at 1665 MHz and about $4''$ at 1667 MHz, assuming the ATCA position is correct.

The *relative* positions for maser features in any given OH transition and polarization should not be significantly affected by atmospheric or ionospheric propagation effects, since such effects (and other systematic errors) cancel almost completely over the small field of view (e.g., leaving $\approx 10^{-5}$ of the original error for a $2''$ region). However, the cancellation of systematic errors in the relative positions among *different* OH transitions is not so good. As mentioned in § 3, different transitions were observed sequentially, allowing for temporal variations in propagation delays to enter significantly. While it is difficult to quantify this effect, one might expect the relative positions errors among different transitions to be a fraction (perhaps 1/4 to 1/2) of the absolute position error. Empirically, this seems to be the case for the well-studied source G133.946+1.064 (W3 OH), where different transitions appear registered to an accuracy of $\approx 0\farcs1$. Indeed, for most sources, the OH maser features from different ground-state transitions overlap on the sky. In a few cases, however, the features in the two transitions seem to be spatially separated. For example, in G358.235+0.116, G345.505+0.347, G344.581−0.022, and G337.707−0.051 the 1665 and 1667 MHz OH masers clusters are separated by 0.″3, 1″, 3″, and 4″, respectively. These separations are not likely to be real. As for the case of the absolute position errors, the position differences among different OH transitions seem to grow dramatically at very low source declinations.

9. COMMENTS

The entire bandwidth (all 256 channels) was correlated for the sources at three "pointing positions" (the Sgr B2 and W51 sources and G351.775−0.538). Since we made no corrections for bandpass response, the amplitude of the signal (and noise) rolls off toward the edges of the band. Caution should be exercised when assessing maser features in the outer one-eighth of the band in these spectra. This is not a problem for the vast majority of sources, where we only used (and display) the inner 128 spectral channels.

For some sources (e.g., G126.715−0.822 and G348.698−1.027) the spectral "noise" seems to be different for the two polarizations. This may be caused by polarized interference. Also, the "noise level" in the spectra of a few sources seems to be systematically biased above the zero level (e.g., by about 0.3 Jy for G5.886−0.393). These offsets are probably due to the detection of the continuum emission from H II regions at 1.6 GHz.

We thank James Caswell for comments on an earlier version of the text. M. J. R. thanks the Alexander von Humboldt Foundation for a Senior Research Award which funded a long term visit to the Max-Planck-Institut für Radioastronomie where the paper was completed.

TABLE 3

G0.375+0.041

Trans.	S (Jy)	v_{LSR} (km s^{-1})	Δv[a] (km s^{-1})	$\Delta\theta_x$[b] (arcsec)	$\Delta\theta_y$[b] (arcsec)	Trans.	S (Jy)	v_{LSR} (km s^{-1})	Δv[a] (km s^{-1})	$\Delta\theta_x$[b] (arcsec)	$\Delta\theta_y$[b] (arcsec)
1665 R......	1.35	39.43	0.35	−0.167	−0.372	1665 R......	1.40	31.92	0.27	0.200	−0.032
	1.00	37.93	0.29	0.112	−0.151	1665 L......	0.50	39.50	0.96	−0.116	−0.261
	1.11	36.70	0.44	0.232	0.167		0.51	38.77	0.46	0.176	−0.081
	1.38	36.44	0.41	0.295	0.064		0.43	38.12	0.38	0.122	−0.204
	3.38	35.71	0.51	0.020	−0.012		1.05	37.37	0.54	0.047	0.002
	5.88	35.41	0.37	−0.018	−0.008		5.00	35.74	0.43	0.057	−0.173
	1.47	33.00	0.26	0.081	0.027		7.45	33.93	0.33	0.000	0.000
	1.02	32.63	0.23	0.181	−0.136						

[a] Line width (FWHM) determined by fitting a Gaussian profile to the three highest points.
[b] East ($\Delta\theta_x$) and north ($\Delta\theta_y$) offsets from map center.

TABLE 4

G0.547−0.852 (RCW 142)

Trans.	S (Jy)	v_{LSR} (km s^{-1})	Δv (km s^{-1})	$\Delta\theta_x$ (arcsec)	$\Delta\theta_y$ (arcsec)	Trans.	S (Jy)	v_{LSR} (km s^{-1})	Δv (km s^{-1})	$\Delta\theta_x$ (arcsec)	$\Delta\theta_y$ (arcsec)
1665 R......	1.38	19.18	0.34	0.255	−0.212	1665 L......	0.65	8.28	0.59	0.218	−0.129
	1.93	15.08	0.36	−0.040	−0.018	1667 R......	0.22	15.27	0.34	0.395	0.448
	1.03	13.26	0.44	0.116	−0.232		0.40	13.75	0.42	0.014	0.018
	1.01	12.95	0.45	0.097	−0.238		1.26	13.00	0.88	0.001	−0.003
	0.66	12.57	0.36	0.029	−0.344		1.05	11.82	0.49	−0.001	0.030
	0.60	12.19	0.34	0.140	−0.364		0.34	10.91	0.41	0.084	0.375
	0.74	11.39	0.44	0.033	−0.473		0.43	10.14	0.43	0.041	0.238
	0.74	11.00	0.32	0.041	−0.397		0.34	9.03	0.51	0.193	0.495
	0.73	10.76	0.46	0.063	−0.217		0.90	7.60	0.48	0.155	0.421
	0.68	8.85	0.29	0.184	−0.161		3.81	6.33	0.39	0.204	0.521
	0.58	8.10	0.45	0.175	−0.257		0.74	5.09	0.37	0.169	0.532
1665 L......	0.30	19.95	0.38	0.091	−0.387		1.00	4.52	0.34	0.137	0.570
	0.18	19.15	0.71	0.275	−0.217	1667 L......	0.25	17.33	0.31	0.005	0.419
	1.39	17.99	0.27	−0.092	0.058		3.24	13.88	0.37	0.011	−0.010
	0.21	17.14	0.42	0.349	−0.366		5.22	12.90	0.49	0.000	0.000
	1.82	13.53	0.64	0.015	−0.578		0.92	10.55	0.50	0.042	0.142
	3.48	12.98	0.44	0.017	−0.551		0.85	7.46	0.93	0.153	0.474
	0.75	11.88	0.52	0.118	−0.191		0.85	7.23	0.82	0.133	0.518
	0.60	11.18	0.70	0.157	−0.177		2.93	5.88	0.31	0.199	0.552
	0.75	10.40	0.49	0.162	−0.140		0.50	5.34	0.43	0.177	0.510
	0.63	8.63	0.46	0.190	−0.183						

TABLE 5

G0.658−0.043 (Sgr B2S)

Trans.	S (Jy)	v_{LSR} (km s^{-1})	Δv (km s^{-1})	$\Delta\theta_x$ (arcsec)	$\Delta\theta_y$ (arcsec)	Trans.	S (Jy)	v_{LSR} (km s^{-1})	Δv (km s^{-1})	$\Delta\theta_x$ (arcsec)	$\Delta\theta_y$ (arcsec)
1665 R......	0.51	77.17	0.29	0.191	−0.519	1665 L......	17.83	71.94	0.60	−0.441	−0.768
	5.11	76.68	0.41	−0.433	−0.741		12.70	69.71	0.76	−0.413	−0.590
	4.44	76.01	0.41	−0.234	−0.685		184.93	67.83	0.60	0.000	0.000
	7.44	75.60	0.39	0.374	−0.439		51.19	66.51	0.47	−0.129	−0.099
	6.15	74.44	0.39	−0.445	−0.671		0.93	48.85	0.69	−5.690	−1.103
	89.63	73.87	0.45	−0.389	−0.602		2.22	48.41	0.40	−5.747	−1.266
	3.03	73.06	0.34	−0.346	−0.537		0.63	47.78	0.42	−5.691	−1.324
	3.96	72.78	0.39	−0.209	−0.438	1667 R......	1.83	73.85	0.50	−0.269	−0.318
	10.81	72.06	0.47	−0.017	−0.043		0.68	72.96	0.39	−0.248	−0.330
	3.60	71.40	0.39	0.081	−0.248		0.69	72.62	0.40	−0.292	−0.402
	24.64	70.22	0.68	−0.092	−0.087		1.48	72.18	0.31	−0.283	−0.277
	27.77	69.77	0.78	−0.030	−0.022		17.91	69.23	0.56	0.181	0.242
	9.93	68.91	0.37	−0.008	0.013		1.17	67.86	0.65	0.047	0.096
	2.79	68.29	0.57	−0.092	−0.057	1665 L......	0.50	75.94	0.27	0.586	−0.155
	2.78	67.96	0.67	−0.070	−0.054		4.54	70.58	0.31	−0.337	−0.375
	0.82	66.46	0.41	−0.208	−0.044		2.60	70.24	0.61	−0.332	−0.401
	1.34	50.69	0.34	−5.575	−0.943		7.59	69.68	0.31	−0.274	−0.313
	0.73	48.51	0.41	−5.677	−1.172		26.13	69.05	0.46	0.346	0.460
	0.54	48.11	0.34	−5.678	−1.199		14.48	67.97	0.74	0.111	0.187
1665 L......	0.54	76.58	0.36	0.423	−0.465		11.73	67.24	0.40	0.069	0.132
	6.78	75.64	0.31	0.410	−0.440		0.89	47.23	0.35	−5.577	−1.021

TABLE 6

G0.666−0.034 (Sgr B2M)

Trans.	S (Jy)	v_{LSR} (km s^{-1})	Δv (km s^{-1})	$\Delta\theta_x$ (arcsec)	$\Delta\theta_y$ (arcsec)	Trans.	S (Jy)	v_{LSR} (km s^{-1})	Δv (km s^{-1})	$\Delta\theta_x$ (arcsec)	$\Delta\theta_y$ (arcsec)
1665 R......	3.37	72.66	0.24	2.247	−2.149	1665 L......	0.81	49.20	0.45	0.176	1.682
	1.62	65.97	0.53	0.554	−0.041	1667 R......	1.00	61.28	0.48	0.078	0.103
	2.07	64.79	0.43	0.493	−0.036		0.62	59.76	0.51	0.393	0.738
	0.56	64.08	0.52	−0.371	−2.649		0.83	59.06	0.43	0.357	0.938
	0.88	63.60	0.36	−0.433	−2.752		1.95	58.06	0.94	0.295	1.106
	0.42	62.66	0.49	−0.033	0.051		10.34	56.04	0.50	0.657	0.945
	50.17	61.28	0.46	0.000	0.000		2.53	55.06	0.62	0.570	1.020
	24.38	60.18	0.44	0.271	0.358		0.69	53.64	0.50	0.515	1.704
	10.14	59.25	0.88	0.310	0.337		22.75	52.15	0.59	0.399	1.962
	10.35	57.99	0.92	0.079	0.865		2.71	49.88	0.61	0.346	1.488
	11.16	57.59	0.67	0.123	0.885		1.50	49.35	0.98	0.352	1.546
	7.76	55.76	0.56	−2.182	1.293		0.52	47.70	0.34	0.390	1.690
	0.61	54.05	0.39	0.558	1.567		4.01	46.15	0.47	0.409	1.944
	1.11	52.97	0.70	0.674	1.621	1667 L......	0.53	67.31	0.43	0.638	−0.276
	1.01	52.56	1.03	0.344	1.518		0.52	60.17	0.45	0.280	1.099
	1.37	51.95	0.60	0.121	1.389		1.03	59.42	0.54	0.306	1.036
	1.00	51.45	1.02	0.268	1.514		2.13	58.65	0.50	0.378	1.545
	5.63	50.17	0.80	0.352	1.729		1.75	57.80	0.41	0.468	1.123
	5.41	49.25	0.63	0.111	1.262		1.40	57.38	0.89	0.637	0.974
	3.22	48.83	0.83	0.102	1.259		1.02	56.04	0.48	0.585	1.038
	0.44	47.86	0.36	−0.212	1.444		2.01	51.84	0.51	0.351	1.517
	0.62	46.56	0.58	0.160	1.689		0.99	51.29	0.97	0.383	1.540
1665 L......	5.18	68.77	0.33	0.551	0.037		0.55	50.46	0.64	0.378	1.598
	2.40	63.83	0.33	−0.137	0.036	1612 R......	1.02	66.45	0.44	0.406	0.241
	1.10	63.49	0.91	−0.159	−0.011		0.61	60.54	0.37	−0.779	1.572
	29.61	62.27	0.30	0.264	0.492		1.41	59.26	0.54	0.077	1.218
	7.06	61.73	0.36	0.223	0.469		0.42	54.58	0.97	0.726	1.992
	3.13	61.21	0.52	0.014	−1.643	1612 L......	1.20	67.40	0.36	0.414	0.327
	4.82	60.73	0.39	−0.106	−1.692		1.36	66.83	0.33	0.080	0.020
	4.67	60.33	0.56	0.131	0.824		0.50	60.89	0.39	−0.727	1.528
	1.76	59.35	0.82	0.125	0.785		1.35	60.09	0.52	0.071	1.213
	1.05	58.81	0.71	0.150	0.867		0.56	55.93	0.38	0.731	2.012
	1.02	57.59	0.46	0.190	0.943	1720 R......	1.10	63.29	0.38	0.036	−2.395
	8.69	55.74	0.61	−2.108	1.283		14.19	61.26	0.32	−1.222	−6.397
	8.60	55.44	1.47	−2.077	1.294		1.89	60.71	0.46	−1.221	−6.445
	3.18	54.68	0.69	−0.773	1.189	1720 L......	1.65	62.37	0.39	−0.024	−2.423
	1.61	53.68	0.99	−0.045	1.240		6.93	61.09	0.28	−1.217	−6.374
	6.24	52.51	0.44	0.086	1.205		1.61	60.59	0.39	−1.220	−6.417

TABLE 7

G0.670−0.058 (Sgr B2)

Trans.	S (Jy)	v_{LSR} (km s^{-1})	Δv (km s^{-1})	$\Delta\theta_x$ (arcsec)	$\Delta\theta_y$ (arcsec)	Trans.	S (Jy)	v_{LSR} (km s^{-1})	Δv (km s^{-1})	$\Delta\theta_x$ (arcsec)	$\Delta\theta_y$ (arcsec)
1612 R......	4.09	67.22	0.69	0.000	0.000	1612 L......	3.84	67.37	0.85	−0.023	−0.008
	0.44	64.79	0.57	−1.888	0.987		0.56	64.85	0.41	−1.786	0.820

TABLE 8

G0.672−0.031 (Sgr B2N)

Trans.	S (Jy)	v_{LSR} (km s^{-1})	Δv (km s^{-1})	$\Delta\theta_x$ (arcsec)	$\Delta\theta_y$ (arcsec)	Trans.	S (Jy)	v_{LSR} (km s^{-1})	Δv (km s^{-1})	$\Delta\theta_x$ (arcsec)	$\Delta\theta_y$ (arcsec)
1665 R......	3.54	55.62	0.34	0.091	−0.023	1667 R......	0.51	49.89	0.44	0.214	0.136
	1.32	55.06	0.47	0.107	−0.007		0.52	49.64	0.33	0.230	−0.020
	1.01	54.72	0.44	0.079	−0.015		2.52	47.38	0.61	0.160	0.139
	0.63	51.03	0.31	0.038	−0.068		1.82	46.92	0.53	0.162	0.151
	4.28	49.78	0.30	0.000	0.000		1.05	46.52	0.50	0.190	0.195
	3.76	47.34	0.44	−0.028	−0.049		0.77	46.21	0.52	0.160	0.171
	1.02	46.42	0.54	−0.010	−0.031	1667 L......	1.62	48.02	0.42	0.200	0.111
1665 L......	3.88	54.41	0.31	0.061	−0.017		1.00	47.39	0.41	0.152	0.110

TABLE 9

G0.678−0.027 (Sgr B2)

Trans.	S (Jy)	v_{LSR} (km s^{-1})	Δv (km s^{-1})	$\Delta\theta_x$ (arcsec)	$\Delta\theta_y$ (arcsec)	Trans.	S (Jy)	v_{LSR} (km s^{-1})	Δv (km s^{-1})	$\Delta\theta_x$ (arcsec)	$\Delta\theta_y$ (arcsec)
1665 R......	0.61	71.10	0.64	−0.623	3.235		3.18	69.27	0.60	−0.139	0.198
	2.69	62.02	0.33	−0.173	0.323	1612 L......	0.60	64.77	0.44	0.323	0.080
1665 L......	0.66	73.57	0.51	−0.300	−0.396		0.58	64.46	0.41	0.323	0.199
	6.95	70.11	0.48	0.000	0.000						

TABLE 10

G2.143+0.010

Trans.	S (Jy)	v_{LSR} (km s^{-1})	Δv (km s^{-1})	$\Delta\theta_x$ (arcsec)	$\Delta\theta_y$ (arcsec)	Trans.	S (Jy)	v_{LSR} (km s^{-1})	Δv (km s^{-1})	$\Delta\theta_x$ (arcsec)	$\Delta\theta_y$ (arcsec)
1665 R......	0.50	61.19	0.43	−0.210	0.133	1667 R......	1.10	60.14	0.36	−0.034	−0.141
	0.63	60.53	0.55	−0.215	0.183		0.92	59.60	0.69	−0.215	0.235
	3.86	59.71	0.49	−0.295	0.210		0.96	59.26	0.52	−0.224	0.258
	2.87	59.34	0.66	−0.323	0.270		0.46	56.10	0.54	−0.040	−0.007
	1.94	59.01	0.50	−0.360	0.354		8.15	53.69	0.86	0.000	0.000
	0.24	56.96	0.41	−0.217	0.416	1667 L......	0.43	62.27	0.39	0.000	−0.057
1665 L......	3.85	61.82	0.38	−0.038	−0.353		0.36	61.41	0.37	0.103	−0.372
	2.33	60.60	0.31	−0.396	0.455		2.57	59.26	0.35	−0.220	0.288
	4.45	59.76	0.37	−0.394	0.422		0.38	53.71	0.54	−0.027	−0.042
1667 R......	0.25	62.18	0.56	0.037	0.155						

TABLE 11

G5.886−0.393

Trans.	S (Jy)	v_{LSR} (km s^{-1})	Δv (km s^{-1})	$\Delta\theta_x$ (arcsec)	$\Delta\theta_y$ (arcsec)	Trans.	S (Jy)	v_{LSR} (km s^{-1})	Δv (km s^{-1})	$\Delta\theta_x$ (arcsec)	$\Delta\theta_y$ (arcsec)
1665 R......	2.12	14.81	0.38	−4.162	−1.759	1665 L......	1.78	6.85	0.72	−4.088	−1.500
	1.65	14.43	0.72	−4.108	−1.775		1.21	5.77	0.56	−4.016	−1.651
	0.62	13.87	0.59	−4.112	−1.708	1667 R......	3.64	15.16	0.61	−3.998	−2.089
	0.45	13.43	0.38	−4.092	−1.672		4.33	14.66	0.75	−3.964	−2.010
	1.75	12.44	1.09	−3.913	−1.656		4.11	14.39	0.79	−3.967	−2.010
	0.91	11.92	0.62	−3.924	−1.587		1.14	12.63	0.47	−3.877	−1.773
	1.13	11.60	0.44	−3.885	−1.630		0.59	11.91	1.10	−3.919	−1.682
	1.12	10.93	0.22	−1.564	−1.259		0.74	11.45	0.55	−3.975	−1.779
	3.04	10.41	0.31	−0.160	0.185		7.86	10.23	0.28	−0.011	0.005
	0.86	9.72	0.33	−0.212	0.166		0.96	9.44	0.35	−0.096	0.020
	1.06	9.20	1.06	−0.254	0.107		0.83	8.88	0.44	−0.131	−0.100
	0.35	8.45	0.42	−4.263	−1.294		0.50	7.87	0.67	−3.797	−1.980
	0.47	7.59	0.45	−3.359	−1.268		1.48	7.08	0.59	−3.732	−1.951
	1.89	7.21	0.36	−3.054	−1.092		0.54	5.93	0.80	−3.673	−2.053
	0.54	6.42	0.31	−3.467	−1.481		0.74	5.18	0.94	−3.498	−2.080
1665 L......	1.34	17.20	0.51	−4.902	1.959	1667 L......	2.58	15.15	0.69	−3.932	−2.029
	2.92	14.73	0.41	−4.060	−1.765		6.43	14.41	0.58	−3.958	−1.963
	3.26	14.31	0.75	−4.056	−1.756		5.05	13.39	0.51	−3.906	−1.827
	3.43	14.02	0.95	−4.089	−1.725		0.55	12.19	0.51	−3.862	−1.761
	5.61	13.50	0.48	−4.062	−1.626		0.94	11.45	0.36	−3.908	−1.875
	1.15	12.65	0.88	−3.873	−1.631		0.67	11.06	1.51	−2.641	−1.664
	0.73	11.77	0.69	−4.584	0.704		8.99	9.71	0.28	0.000	0.000
	1.59	11.22	0.63	−4.199	−1.378		0.67	8.91	0.38	−1.392	−0.648
	2.89	10.94	0.27	−2.879	−1.299		0.76	8.34	0.34	−0.105	−0.094
	1.04	9.96	0.55	−4.378	−1.250		0.52	7.00	1.03	−3.765	−1.871
	4.30	9.52	0.25	−0.153	0.202		1.04	6.17	1.64	−3.801	−1.907
	0.93	8.55	1.37	−2.983	−0.799		1.47	4.94	0.64	−3.464	−2.053
	1.69	8.16	0.33	−1.577	−0.385						

TABLE 12

G6.049−1.447

Trans.	S (Jy)	v_{LSR} (km s^{-1})	Δv (km s^{-1})	$\Delta\theta_x$ (arcsec)	$\Delta\theta_y$ (arcsec)	Trans.	S (Jy)	v_{LSR} (km s^{-1})	Δv (km s^{-1})	$\Delta\theta_x$ (arcsec)	$\Delta\theta_y$ (arcsec)
1665 R......	6.95	11.13	0.96	0.000	0.000	1665 L......	6.84	11.12	0.60	−0.005	0.001
	5.28	10.65	0.49	−0.021	−0.027						

TABLE 13

G9.622+0.195

Trans.	S (Jy)	v_{LSR} (km s^{-1})	Δv (km s^{-1})	$\Delta\theta_x$ (arcsec)	$\Delta\theta_y$ (arcsec)	Trans.	S (Jy)	v_{LSR} (km s^{-1})	Δv (km s^{-1})	$\Delta\theta_x$ (arcsec)	$\Delta\theta_y$ (arcsec)
1665 R......	4.22	5.81	0.42	3.119	−12.308	1667 R......	0.29	6.02	0.41	1.674	−5.454
	2.39	4.87	0.20	0.492	−2.905		0.85	4.81	0.38	1.809	−5.200
	2.72	3.86	0.39	1.519	−5.561		1.89	4.28	0.43	1.756	−5.342
	0.27	2.86	0.37	1.332	−5.303		0.25	3.06	0.68	1.696	−5.162
	8.62	1.75	0.31	−0.692	−0.361		0.51	2.28	0.25	1.416	−5.101
	7.52	1.25	0.65	−0.685	−0.344		2.08	1.42	0.43	−0.034	0.016
1665 L......	0.88	7.03	0.36	1.574	−5.593		2.12	0.64	0.40	−0.476	−0.169
	1.40	5.49	0.45	1.514	−5.653	1667 L......	4.76	7.13	0.28	1.797	−5.389
	1.41	3.93	0.40	1.556	−5.586		0.77	6.02	...	1.706	−5.359
	8.01	1.78	0.26	−0.131	−1.225		0.69	4.78	...	1.791	−5.334
	2.48	−1.05	0.36	−0.699	−0.353		0.59	3.96	...	1.770	−5.201
	1.66	−3.97	0.33	−0.523	−0.436		0.60	2.31	...	0.172	−0.900
1667 R......	0.89	7.17	0.49	1.791	−5.423		9.72	1.48	0.39	0.000	0.000

TABLE 14

G10.624−0.385

Trans.	S (Jy)	v_{LSR} (km s^{-1})	Δv (km s^{-1})	$\Delta\theta_x$ (arcsec)	$\Delta\theta_y$ (arcsec)	Trans.	S (Jy)	v_{LSR} (km s^{-1})	Δv (km s^{-1})	$\Delta\theta_x$ (arcsec)	$\Delta\theta_y$ (arcsec)
1665 R......	0.45	3.21	0.38	−0.450	0.800	1665 L......	0.58	−1.32	0.31	0.083	0.054
	0.54	0.35	0.36	0.111	0.151		1.44	−1.91	0.39	0.024	0.031
	0.99	−0.48	0.30	0.109	0.082		9.94	−2.26	0.28	0.001	−0.010
	0.69	−1.13	0.36	0.267	0.020	1667 R......	1.25	0.10	0.34	2.015	−0.275
	0.92	−1.31	0.31	0.261	0.063		0.54	−0.54	0.27	0.052	−0.080
	4.46	−1.90	0.40	0.028	0.009		0.70	−0.78	0.28	−0.027	−0.043
	29.90	−2.31	0.33	0.000	0.000		0.63	−1.12	0.46	−0.032	−0.017
	0.76	−2.85	0.21	0.597	−0.274		0.69	−1.32	0.50	−0.027	−0.028
1665 L......	0.52	2.87	0.42	2.014	−0.043		22.37	−1.98	0.24	−0.041	−0.126
	0.44	1.21	0.48	0.255	0.154	1667 L......	0.80	2.08	0.30	1.988	−0.225
	2.88	0.06	0.37	0.042	0.024		22.01	−0.58	0.31	−0.044	−0.127
	6.61	−0.51	0.55	−0.021	0.068		2.08	−1.96	0.24	−0.066	−0.109

TABLE 15

G12.210−0.102

Trans.	S (Jy)	v_{LSR} (km s^{-1})	Δv (km s^{-1})	$\Delta\theta_x$ (arcsec)	$\Delta\theta_y$ (arcsec)	Trans.	S (Jy)	v_{LSR} (km s^{-1})	Δv (km s^{-1})	$\Delta\theta_x$ (arcsec)	$\Delta\theta_y$ (arcsec)
1665 R......	0.93	27.04	0.47	−1.911	−0.223	1665 L......	1.17	21.77	0.27	0.000	0.000

TABLE 16

G12.216−0.117

Trans.	S (Jy)	v_{LSR} (km s^{-1})	Δv (km s^{-1})	$\Delta\theta_x$ (arcsec)	$\Delta\theta_y$ (arcsec)	Trans.	S (Jy)	v_{LSR} (km s^{-1})	Δv (km s^{-1})	$\Delta\theta_x$ (arcsec)	$\Delta\theta_y$ (arcsec)
1665 R......	2.91	29.01	0.49	−0.019	−0.045	1667 R......	4.28	29.06	0.49	0.038	−0.036
	11.94	27.59	0.58	0.027	−0.031		2.98	28.07	0.86	0.107	−0.073
1665 L......	15.26	29.08	0.48	0.000	0.000		3.88	27.71	0.56	0.169	−0.091
	0.96	27.74	0.36	0.019	−0.080	1667 L......	3.78	30.58	0.70	−0.128	−0.274
	0.47	27.18	0.98	0.102	−0.377		11.93	28.82	0.44	0.113	−0.032
1667 R......	2.79	30.69	0.39	−0.131	−0.286		0.39	26.85	0.55	0.147	−0.721
	4.05	30.37	0.36	−0.098	−0.277						

TABLE 17

G12.680−0.181 (W33 B)

Trans.	S (Jy)	v_{LSR} (km s^{-1})	Δv (km s^{-1})	$\Delta\theta_x$ (arcsec)	$\Delta\theta_y$ (arcsec)	Trans.	S (Jy)	v_{LSR} (km s^{-1})	Δv (km s^{-1})	$\Delta\theta_x$ (arcsec)	$\Delta\theta_y$ (arcsec)
1665 R......	0.38	66.08	0.41	0.066	0.143	1665 L......	0.83	59.68	0.39	−0.036	−0.015
	0.57	65.32	0.46	−0.169	0.143		0.67	59.04	0.40	−0.068	−0.001
	1.11	64.42	0.56	−0.085	0.044		0.90	56.89	0.35	−0.168	−0.212
	1.52	64.04	0.45	−0.096	0.070	1667 R......	0.32	66.20	0.60	−0.321	0.028
	4.54	63.34	0.41	0.032	0.010		0.57	65.64	0.52	−0.213	−0.056
	2.59	62.28	0.51	0.022	−0.003		1.52	64.29	0.52	−0.189	−0.133
	2.67	61.73	2.36	0.023	0.010		1.52	63.64	1.10	−0.152	−0.133
	2.61	61.16	0.72	0.039	−0.009		1.84	63.37	0.48	−0.132	−0.150
	10.48	59.74	0.38	−0.061	−0.004		3.88	62.52	0.46	−0.115	−0.158
	7.56	59.11	0.31	−0.067	0.004		3.19	62.14	0.94	−0.122	−0.161
	4.27	58.57	0.38	−0.065	−0.010		0.90	61.09	0.50	−0.188	−0.107
	0.34	54.92	0.73	−0.225	−0.184		1.47	60.01	0.46	−0.187	−0.169
1665 L......	0.73	65.53	0.34	−0.141	0.118		0.66	59.38	0.35	−0.294	−0.174
	1.23	65.24	0.38	−0.101	0.085	1667 L......	0.58	65.66	0.52	−0.178	−0.065
	2.57	64.95	0.37	−0.056	0.050		2.92	64.81	0.69	−0.167	−0.147
	21.27	64.46	0.41	0.000	0.000		5.51	64.50	0.45	−0.147	−0.161
	3.54	63.86	0.41	−0.059	0.034		0.96	63.72	0.65	−0.230	−0.054
	3.38	63.46	0.40	−0.092	0.041		2.29	62.75	0.64	−0.133	−0.156
	3.45	62.93	0.81	−0.095	0.026		2.65	62.56	0.49	−0.103	−0.172
	5.32	62.37	0.48	0.055	−0.031		1.03	61.66	0.58	−0.219	−0.191
	0.63	61.35	0.50	−0.054	0.069		0.29	60.58	0.45	−0.186	0.078
	3.96	60.78	0.51	−0.163	0.189						

TABLE 18

G12.890+0.488

Trans.	S (Jy)	v_{LSR} (km s^{-1})	Δv (km s^{-1})	$\Delta\theta_x$ (arcsec)	$\Delta\theta_y$ (arcsec)	Trans.	S (Jy)	v_{LSR} (km s^{-1})	Δv (km s^{-1})	$\Delta\theta_x$ (arcsec)	$\Delta\theta_y$ (arcsec)
1665 R......	0.89	35.19	0.32	0.010	0.072	1665 L......	3.97	33.37	1.14	0.008	0.030
	0.17	34.14	...	−0.010	0.085		4.16	33.10	0.35	0.000	0.000
	0.64	33.00	0.46	0.015	0.034		2.13	32.81	0.29	0.006	−0.051
	0.70	32.82	0.28	0.099	0.107		0.37	31.59	0.25	2.705	−0.279
	0.29	31.53	...	1.102	0.088						

TABLE 19

G12.908−0.259 (W33 A)

Trans.	S (Jy)	v_{LSR} (km s^{-1})	Δv (km s^{-1})	$\Delta\theta_x$ (arcsec)	$\Delta\theta_y$ (arcsec)	Trans.	S (Jy)	v_{LSR} (km s^{-1})	Δv (km s^{-1})	$\Delta\theta_x$ (arcsec)	$\Delta\theta_y$ (arcsec)
1665 R......	12.61	40.52	0.33	0.427	0.195	1665 L......	16.03	34.47	0.37	0.164	−0.109
	8.36	39.93	0.52	0.103	0.020		5.55	33.59	0.69	0.174	−0.212
	3.54	39.55	0.51	0.274	0.160		4.99	32.37	0.50	0.147	−0.067
	3.49	39.23	0.55	0.350	0.203		1.26	31.17	0.50	0.156	−0.061
	6.01	38.91	0.42	0.345	0.162		0.46	28.44	0.31	0.176	−0.019
	44.98	38.44	0.43	0.458	0.210		0.37	27.73	0.25	0.193	0.064
	38.97	37.92	0.45	0.156	−0.005	1667 R......	5.07	40.45	0.75	0.138	0.145
	30.33	37.45	0.51	0.076	−0.086		6.34	39.76	0.41	0.244	0.164
	41.78	37.15	0.45	0.100	−0.057		9.35	38.96	0.34	0.747	0.500
	2.66	35.74	0.50	0.159	−0.058		5.36	38.28	0.48	0.566	0.301
	2.30	34.72	0.33	0.196	−0.034		4.12	37.70	1.04	0.422	0.187
	1.78	34.26	0.65	0.210	−0.041		8.47	36.49	0.40	0.298	0.120
	4.66	33.60	0.34	0.189	−0.051		0.85	35.14	0.36	0.590	−0.227
	0.92	32.46	0.30	0.190	−0.269		0.56	33.00	0.36	0.719	0.108
	0.89	32.28	0.52	0.182	−0.199	1667 L......	0.63	41.64	0.30	0.310	0.135
	0.65	31.72	0.32	0.209	−0.198		1.52	40.70	0.32	−0.058	0.125
1665 L......	6.16	40.52	0.39	0.490	0.215		67.18	39.95	0.58	0.160	0.136
	87.88	39.84	0.45	0.000	0.000		10.60	38.98	0.42	0.737	0.511
	12.93	38.40	0.33	0.503	0.222		2.28	38.24	0.64	0.375	0.200
	25.52	37.64	0.30	0.129	−0.028		2.33	37.80	0.48	0.365	0.198
	14.90	36.91	0.48	0.158	−0.013		0.90	36.90	0.73	0.402	0.147
	13.77	36.57	0.41	0.186	0.013		1.18	36.54	0.78	0.408	0.176
	7.72	36.04	0.92	0.151	−0.080		0.90	32.76	0.35	1.065	0.201
	32.69	35.46	0.52	0.157	−0.108		1.14	30.84	0.26	0.500	0.319

TABLE 20

G17.639+0.155

Trans.	S (Jy)	v_{LSR} (km s^{-1})	Δv (km s^{-1})	$\Delta\theta_x$ (arcsec)	$\Delta\theta_y$ (arcsec)	Trans.	S (Jy)	v_{LSR} (km s^{-1})	Δv (km s^{-1})	$\Delta\theta_x$ (arcsec)	$\Delta\theta_y$ (arcsec)
1665 R......	0.22	23.31	0.29	1.919	0.658	1665 L......	1.86	20.92	0.31	−0.442	0.239
	2.22	20.42	0.28	−0.384	0.266		3.16	19.95	0.25	0.000	0.000
	2.78	20.01	0.31	−0.210	0.144						

TABLE 21

G20.081−0.135

Trans.	S (Jy)	v_{LSR} (km s^{-1})	Δv (km s^{-1})	$\Delta\theta_x$ (arcsec)	$\Delta\theta_y$ (arcsec)	Trans.	S (Jy)	v_{LSR} (km s^{-1})	Δv (km s^{-1})	$\Delta\theta_x$ (arcsec)	$\Delta\theta_y$ (arcsec)
1665 R......	0.43	50.57	0.32	0.064	0.145	1665 R......	0.71	42.92	0.41	0.131	−0.017
	1.42	49.79	0.42	−0.007	0.020	1665 L......	0.34	47.83	0.34	0.128	−0.299
	1.03	49.16	0.57	0.040	−0.077		11.10	46.60	0.37	0.000	0.000
	2.22	48.64	0.39	0.157	−0.140		4.58	45.47	0.32	0.026	−0.049
	1.25	48.19	0.63	0.189	−0.205		0.23	43.77	0.58	0.266	−0.165
	1.25	45.54	0.24	0.344	0.099		0.64	42.90	0.50	0.216	−0.147

TABLE 22

G28.147 − 0.005

Trans.	S (Jy)	v_{LSR} (km s^{-1})	Δv (km s^{-1})	$\Delta\theta_x$ (arcsec)	$\Delta\theta_y$ (arcsec)	Trans.	S (Jy)	v_{LSR} (km s^{-1})	Δv (km s^{-1})	$\Delta\theta_x$ (arcsec)	$\Delta\theta_y$ (arcsec)
1665 R......	0.35	102.72	0.30	−0.003	−0.106	1665 L......	2.39	102.12	0.25	0.000	0.000
	0.54	100.49	0.24	0.027	0.038						

TABLE 23

G28.199 − 0.048

Trans.	S (Jy)	v_{LSR} (km s^{-1})	Δv (km s^{-1})	$\Delta\theta_x$ (arcsec)	$\Delta\theta_y$ (arcsec)	Trans.	S (Jy)	v_{LSR} (km s^{-1})	Δv (km s^{-1})	$\Delta\theta_x$ (arcsec)	$\Delta\theta_y$ (arcsec)
1665 R......	1.11	99.51	0.39	1.220	−0.485	1665 L......	2.86	93.23	0.31	0.018	−0.023
	1.05	99.05	0.37	1.135	−0.478		0.84	92.73	0.38	0.123	−0.044
	2.39	97.92	0.51	0.860	−0.423	1667 R......	0.40	98.73	0.43	1.251	−0.585
	3.09	97.31	0.58	0.897	−0.444		2.11	97.07	0.51	0.845	−0.481
	11.23	96.71	0.40	0.493	−0.211		0.80	96.12	1.01	0.561	−0.345
	1.60	95.55	0.72	0.512	−0.194		0.85	95.88	0.63	0.497	−0.299
	19.23	94.89	0.27	0.000	0.000		0.69	95.34	0.47	1.275	−0.333
	0.54	93.98	0.27	1.254	−0.258		0.62	94.69	0.62	1.161	−0.287
1665 L......	0.39	100.69	0.65	1.214	−0.494		2.41	94.21	0.23	0.236	−0.133
	4.11	98.38	0.32	1.170	−0.506	1667 L......	1.02	97.16	0.60	1.131	−0.562
	5.76	96.97	0.70	0.972	−0.472		0.57	96.07	0.88	0.873	−0.442
	4.23	96.18	0.65	0.827	−0.370		1.45	95.40	0.31	1.327	−0.328
	11.48	94.92	0.35	−0.016	0.005		0.35	94.08	0.30	0.367	−0.036
	1.22	94.30	0.80	0.180	−0.017		0.38	93.64	0.33	0.559	−0.213
	3.07	93.74	0.80	1.338	−0.277		0.86	92.95	0.39	0.342	−0.083

TABLE 24

G30.589 − 0.044

Trans.	S (Jy)	v_{LSR} (km s^{-1})	Δv (km s^{-1})	$\Delta\theta_x$ (arcsec)	$\Delta\theta_y$ (arcsec)	Trans.	S (Jy)	v_{LSR} (km s^{-1})	Δv (km s^{-1})	$\Delta\theta_x$ (arcsec)	$\Delta\theta_y$ (arcsec)
1665 R......	0.28	41.38	0.26	1.088	−0.356	1665 L......	7.62	37.10	0.75	0.005	−0.025
	1.00	39.71	0.34	0.053	0.238		0.90	36.09	0.31	0.013	0.009
	1.36	38.72	0.38	0.047	−0.044	1667 R......	2.23	38.12	0.29	0.907	−0.416
	7.80	36.96	0.53	0.000	0.000		5.27	37.39	0.42	0.985	−0.387
	7.48	36.09	0.28	−0.015	0.155		4.50	36.94	0.66	0.995	−0.366
1665 L......	2.26	44.20	0.35	−0.061	−0.109		4.86	36.64	0.38	1.046	−0.287
	1.53	41.75	0.29	−0.034	−0.099	1667 L......	0.31	39.15	0.44	1.112	−0.231
	1.33	39.77	0.34	0.066	0.148		0.88	38.22	0.88	0.957	−0.436
	4.30	38.85	0.31	0.106	0.007		6.74	37.50	0.45	0.987	−0.390
	0.64	38.19	0.62	0.007	−0.016		4.32	36.95	1.55	1.005	−0.372

TABLE 25

G30.703 − 0.069

Trans.	S (Jy)	v_{LSR} (km s^{-1})	Δv (km s^{-1})	$\Delta\theta_x$ (arcsec)	$\Delta\theta_y$ (arcsec)	Trans.	S (Jy)	v_{LSR} (km s^{-1})	Δv (km s^{-1})	$\Delta\theta_x$ (arcsec)	$\Delta\theta_y$ (arcsec)
1665 R......	0.74	96.33	0.43	0.257	−0.723	1667 R......	0.87	95.98	0.39	0.371	−0.943
	0.93	95.72	0.46	0.166	−0.735		0.93	95.24	0.32	0.329	−0.759
	0.56	95.14	0.33	0.234	−0.561		11.86	91.18	0.34	0.047	−0.248
	16.93	91.17	0.36	0.000	0.000		2.91	88.22	0.47	0.381	−0.416
	0.24	89.42	0.76	−0.183	0.186		1.13	87.77	0.36	0.078	−0.442
	1.90	88.25	0.35	0.424	−0.129		1.00	86.54	0.25	−0.021	−0.312
	0.31	82.58	0.36	0.408	−0.131		0.55	85.42	0.26	0.072	−0.218
	0.33	82.22	0.43	0.459	−0.145	1667 L......	0.54	95.67	0.51	0.425	−1.004
1665 L......	0.81	95.79	0.42	0.312	−0.757		0.74	95.13	0.52	0.371	−0.730
	0.52	95.15	0.87	0.284	−0.478		0.57	94.09	0.24	0.077	−0.872
	2.18	90.98	0.54	−0.011	0.031		5.30	90.91	0.33	−0.117	−0.026
	2.69	88.25	0.39	0.405	−0.139		3.17	88.26	0.43	0.446	−0.388
	0.57	86.70	0.83	0.334	−0.133		14.90	87.59	0.30	0.001	−0.420
	0.67	86.40	0.61	0.340	−0.160		1.14	86.65	0.20	0.021	−0.337
	0.22	85.61	0.39	0.419	−0.116		2.36	86.28	0.21	0.121	−0.342
1667 R......	1.18	96.42	0.45	0.474	−0.857		0.69	84.72	0.33	0.463	−0.395

TABLE 26

G31.412+0.307

Trans.	S (Jy)	v_{LSR} (km s^{-1})	Δv (km s^{-1})	$\Delta\theta_x$ (arcsec)	$\Delta\theta_y$ (arcsec)	Trans.	S (Jy)	v_{LSR} (km s^{-1})	Δv (km s^{-1})	$\Delta\theta_x$ (arcsec)	$\Delta\theta_y$ (arcsec)
1665 R......	0.81	102.96	0.70	1.184	0.308	1667 R......	2.74	103.48	0.73	1.371	0.414
	0.22	101.35	0.47	1.144	0.085		0.60	101.58	0.41	0.746	0.108
	0.23	100.79	0.62	0.877	−0.008		0.74	100.34	0.50	0.319	−0.092
	0.29	99.69	0.54	1.230	0.839		1.38	99.15	0.43	0.480	0.008
	1.34	98.46	0.33	0.524	−0.069		10.47	97.84	0.46	0.000	0.000
	2.35	97.76	0.40	−0.133	−0.090		3.46	97.03	0.50	0.002	−0.035
	0.82	96.06	0.39	1.005	−0.407		1.22	95.95	0.50	0.174	−0.082
	0.47	95.42	0.43	0.560	−0.154		0.85	95.61	0.92	0.171	−0.161
	1.65	94.87	0.27	1.230	−0.550		0.35	94.76	0.47	−0.069	−0.100
	0.20	93.40	0.50	−0.472	−0.117		0.38	94.20	0.44	−0.215	−0.008
	0.23	92.22	0.44	−0.281	−0.317		1.03	93.38	0.52	−0.280	−0.004
1665 L......	0.80	103.77	0.43	1.264	0.308		1.13	92.20	0.49	−0.232	0.005
	0.77	102.78	0.61	1.151	0.212	1667 L......	0.47	105.39	0.38	1.617	0.419
	1.13	101.83	0.67	1.031	−0.301		0.41	104.92	0.62	1.412	0.502
	4.63	101.43	0.36	1.064	−0.338		3.61	103.87	0.54	1.383	0.410
	2.20	100.56	0.38	1.070	−0.322		0.54	102.68	0.60	1.099	0.300
	0.38	99.15	0.38	0.586	−0.079		0.79	102.17	0.49	0.922	0.077
	2.88	98.46	0.33	0.372	−0.093		0.67	101.62	0.59	0.869	−0.096
	0.80	97.89	0.51	0.306	−0.073		0.81	101.04	0.51	0.456	−0.049
	0.35	97.21	1.09	0.794	−0.008		0.64	100.48	0.71	0.352	−0.047
	0.29	96.83	0.63	0.866	0.025		1.25	99.12	0.45	0.489	−0.004
	0.50	94.87	0.23	1.161	−0.488		4.21	98.07	0.65	0.161	0.007
	0.64	93.64	0.42	1.051	−0.463		2.56	97.05	0.80	0.022	−0.042
	0.36	92.55	0.43	0.377	−0.433		1.17	95.82	0.53	0.015	−0.111
1667 R......	0.54	105.70	0.40	1.592	0.436		0.46	94.67	0.60	−0.104	−0.093
	0.39	105.10	0.50	1.574	0.467		0.77	93.44	0.67	−0.272	−0.035
	0.47	104.53	0.41	1.478	0.456		0.69	92.20	0.46	−0.149	−0.107

TABLE 27

G32.744−0.076

Trans.	S (Jy)	v_{LSR} (km s^{-1})	Δv (km s^{-1})	$\Delta\theta_x$ (arcsec)	$\Delta\theta_y$ (arcsec)	Trans.	S (Jy)	v_{LSR} (km s^{-1})	Δv (km s^{-1})	$\Delta\theta_x$ (arcsec)	$\Delta\theta_y$ (arcsec)
1665 R......	0.96	39.57	0.31	−0.086	0.562	1665 L......	1.13	35.00	0.44	0.040	0.068
	0.40	37.30	0.45	−0.307	0.891		0.84	34.56	0.50	0.041	0.074
	0.45	34.01	0.27	−0.202	0.121		2.17	33.77	0.29	0.000	0.000
	1.68	32.42	0.51	0.026	0.014		1.27	33.38	0.30	−0.111	−0.173
	0.69	31.01	0.52	−0.069	−0.286		0.63	32.83	0.57	0.025	−0.246
	0.56	30.21	0.45	−0.101	−0.250		0.18	31.59	0.41	−0.108	−0.418
	0.19	25.77	0.32	0.089	−0.190		0.37	30.94	0.33	0.050	−0.402
1665 L......	0.28	40.22	0.29	−0.319	0.436		0.45	30.35	0.36	−0.015	−0.444
	0.56	37.11	0.49	−0.235	0.770		0.25	25.82	0.32	−0.008	−0.284
	0.59	36.71	0.38	−0.134	0.576						

TABLE 28

G34.257+0.154

Trans.	S (Jy)	v_{LSR} (km s^{-1})	Δv (km s^{-1})	$\Delta\theta_x$ (arcsec)	$\Delta\theta_y$ (arcsec)	Trans.	S (Jy)	v_{LSR} (km s^{-1})	Δv (km s^{-1})	$\Delta\theta_x$ (arcsec)	$\Delta\theta_y$ (arcsec)
1665 R......	0.73	62.49	...	0.000	1.902	1665 L......	15.90	58.15	0.38	−0.092	−0.087
	6.68	59.56	0.40	0.355	1.808		0.36	57.43	0.38	−0.827	−1.490
	16.36	59.11	0.35	0.396	1.812		24.59	55.89	0.33	0.460	1.779
	80.57	58.24	0.36	−0.075	−0.097		0.55	54.70	0.22	−2.065	−1.694
	0.61	57.33	0.40	−0.634	−1.156		0.50	53.86	0.21	−0.445	1.211
	2.92	56.50	0.24	−0.374	−0.801	1667 R......	66.09	58.49	0.36	−0.001	0.003
	0.43	55.74	0.73	−0.625	−1.160		10.56	57.41	0.27	−0.793	−1.654
	0.36	51.56	0.51	−0.449	1.226	1667 L......	1.27	62.30	0.36	−1.562	2.616
1665 L......	2.24	62.77	0.30	−1.658	2.553		1.35	60.58	0.43	0.012	−0.011
	3.78	61.22	0.41	−0.087	−0.078		111.38	58.64	0.36	0.000	0.000
	1.66	59.88	0.26	0.010	1.879		2.24	57.97	0.27	−0.754	−1.679
	1.50	59.51	0.34	0.026	0.607		7.32	57.49	0.31	−0.798	−1.653
	3.35	58.94	0.35	0.040	1.927						

TABLE 29

G35.024+0.350

Trans.	S (Jy)	v_{LSR} (km s^{-1})	Δv (km s^{-1})	$\Delta\theta_x$ (arcsec)	$\Delta\theta_y$ (arcsec)	Trans.	S (Jy)	v_{LSR} (km s^{-1})	Δv (km s^{-1})	$\Delta\theta_x$ (arcsec)	$\Delta\theta_y$ (arcsec)
1665 R......	0.23	51.37	0.45	−0.167	0.231	1665 L......	1.94	46.71	0.46	−0.008	0.106
	2.08	48.19	0.52	−0.052	−0.081		0.17	45.77	0.45	−0.062	−0.035
	7.89	47.81	0.36	0.009	0.066		2.72	44.62	0.24	−0.028	−0.009
	9.02	47.03	0.32	0.000	0.000		0.54	43.86	0.80	0.023	−0.033
	1.84	44.64	0.25	−0.027	−0.001		2.16	42.84	0.20	0.055	0.092
1665 L......	0.63	51.34	0.26	−0.214	0.392		0.32	40.93	0.38	0.082	0.201
	5.51	47.79	0.35	0.042	0.171		0.47	40.44	0.44	0.036	0.208
	1.86	46.93	0.47	−0.029	0.095						

TABLE 30

G35.197−0.743

Trans.	S (Jy)	v_{LSR} (km s^{-1})	Δv (km s^{-1})	$\Delta\theta_x$ (arcsec)	$\Delta\theta_y$ (arcsec)	Trans.	S (Jy)	v_{LSR} (km s^{-1})	Δv (km s^{-1})	$\Delta\theta_x$ (arcsec)	$\Delta\theta_y$ (arcsec)
1665 R......	0.71	37.47	0.40	−0.914	1.858	1665 L......	2.02	35.79	0.30	−0.422	1.210
	1.63	37.02	0.39	−0.924	1.851		0.67	30.39	0.29	0.388	−0.050
	1.25	36.58	0.67	−0.929	1.838		0.32	30.02	0.54	0.384	−0.069
	2.95	36.01	0.29	−0.935	1.828		0.67	29.14	0.72	−0.058	0.019
	1.35	34.23	0.20	−0.355	1.083		1.80	28.75	0.29	0.330	−0.176
	2.66	30.24	0.20	0.566	0.204		2.01	26.71	0.32	0.015	−0.012
	4.64	29.20	0.39	−0.059	0.045		1.11	26.36	0.29	0.053	−0.012
	5.39	28.81	0.32	0.000	0.000		1.04	25.11	0.34	0.331	−0.006
1665 L......	0.49	36.63	0.28	−0.275	1.003						

TABLE 31

G35.200−1.736

Trans.	S (Jy)	v_{LSR} (km s^{-1})	Δv (km s^{-1})	$\Delta\theta_x$ (arcsec)	$\Delta\theta_y$ (arcsec)	Trans.	S (Jy)	v_{LSR} (km s^{-1})	Δv (km s^{-1})	$\Delta\theta_x$ (arcsec)	$\Delta\theta_y$ (arcsec)
1665 R......	6.03	45.96	0.24	0.075	0.029	1665 R......	0.46	39.02	0.43	0.122	−0.091
	0.62	45.61	0.32	0.016	0.039	1665 L......	1.96	45.98	0.25	0.120	0.013
	2.61	44.48	0.28	0.177	0.179		0.90	45.56	0.55	0.115	0.061
	0.56	43.22	0.39	0.035	−0.047		0.79	44.74	0.43	0.119	0.051
	1.12	42.14	0.41	0.034	−0.004		13.29	42.95	0.33	0.000	0.000
	1.50	41.65	0.35	0.062	−0.049		5.93	41.87	0.34	−0.011	−0.011
	1.63	40.33	0.27	0.054	−0.079		5.61	39.03	0.33	0.062	−0.090

TABLE 32

G35.577−0.029

Trans.	S (Jy)	v_{LSR} (km s^{-1})	Δv (km s^{-1})	$\Delta\theta_x$ (arcsec)	$\Delta\theta_y$ (arcsec)	Trans.	S (Jy)	v_{LSR} (km s^{-1})	Δv (km s^{-1})	$\Delta\theta_x$ (arcsec)	$\Delta\theta_y$ (arcsec)
1665 R......	52.63	49.02	0.28	0.000	0.000	1667 R......	0.29	50.25	0.31	0.180	−0.159
	2.84	48.25	0.39	−0.088	0.148		0.49	49.02	0.37	0.107	−0.092
	0.95	47.64	0.40	−0.096	0.116		0.57	48.25	0.41	0.098	0.030
1665 L......	2.95	51.88	0.22	−0.002	−0.094	1667 L......	11.56	50.27	0.24	0.172	−0.158
	7.20	50.80	0.30	−0.006	−0.115		0.40	48.96	0.41	0.119	−0.054
	2.75	49.90	0.31	−0.035	−0.087		0.50	48.28	0.31	0.024	0.073
	29.45	48.94	0.42	−0.032	0.067						

TABLE 33

G40.622−0.137

Trans.	S (Jy)	v_{LSR} (km s^{-1})	Δv (km s^{-1})	$\Delta\theta_x$ (arcsec)	$\Delta\theta_y$ (arcsec)	Trans.	S (Jy)	v_{LSR} (km s^{-1})	Δv (km s^{-1})	$\Delta\theta_x$ (arcsec)	$\Delta\theta_y$ (arcsec)
1665 R......	2.16	35.74	0.31	−0.674	0.180	1667 R......	0.28	32.59	0.41	0.038	−0.020
	0.56	35.13	0.42	−0.695	0.166		1.02	31.68	0.46	−0.439	0.045
	1.02	34.76	0.30	−0.695	0.196		1.96	30.75	0.31	0.199	0.069
	2.48	34.06	0.30	−0.687	−0.079		1.03	29.79	0.27	0.023	−0.018
	39.62	32.63	0.35	−0.008	0.007		0.38	29.04	1.99	−0.196	0.067
	1.25	31.99	0.28	−0.635	0.069		0.44	27.39	0.41	−0.183	−0.016
	0.93	31.11	0.24	−0.523	0.103		1.08	26.72	0.37	−0.156	0.023
	0.91	30.01	0.21	0.096	0.065		0.40	25.98	0.48	−0.103	0.006
	2.07	29.13	0.20	0.055	−0.074		0.29	25.16	0.53	−0.154	0.024
	1.16	28.73	0.34	−0.037	0.221	1667 L......	0.91	35.55	0.31	−0.547	0.259
	0.76	28.04	0.28	−0.109	0.209		0.31	34.45	0.30	−0.504	0.125
1665 L......	1.31	34.47	0.34	−0.723	0.183		0.79	32.55	0.32	0.035	0.023
	97.49	32.57	0.29	0.000	0.000		18.97	31.97	0.31	0.131	−0.006
	1.29	29.73	0.38	0.136	0.442		2.88	31.53	0.29	0.148	0.090
	1.26	25.76	0.34	−0.338	0.086		1.39	30.84	0.30	0.151	0.065
1667 R......	0.71	36.05	0.36	−0.560	0.259		1.75	29.32	0.18	−0.278	0.164
	0.88	35.50	0.36	−0.534	0.223		1.13	27.08	0.51	−0.140	0.004
	0.23	34.74	0.34	−0.576	0.149		1.63	25.43	0.52	−0.169	0.000

TABLE 34

G43.148+0.015 (W49)

Trans.	S (Jy)	v_{LSR} (km s^{-1})	Δv (km s^{-1})	$\Delta\theta_x$ (arcsec)	$\Delta\theta_y$ (arcsec)	Trans.	S (Jy)	v_{LSR} (km s^{-1})	Δv (km s^{-1})	$\Delta\theta_x$ (arcsec)	$\Delta\theta_y$ (arcsec)
1665 L......	7.05	13.65	0.92	0.000	0.000	1667 L......	1.40	12.72	0.38	0.537	0.277
1667 R......	0.47	14.53	0.38	−1.526	−2.624		0.56	9.78	0.41	−1.537	−2.515
	1.16	12.35	0.39	0.495	0.229		0.66	9.53	0.49	−6.090	−2.944
	0.76	7.89	0.49	−9.606	−2.627		1.35	8.44	0.53	−9.519	−2.495
1667 L......	1.08	13.99	0.90	0.541	0.288	1612 R......	2.43	13.82	0.79	−5.195	0.964
	1.25	13.21	0.34	0.507	0.223	1612 L......	2.30	13.20	0.25	−5.230	0.959

TABLE 35

G43.165−0.028 (W49 S)

Trans.	S (Jy)	v_{LSR} (km s^{-1})	Δv (km s^{-1})	$\Delta\theta_x$ (arcsec)	$\Delta\theta_y$ (arcsec)	Trans.	S (Jy)	v_{LSR} (km s^{-1})	Δv (km s^{-1})	$\Delta\theta_x$ (arcsec)	$\Delta\theta_y$ (arcsec)
1665 R......	2.71	24.05	0.66	0.369	−0.375	1667 R......	1.52	22.58	0.78	0.641	−0.026
	3.80	23.66	0.50	0.359	−0.344		1.63	22.32	0.55	0.575	−0.045
	6.59	22.55	0.51	0.177	−0.367		14.77	21.45	0.35	−0.174	−0.149
	13.48	22.16	0.34	0.172	−0.383		4.93	20.84	0.55	−0.117	−0.143
	2.13	21.42	0.67	−0.405	−0.416		4.79	20.47	0.64	−0.110	−0.144
	13.40	20.95	0.37	−0.520	−0.396		16.36	20.02	0.34	0.613	−0.026
	7.13	19.74	0.33	−0.473	−0.399		1.82	19.03	0.30	0.050	−0.120
	4.03	17.83	0.39	0.951	−1.212		0.50	18.23	0.48	0.290	0.351
	19.16	17.03	0.43	0.057	0.141		2.31	16.90	0.71	0.348	0.403
	230.48	16.23	0.31	0.000	0.000		4.82	16.33	0.63	0.303	0.365
	22.25	15.44	0.69	0.010	−0.032		1.85	15.45	1.45	0.580	−1.055
	16.50	14.52	0.64	0.308	−1.694		0.45	14.35	0.52	0.609	−1.696
	35.31	13.69	0.61	0.337	−1.487		0.35	13.70	1.01	0.682	−1.591
	31.21	13.16	0.69	0.316	−1.464	1667 L......	14.28	19.83	0.47	0.219	−0.090
	7.47	12.20	1.15	0.288	−1.353		28.50	19.25	0.52	0.527	−0.031
	1.23	10.70	1.39	0.056	−1.165		1.22	17.59	0.94	0.001	−0.061
1665 L......	0.80	22.38	0.38	1.032	−1.177		13.94	16.99	0.29	−0.117	−0.121
	45.65	19.11	0.36	0.187	−0.356		3.62	15.79	0.75	0.290	0.425
	42.54	18.73	0.78	0.130	−0.336		0.52	14.08	0.46	0.611	−1.415
	63.44	18.36	0.43	0.017	−0.389	1720 R......	2.56	15.90	0.53	0.363	−0.373
	56.46	17.88	0.48	−0.389	−0.398		1.44	14.95	0.54	0.345	−0.369
	52.88	17.71	0.68	−0.520	−0.399		7.32	12.95	0.69	0.355	−0.367
	38.69	16.41	0.59	−0.398	−0.348		13.34	12.37	0.58	0.333	−0.356
	64.26	15.32	0.42	0.008	−0.005	1720 L......	118.83	15.12	1.34	0.363	−0.357
	15.01	14.47	0.54	0.307	−1.674		143.19	14.67	0.61	0.361	−0.353
	26.65	13.23	0.79	0.324	−1.483		5.93	13.39	0.50	0.363	−0.373
	17.79	12.18	0.47	0.255	−1.532		1.95	11.54	0.89	0.333	−0.352

TABLE 36

G43.167+0.010 (W49 N)

Trans.	S (Jy)	v_{LSR} (km s^{-1})	Δv (km s^{-1})	$\Delta\theta_x$ (arcsec)	$\Delta\theta_y$ (arcsec)	Trans.	S (Jy)	v_{LSR} (km s^{-1})	Δv (km s^{-1})	$\Delta\theta_x$ (arcsec)	$\Delta\theta_y$ (arcsec)
1665 R......	5.13	23.19	0.23	−0.553	0.995	1667 R......	4.56	18.17	0.95	0.512	0.276
	2.70	21.24	0.35	−0.006	0.199		4.74	17.73	1.11	0.519	0.484
	20.39	20.01	0.34	−0.053	0.728		6.57	17.05	0.50	0.780	0.922
	21.09	19.54	0.32	−0.132	0.888		4.24	16.49	0.52	0.740	0.786
	50.34	18.16	0.40	0.152	0.000		6.29	15.46	0.43	0.435	0.326
	108.61	17.03	0.61	0.156	−0.013		3.36	14.29	0.44	−0.831	0.145
	67.14	15.75	0.37	0.147	0.008		1.73	13.68	0.36	1.141	2.157
	21.02	15.17	0.34	−0.728	0.322		1.81	13.11	0.37	1.364	0.699
	2.64	14.07	0.48	−0.389	0.482		2.34	12.36	0.41	0.442	0.582
	4.35	13.30	0.59	−1.180	−0.244		4.14	11.61	0.57	1.397	0.930
	6.53	12.28	0.38	0.914	1.605		2.41	10.35	0.49	1.349	0.838
	6.26	11.95	0.70	0.902	2.265		0.95	9.54	1.14	1.326	0.739
	12.09	10.98	0.49	0.578	0.476		1.29	9.17	0.73	1.364	0.725
	17.03	10.38	0.38	0.789	0.661		0.92	8.74	0.66	1.632	1.916
	3.19	9.33	0.79	0.628	0.467		6.01	7.97	0.31	4.932	3.165
	33.46	7.90	0.37	0.645	0.442	1667 L......	0.54	24.11	0.50	0.412	0.134
1665 L......	1.29	23.14	0.28	−0.507	0.829		17.10	21.38	0.39	0.504	0.205
	0.64	22.51	0.69	−0.294	0.670		7.42	21.00	1.98	0.581	0.259
	1.57	22.15	0.26	−0.145	0.306		47.24	19.09	0.59	0.506	0.275
	169.07	21.04	0.41	0.000	0.000		10.27	18.49	0.74	0.516	0.384
	7.22	20.36	0.74	−0.493	0.206		5.55	17.89	1.19	0.569	0.467
	10.01	19.93	0.61	−0.179	0.077		5.49	16.79	0.52	0.444	0.347
	8.39	19.62	0.62	−0.077	0.495		1.58	16.33	0.39	−0.880	1.855
	58.33	18.29	0.42	0.025	0.483		3.12	15.85	0.27	1.366	2.236
	21.64	17.64	0.35	0.038	0.524		1.51	15.38	0.51	1.417	2.273
	91.73	16.98	0.67	0.160	−0.047		2.46	14.60	0.32	−0.089	0.002
	47.26	15.77	0.44	0.115	0.170		2.18	14.01	0.61	0.003	0.248
	8.47	14.63	0.34	0.549	0.410		1.59	13.46	0.75	−0.662	−0.374
	24.06	13.82	0.43	0.980	2.056		1.03	12.90	0.52	1.275	1.984
	3.31	13.11	0.45	0.185	0.660		0.94	12.30	0.54	1.357	1.011
	81.32	12.18	0.60	0.952	2.167		1.38	11.21	0.42	1.169	0.782
	20.42	11.15	0.51	0.641	0.467		2.21	10.46	0.43	1.384	0.830
	14.05	10.48	0.39	0.758	0.568		0.74	9.49	0.67	3.054	0.989
	8.26	9.97	0.54	0.678	0.441		2.35	8.29	0.51	3.898	1.267
	12.93	9.34	0.49	0.674	0.459	1612 R......	0.69	18.85	0.42	−4.908	2.801
	1.24	8.74	0.39	−4.815	−0.629		2.56	15.66	0.73	−4.295	3.342
	10.01	7.88	0.37	0.659	0.434		24.11	14.76	0.35	−4.289	3.411
1667 R......	0.55	24.53	0.48	0.210	1.337		0.88	14.07	0.56	−4.302	3.299
	2.38	21.88	0.35	0.416	0.335	1612 L......	0.56	20.54	0.36	−4.958	2.794
	0.94	21.37	0.53	0.251	0.327		0.63	16.22	0.44	−4.359	2.836
	3.50	20.89	0.35	0.484	0.291		0.83	15.84	0.44	−4.300	2.864
	1.77	20.03	0.53	0.510	0.326		3.16	15.00	0.49	−4.325	3.391
	2.66	19.58	0.36	0.682	0.409		7.70	14.07	0.42	−4.314	3.408
	3.63	18.92	0.54	0.490	0.309		0.55	13.49	0.43	−4.236	3.327

TABLE 37

G43.796−0.127

Trans.	S (Jy)	v_{LSR} (km s^{-1})	Δv (km s^{-1})	$\Delta\theta_x$ (arcsec)	$\Delta\theta_y$ (arcsec)	Trans.	S (Jy)	v_{LSR} (km s^{-1})	Δv (km s^{-1})	$\Delta\theta_x$ (arcsec)	$\Delta\theta_y$ (arcsec)
1665 R......	0.71	44.74	0.19	−0.427	0.191		0.71	40.04	0.39	0.040	0.015
	28.19	44.14	0.23	0.008	0.153		2.04	39.14	0.36	0.016	0.054
	1.11	43.29	0.48	−0.072	0.160	1667 R......	1.45	43.01	0.48	−0.011	0.060
	1.45	42.93	0.34	0.087	0.241		1.74	42.50	0.48	0.023	0.027
	1.62	42.71	0.32	0.063	0.294		1.39	41.87	0.36	−0.010	0.012
	0.87	42.48	0.42	−0.015	0.300		0.98	41.60	0.80	0.007	0.042
	76.86	41.62	0.56	0.031	−0.003		2.95	40.16	0.28	−0.245	0.213
	1.35	40.16	0.46	−0.361	0.250	1667 L......	0.16	44.22	0.35	−0.229	0.149
1665 L......	0.55	45.38	0.32	−0.334	0.276		1.23	43.44	0.38	−0.587	0.127
	16.35	44.20	0.28	−0.002	0.148		3.82	42.52	0.29	0.020	0.009
	4.43	43.52	0.46	−0.537	−0.025		2.45	41.91	0.40	0.011	0.028
	0.81	42.36	0.40	−0.497	0.051		0.90	41.51	0.66	−0.056	0.079
	94.26	41.52	0.43	0.000	0.000		0.34	40.37	0.25	0.044	0.186

TABLE 38

G45.071+0.134

Trans.	S (Jy)	v_{LSR} (km s^{-1})	Δv (km s^{-1})	$\Delta\theta_x$ (arcsec)	$\Delta\theta_y$ (arcsec)	Trans.	S (Jy)	v_{LSR} (km s^{-1})	Δv (km s^{-1})	$\Delta\theta_x$ (arcsec)	$\Delta\theta_y$ (arcsec)
1665 R......	6.86	62.16	0.46	−0.156	1.346	1665 L......	14.23	53.93	0.66	−0.096	−0.016
	11.04	60.07	0.43	−0.221	−0.134		6.53	53.57	0.33	−0.111	−0.005
	0.83	59.17	0.52	−0.247	−0.169		8.65	52.96	0.27	−0.115	−0.015
	1.28	58.66	0.28	−0.286	−0.174	1667 R......	0.60	62.93	0.33	−0.499	0.081
	65.18	56.51	0.45	0.000	0.000		0.26	59.09	0.36	0.458	0.199
	7.36	55.90	0.28	−0.114	−0.005		0.92	57.18	0.63	0.316	0.219
	9.38	54.20	0.27	−0.096	−0.009		3.81	56.34	0.43	0.316	0.214
1665 L......	1.29	65.84	0.26	−0.274	−0.155		0.74	55.94	1.74	0.298	0.224
	0.46	64.26	0.25	−0.207	1.374		2.17	55.26	0.29	0.229	0.233
	0.61	62.17	0.48	−0.341	0.829		1.19	54.55	0.59	0.205	0.242
	0.88	61.20	0.48	−0.641	−0.231	1667 L......	0.75	61.45	0.43	−0.528	0.077
	0.79	60.96	0.45	−0.209	0.734		3.17	55.80	0.37	0.287	0.174
	1.45	60.53	0.27	−0.784	−0.255		5.95	55.31	0.30	0.308	0.202
	0.60	57.08	0.24	0.644	−0.480		1.01	54.05	0.39	0.208	0.232
	5.14	54.59	0.45	−0.041	−0.051		6.20	53.53	0.27	0.199	0.229

TABLE 39

G45.122+0.133

Trans.	S (Jy)	v_{LSR} (km s^{-1})	Δv (km s^{-1})	$\Delta\theta_x$ (arcsec)	$\Delta\theta_y$ (arcsec)	Trans.	S (Jy)	v_{LSR} (km s^{-1})	Δv (km s^{-1})	$\Delta\theta_x$ (arcsec)	$\Delta\theta_y$ (arcsec)
1665 R......	1.50	55.86	0.44	0.316	−0.462	1665 L......	2.88	54.06	0.27	0.359	−0.449
	2.59	55.30	0.47	0.302	−0.298	1667 R......	1.23	55.31	0.25	0.069	0.012
	2.01	54.49	0.96	0.349	−0.429		0.28	53.76	0.32	0.718	−0.232
	4.66	54.08	0.29	0.361	−0.432		2.04	52.18	0.37	0.225	−0.057
	0.69	52.35	0.33	0.299	−0.498	1667 L......	12.55	56.57	0.26	0.000	0.000
1665 L......	2.93	57.08	0.24	−0.182	−0.061		0.38	54.29	0.31	0.571	−0.179
	4.13	55.78	0.60	0.326	−0.450		1.85	52.98	0.43	0.228	−0.056
	6.49	55.43	0.44	0.391	−0.436						

TABLE 40

G45.455+0.060

Trans.	S (Jy)	v_{LSR} (km s^{-1})	Δv (km s^{-1})	$\Delta\theta_x$ (arcsec)	$\Delta\theta_y$ (arcsec)	Trans.	S (Jy)	v_{LSR} (km s^{-1})	Δv (km s^{-1})	$\Delta\theta_x$ (arcsec)	$\Delta\theta_y$ (arcsec)
1665 R......	0.88	55.09	0.33	0.000	0.000						

TABLE 41

G45.465+0.047

Trans.	S (Jy)	v_{LSR} (km s^{-1})	Δv (km s^{-1})	$\Delta\theta_x$ (arcsec)	$\Delta\theta_y$ (arcsec)	Trans.	S (Jy)	v_{LSR} (km s^{-1})	Δv (km s^{-1})	$\Delta\theta_x$ (arcsec)	$\Delta\theta_y$ (arcsec)
1665 R......	1.40	69.76	0.28	0.067	−0.025	1665 R......	1.13	63.83	0.34	−0.233	0.065
	4.27	68.20	0.56	−0.005	0.012		0.70	63.28	0.28	−0.447	−0.501
	1.13	67.52	0.51	−0.011	0.030		0.41	62.30	0.26	0.081	0.325
	1.97	67.12	0.46	−0.002	0.031	1665 L......	5.25	67.24	0.42	0.007	0.188
	1.47	66.62	0.54	0.011	0.030		18.77	65.98	0.36	0.000	0.000
	3.05	66.04	0.31	0.014	−0.015		15.27	65.32	0.41	0.012	0.005
	1.59	65.76	0.71	−0.008	−0.018		4.59	63.78	0.33	0.053	−0.050
	0.83	64.45	0.33	−0.046	0.288		0.25	62.34	0.26	0.218	0.563
	0.98	64.14	0.61	−0.224	0.144						

TABLE 42

G45.472+0.134

Trans.	S (Jy)	v_{LSR} (km s^{-1})	Δv (km s^{-1})	$\Delta\theta_x$ (arcsec)	$\Delta\theta_y$ (arcsec)	Trans.	S (Jy)	v_{LSR} (km s^{-1})	Δv (km s^{-1})	$\Delta\theta_x$ (arcsec)	$\Delta\theta_y$ (arcsec)
1665 L......	0.57	64.76	0.24	−0.780	−0.471	1665 L......	3.59	58.91	0.32	−0.016	−0.008
	35.42	59.41	0.26	0.000	0.000		4.22	58.59	0.26	0.000	0.013

TABLE 43

G49.469−0.370 (W51)

Trans.	S (Jy)	v_{LSR} (km s^{-1})	Δv (km s^{-1})	$\Delta\theta_x$ (arcsec)	$\Delta\theta_y$ (arcsec)	Trans.	S (Jy)	v_{LSR} (km s^{-1})	Δv (km s^{-1})	$\Delta\theta_x$ (arcsec)	$\Delta\theta_y$ (arcsec)
1665 R......	2.50	73.82	0.29	0.000	0.000	1665 L......	0.64	70.46	0.42	−0.081	0.025

TABLE 44

G49.488−0.387 (W51 M)

Trans.	S (Jy)	v_{LSR} (km s^{-1})	Δv (km s^{-1})	$\Delta\theta_x$ (arcsec)	$\Delta\theta_y$ (arcsec)	Trans.	S (Jy)	v_{LSR} (km s^{-1})	Δv (km s^{-1})	$\Delta\theta_x$ (arcsec)	$\Delta\theta_y$ (arcsec)
1665 R......	0.75	71.67	0.72	−0.436	6.647	1667 R......	0.61	66.11	0.62	−0.309	6.414
	1.77	67.54	0.77	−0.641	6.213		0.73	64.86	0.63	−0.340	6.437
	0.95	65.52	0.35	−0.151	6.537		0.69	63.85	0.58	−0.436	6.096
	2.79	64.47	0.70	−0.130	6.553		7.20	61.94	0.48	0.235	−0.442
	0.52	62.88	0.37	−0.299	−0.910		1.36	61.03	0.66	−0.797	3.302
	1.28	62.12	0.39	−0.163	−0.928		2.44	60.01	0.60	0.065	−0.016
	1.89	61.38	0.76	0.118	−0.317		0.92	58.84	0.65	−0.998	5.634
	3.73	60.59	0.49	0.078	−0.128		1.71	58.28	0.68	−0.330	−0.087
	9.69	59.42	0.93	0.021	0.016		0.34	56.80	0.42	−0.782	0.996
	166.86	58.26	0.54	0.000	0.000		0.49	55.91	0.36	−0.772	5.568
	0.79	56.57	0.51	−0.764	2.512		1.07	48.91	0.68	−0.042	5.640
	1.25	55.93	0.46	−0.558	1.165	1667 L......	0.90	70.18	0.37	−1.072	6.522
	0.84	55.43	0.31	−0.815	5.446		0.92	68.28	0.35	−0.428	6.417
1665 L......	0.63	69.03	0.41	−0.437	6.625		4.50	61.87	0.46	0.134	−0.413
	1.63	67.42	0.29	−0.166	6.524		2.13	61.14	0.52	0.051	−0.224
	1.11	64.50	0.70	−0.044	6.607		2.11	60.26	0.90	0.014	−0.254
	0.85	62.41	0.82	−1.857	0.768		2.53	59.93	0.49	0.073	−0.007
	4.78	61.58	0.45	0.122	0.060		1.29	59.47	0.72	−1.276	5.186
	5.30	60.67	0.49	0.009	−0.084		1.04	59.08	0.61	−1.282	5.218
	68.81	59.26	0.62	0.030	−0.011		4.53	54.16	0.33	−0.939	5.933
	61.71	58.85	0.56	0.028	−0.015		1.72	47.02	0.85	−0.086	5.634
	13.59	57.84	0.45	0.075	0.013	1720 R......	61.37	59.56	0.73	−0.940	6.050
	6.34	57.30	0.44	−0.833	5.571		88.31	58.17	0.46	−0.877	6.091
	0.99	56.61	0.39	−0.329	−1.813		8.24	56.47	0.38	−0.962	5.746
	0.37	55.03	0.37	−0.626	5.854		2.20	55.89	1.74	−0.967	5.916
	0.48	54.35	0.61	−0.754	5.508		5.26	55.11	0.95	−1.117	5.734
	1.10	52.51	0.42	0.063	5.827		2.50	53.45	0.39	−1.921	0.050
	1.30	51.89	0.29	−0.090	5.637	1720 L......	0.41	60.59	0.60	−1.137	5.781
	0.34	51.00	0.33	0.425	7.146		2.22	59.54	0.56	−0.973	6.009
	0.45	49.31	0.59	−0.920	5.729		26.13	58.60	0.47	−0.941	6.049
	0.41	48.18	0.53	−0.966	5.770		38.29	56.98	0.55	−0.878	6.092
	1.66	46.65	0.46	0.131	5.742		5.91	55.77	0.44	−0.950	5.756
1667 R......	0.58	72.45	0.58	−1.036	6.517		1.45	55.04	1.32	−0.956	5.853
	0.26	70.94	0.71	−0.633	6.509		2.13	54.56	0.66	−1.393	3.873
	2.04	69.68	0.32	−0.437	6.393		2.76	54.33	0.47	−1.134	5.765
	1.43	68.74	0.35	−0.402	6.567		1.92	52.64	0.33	−1.920	0.064
	0.85	66.52	0.67	−0.430	6.443						

TABLE 45

G49.489−0.368 (W51 N)

Trans.	S (Jy)	v_{LSR} (km s^{-1})	Δv (km s^{-1})	$\Delta\theta_x$ (arcsec)	$\Delta\theta_y$ (arcsec)	Trans.	S (Jy)	v_{LSR} (km s^{-1})	Δv (km s^{-1})	$\Delta\theta_x$ (arcsec)	$\Delta\theta_y$ (arcsec)
1665 L......	1.31	59.89	0.51	0.000	0.000						

TABLE 46

G49.491−0.376 (W51)

Trans.	S (Jy)	v_{LSR} (km s^{-1})	Δv (km s^{-1})	$\Delta\theta_x$ (arcsec)	$\Delta\theta_y$ (arcsec)	Trans.	S (Jy)	v_{LSR} (km s^{-1})	Δv (km s^{-1})	$\Delta\theta_x$ (arcsec)	$\Delta\theta_y$ (arcsec)
1720 R......	0.73	64.77	0.44	0.020	−0.010	1720 L......	1.07	64.02	0.53	0.000	0.000

TABLE 47

G69.540 − 0.976 (ON 1)

Trans.	S (Jy)	v_{LSR} (km s^{-1})	Δv (km s^{-1})	$\Delta\theta_x$ (arcsec)	$\Delta\theta_y$ (arcsec)	Trans.	S (Jy)	v_{LSR} (km s^{-1})	Δv (km s^{-1})	$\Delta\theta_x$ (arcsec)	$\Delta\theta_y$ (arcsec)
1665 R......	21.17	13.11	0.54	0.000	0.000	1665 L......	0.65	10.87	0.29	−0.716	0.518
	15.72	11.86	0.26	0.244	−0.134		0.42	4.03	0.46	0.208	0.838
	0.86	10.75	0.42	−0.646	0.469		13.66	2.46	0.30	0.208	0.872
1665 L......	5.64	15.45	0.34	0.009	−0.059		3.69	1.12	0.23	0.215	0.857
	3.04	15.05	0.50	0.025	−0.060	1667 R......	2.53	13.28	0.30	0.403	−0.193
	4.84	13.97	0.41	0.374	−0.138		0.84	12.89	0.24	0.252	−0.204
	10.74	13.25	0.35	0.015	0.027	1667 L......	6.18	13.64	0.25	0.522	−0.211
	0.35	11.94	0.56	−0.214	0.260						

TABLE 48

G70.293 + 1.601 (K3 − 50)

Trans.	S (Jy)	v_{LSR} (km s^{-1})	Δv (km s^{-1})	$\Delta\theta_x$ (arcsec)	$\Delta\theta_y$ (arcsec)	Trans.	S (Jy)	v_{LSR} (km s^{-1})	Δv (km s^{-1})	$\Delta\theta_x$ (arcsec)	$\Delta\theta_y$ (arcsec)
1665 R......	0.65	−18.86	0.31	−0.132	−0.465	1665 L......	11.84	−19.76	0.25	0.000	0.000
	3.88	−19.49	0.30	0.242	0.127		4.03	−20.39	0.30	0.009	−0.007
	6.05	−21.27	0.38	−0.010	−0.007		2.37	−21.28	0.94	1.710	−1.938
	2.73	−22.27	1.27	1.689	−1.913		1.80	−22.43	0.28	−0.059	−0.445
	2.57	−22.78	2.31	1.705	−1.936	1667 R......	3.56	−21.08	0.38	0.104	0.040
1665 L......	1.95	−17.55	0.31	−0.115	−0.579	1667 L......	3.56	−20.14	0.33	0.108	0.052
	3.06	−19.45	0.43	0.150	0.058		2.60	−20.81	0.46	0.120	0.050

TABLE 49

G70.329 + 1.590 (ON 3)

Trans.	S (Jy)	v_{LSR} (km s^{-1})	Δv (km s^{-1})	$\Delta\theta_x$ (arcsec)	$\Delta\theta_y$ (arcsec)	Trans.	S (Jy)	v_{LSR} (km s^{-1})	Δv (km s^{-1})	$\Delta\theta_x$ (arcsec)	$\Delta\theta_y$ (arcsec)
1665 R......	0.80	−15.70	0.35	0.000	0.000	1665 L......	0.26	−15.82	0.51	−0.075	0.030
	0.57	−16.38	0.45	0.041	0.055		0.33	−17.67	0.41	0.041	0.001
1665 L......	0.50	−14.29	0.33	−0.046	0.028		0.22	−18.32	0.56	0.076	0.017

TABLE 50

G75.761 + 0.340 (ON 2 S)

Trans.	S (Jy)	v_{LSR} (km s^{-1})	Δv (km s^{-1})	$\Delta\theta_x$ (arcsec)	$\Delta\theta_y$ (arcsec)	Trans.	S (Jy)	v_{LSR} (km s^{-1})	Δv (km s^{-1})	$\Delta\theta_x$ (arcsec)	$\Delta\theta_y$ (arcsec)
1667 R......	1.11	0.75	0.32	0.000	0.000						

TABLE 51

G75.782+0.343 (ON 2 N)

Trans.	S (Jy)	v_{LSR} (km s^{-1})	Δv (km s^{-1})	$\Delta\theta_x$ (arcsec)	$\Delta\theta_y$ (arcsec)	Trans.	S (Jy)	v_{LSR} (km s^{-1})	Δv (km s^{-1})	$\Delta\theta_x$ (arcsec)	$\Delta\theta_y$ (arcsec)
1665 R......	36.05	2.54	0.38	0.000	0.000	1667 R......	2.88	2.73	0.77	−0.357	−0.363
	2.85	0.70	0.30	0.877	0.069		1.14	−1.20	0.51	0.656	0.104
	6.63	−0.57	0.69	0.924	0.043		4.61	−1.74	0.25	0.799	−0.599
	3.56	−1.49	0.43	0.847	0.118		1.99	−2.22	0.30	0.794	−0.459
	3.46	−2.18	0.56	0.913	−0.002		24.49	−3.59	0.42	0.829	−0.189
	15.94	−2.87	0.33	0.915	0.032		32.74	−4.07	0.44	0.821	−0.146
	31.45	−3.56	0.36	0.899	0.016		25.80	−4.44	0.46	0.820	−0.157
	1.79	−5.28	0.44	0.893	0.000		21.52	−4.96	0.49	0.820	−0.160
1665 L......	7.38	2.36	0.53	−0.004	−0.261		2.88	−6.55	0.48	0.827	−0.167
	1.55	1.36	0.50	0.816	−0.027		1.13	−7.95	0.41	0.829	−0.310
	2.19	0.98	0.31	0.927	0.020	1667 L......	1.62	4.14	0.47	−0.478	−0.381
	1.57	0.45	0.29	1.022	−0.027		4.39	2.98	0.86	−0.561	−0.301
	0.56	−0.98	0.41	0.878	0.116		0.89	−2.17	0.56	0.816	−0.502
	3.43	−1.59	0.28	0.969	0.020		1.03	−2.65	0.55	0.828	−0.222
	2.58	−2.03	0.55	0.911	0.043		5.55	−4.06	0.44	0.826	−0.163
	6.16	−2.74	1.88	0.904	0.026		16.31	−4.90	0.37	0.834	−0.150
	9.32	−3.39	0.58	0.932	0.004		5.68	−5.37	0.71	0.818	−0.191
	6.05	−4.52	0.47	0.927	0.000		2.82	−6.83	0.34	0.916	−0.457
	8.89	−5.35	0.40	0.910	0.011		3.23	−7.23	0.47	0.965	−0.364
	0.77	−6.24	0.61	0.887	−0.541		2.59	−7.47	0.41	0.961	−0.384
	2.05	−6.69	0.29	1.015	−0.234		0.77	−8.78	0.61	0.806	−0.142
	1.65	−7.15	0.26	0.841	−0.649		0.80	−9.04	0.63	0.814	−0.143
	1.67	−7.88	0.29	1.064	−0.228		0.74	−9.66	0.39	0.800	−0.257
1667 R......	2.08	4.37	0.41	−0.560	−0.329		0.57	−10.18	0.54	0.819	−0.261
	1.75	3.34	0.53	−0.397	−0.423						

TABLE 52

G80.864+0.421

Trans.	S (Jy)	v_{LSR} (km s^{-1})	Δv (km s^{-1})	$\Delta\theta_x$ (arcsec)	$\Delta\theta_y$ (arcsec)	Trans.	S (Jy)	v_{LSR} (km s^{-1})	Δv (km s^{-1})	$\Delta\theta_x$ (arcsec)	$\Delta\theta_y$ (arcsec)
1665 R......	25.40	−8.46	0.25	0.000	0.000	1665 L......	20.15	−8.46	0.25	−0.001	0.007

TABLE 53

G81.721+0.571 (W75 S)

Trans.	S (Jy)	v_{LSR} (km s^{-1})	Δv (km s^{-1})	$\Delta\theta_x$ (arcsec)	$\Delta\theta_y$ (arcsec)	Trans.	S (Jy)	v_{LSR} (km s^{-1})	Δv (km s^{-1})	$\Delta\theta_x$ (arcsec)	$\Delta\theta_y$ (arcsec)
1665 R......	3.88	5.19	0.28	−0.335	0.367	1665 L......	3.05	1.70	0.32	−0.060	0.078
	0.35	4.29	0.30	−0.062	0.152		23.33	1.33	0.29	−0.329	0.343
	0.68	3.54	0.34	−0.256	0.287		16.32	0.94	0.39	−0.342	0.332
	1.48	2.96	0.36	−0.399	0.416		8.22	0.59	0.54	−0.288	0.263
	0.73	2.34	0.34	−0.045	0.367		2.44	−0.28	0.42	−0.388	0.394
	12.73	1.74	0.28	0.010	0.019		7.57	−1.30	0.28	1.650	−0.119
	5.59	1.21	0.36	−0.011	0.005		0.40	−2.07	0.25	1.338	0.750
	26.53	0.65	0.30	0.000	0.000		0.34	−2.80	0.28	0.101	0.101
	4.03	−0.89	0.35	0.060	−0.266	1667 R......	0.71	2.13	0.25	−0.348	0.381
	0.73	−2.31	0.38	1.410	−0.410		1.55	−1.16	0.41	0.083	−0.276
	0.92	−3.06	0.38	1.457	−0.433		0.25	−3.48	0.32	1.826	−0.233
	0.69	−3.59	0.37	1.473	−0.343	1667 L......	0.74	−1.12	0.27	0.162	−0.253
	1.40	−4.00	0.28	1.642	−0.222		0.93	−1.94	···	1.752	−0.097
	0.78	−4.49	0.40	1.269	1.390						

TABLE 54

G81.745+0.590 (W75)

Trans.	S (Jy)	v_{LSR} (km s^{-1})	Δv (km s^{-1})	$\Delta\theta_x$ (arcsec)	$\Delta\theta_y$ (arcsec)	Trans.	S (Jy)	v_{LSR} (km s^{-1})	Δv (km s^{-1})	$\Delta\theta_x$ (arcsec)	$\Delta\theta_y$ (arcsec)
1665 R......	0.83	3.34	0.59	0.007	−0.012	1665 L......	0.56	3.65	0.25	0.114	0.057
	5.20	2.50	0.39	0.000	0.000						

TABLE 55

G81.871+0.781 (W75 N)

Trans.	S (Jy)	v_{LSR} (km s^{-1})	Δv (km s^{-1})	$\Delta\theta_x$ (arcsec)	$\Delta\theta_y$ (arcsec)	Trans.	S (Jy)	v_{LSR} (km s^{-1})	Δv (km s^{-1})	$\Delta\theta_x$ (arcsec)	$\Delta\theta_y$ (arcsec)
1665 R......	46.04	12.47	0.36	0.000	0.000	1665 L......	1.39	4.65	0.52	0.386	1.138
	0.80	11.03	0.42	0.226	0.732		2.50	4.07	0.25	0.296	1.092
	11.31	9.33	0.20	0.187	0.542		5.59	3.69	0.24	0.548	1.465
	2.55	9.06	0.20	0.171	0.529		27.00	3.10	0.32	0.599	−0.104
	2.52	7.36	0.24	0.356	1.200		13.99	0.62	0.39	0.686	−0.217
	19.35	5.74	0.31	0.287	1.049	1667 R......	0.56	12.87	0.51	1.929	−0.663
	5.40	5.24	0.35	0.449	1.276		1.24	12.57	0.24	1.973	−0.650
	30.75	3.09	0.32	0.598	−0.101		0.31	11.96	0.49	0.251	0.078
	0.93	1.89	0.48	0.660	−0.137		19.09	9.26	0.35	0.341	0.449
	17.36	0.63	0.39	0.684	−0.216		4.88	8.11	0.21	0.366	0.608
1665 L......	0.79	13.69	0.29	0.120	−0.040		0.49	6.42	0.32	0.759	0.068
	1.89	12.88	0.26	0.142	−0.035	1667 L......	26.78	9.33	0.36	0.330	0.458
	0.64	12.22	0.38	0.635	−0.208		0.70	6.43	0.25	0.369	0.346
	15.03	9.35	0.20	0.007	0.004		4.74	5.99	0.30	0.361	0.569
	20.65	5.74	0.29	0.264	0.927		9.81	5.43	0.28	0.367	0.625
	16.64	5.17	0.41	0.464	1.275						

TABLE 56

G97.527+3.184

Trans.	S (Jy)	v_{LSR} (km s^{-1})	Δv (km s^{-1})	$\Delta\theta_x$ (arcsec)	$\Delta\theta_y$ (arcsec)	Trans.	S (Jy)	v_{LSR} (km s^{-1})	Δv (km s^{-1})	$\Delta\theta_x$ (arcsec)	$\Delta\theta_y$ (arcsec)
1665 R......	2.41	−65.78	0.24	0.000	0.000	1665 L......	0.14	−67.37	0.32	−0.047	−0.074

TABLE 57

G109.871+2.114 (Cep A)

Trans.	S (Jy)	v_{LSR} (km s^{-1})	Δv (km s^{-1})	$\Delta\theta_x$ (arcsec)	$\Delta\theta_y$ (arcsec)	Trans.	S (Jy)	v_{LSR} (km s^{-1})	Δv (km s^{-1})	$\Delta\theta_x$ (arcsec)	$\Delta\theta_y$ (arcsec)
1665 R......	0.28	−7.10	0.98	1.243	−1.005	1667 R......	0.73	−5.25	0.22	0.059	1.079
	2.65	−11.72	0.35	−0.005	−0.004		0.52	−5.43	0.44	−0.123	1.183
	0.44	−13.30	···	1.623	0.562		0.56	−10.96	···	0.095	0.009
	7.31	−14.24	0.27	1.741	−2.485		4.51	−14.64	0.28	1.839	−2.452
1665 L......	0.29	−5.07	0.61	1.355	−1.084	1667 L......	3.01	−3.14	···	−0.061	1.114
	2.07	−8.00	0.31	0.951	0.852		1.27	−3.42	···	−0.122	1.204
	40.56	−11.56	0.30	0.000	0.000		0.88	−11.39	0.25	0.113	0.006
	5.97	−12.30	0.26	−0.183	−0.131		0.41	−12.33	···	0.025	−0.064
	7.00	−13.90	0.21	1.853	−2.334		3.77	−15.78	0.38	1.846	−2.449
	9.41	−16.22	0.27	1.752	−2.488						

TABLE 58

G111.533+0.757 (NGC 7538)

Trans.	S (Jy)	v_{LSR} (km s^{-1})	Δv (km s^{-1})	$\Delta\theta_x$ (arcsec)	$\Delta\theta_y$ (arcsec)	Trans.	S (Jy)	v_{LSR} (km s^{-1})	Δv (km s^{-1})	$\Delta\theta_x$ (arcsec)	$\Delta\theta_y$ (arcsec)
1665 R......	2.47	−53.00	0.30	−0.014	−0.003	1665 R......	0.63	−60.70	0.40	−0.079	0.276
	0.21	−54.06	0.44	−0.078	−0.381	1665 L......	2.82	−54.33	0.32	0.000	0.000
	0.26	−54.84	0.44	0.113	0.184		0.94	−57.69	0.30	1.174	1.042
	0.63	−57.71	0.36	1.175	1.042		0.25	−60.79	0.45	−0.042	0.221

TABLE 59

G111.543+0.777 (NGC 7538)

Trans.	S (Jy)	v_{LSR} (km s^{-1})	Δv (km s^{-1})	$\Delta\theta_x$ (arcsec)	$\Delta\theta_y$ (arcsec)	Trans.	S (Jy)	v_{LSR} (km s^{-1})	Δv (km s^{-1})	$\Delta\theta_x$ (arcsec)	$\Delta\theta_y$ (arcsec)
1665 R......	1.07	−58.19	0.44	0.391	−0.481	1665 L......	39.90	−59.40	0.31	0.000	0.000
	11.93	−59.32	0.41	0.014	−0.005	1667 R......	3.59	−59.22	0.47	0.225	−0.011
	4.88	−59.82	0.49	−0.014	−0.001	1667 L......	5.80	−59.37	0.56	0.100	0.050
1665 L......	0.70	−58.14	0.44	0.403	−0.415						

TABLE 60

G126.715−0.822

Trans.	S (Jy)	v_{LSR} (km s^{-1})	Δv (km s^{-1})	$\Delta\theta_x$ (arcsec)	$\Delta\theta_y$ (arcsec)	Trans.	S (Jy)	v_{LSR} (km s^{-1})	Δv (km s^{-1})	$\Delta\theta_x$ (arcsec)	$\Delta\theta_y$ (arcsec)
1665 R......	0.50	−5.74	...	−0.004	−0.195	1665 L......	0.63	−10.22	0.60	−0.019	−0.003
1665 L......	0.67	−8.64	0.23	−0.005	−0.051		1.50	−12.06	0.30	0.000	0.000
	0.98	−9.35	0.35	−0.071	−0.059						

TABLE 61

G133.715+1.215 (W3)

Trans.	S (Jy)	v_{LSR} (km s^{-1})	Δv (km s^{-1})	$\Delta\theta_x$ (arcsec)	$\Delta\theta_y$ (arcsec)	Trans.	S (Jy)	v_{LSR} (km s^{-1})	Δv (km s^{-1})	$\Delta\theta_x$ (arcsec)	$\Delta\theta_y$ (arcsec)
1665 R......	0.75	−39.20	...	0.004	−0.088	1665 L......	4.31	−39.29	0.26	0.000	0.000
1665 L......	0.67	−37.59	0.32	−1.124	−2.802		0.64	−40.66	0.27	2.018	3.317
	0.31	−38.12	0.36	−1.111	−2.812		0.38	−43.96	0.48	0.372	−0.376

TABLE 62

G133.946+1.064 (W3 OH)

Trans.	S (Jy)	v_{LSR} (km s^{-1})	Δv (km s^{-1})	$\Delta\theta_x$ (arcsec)	$\Delta\theta_y$ (arcsec)	Trans.	S (Jy)	v_{LSR} (km s^{-1})	Δv (km s^{-1})	$\Delta\theta_x$ (arcsec)	$\Delta\theta_y$ (arcsec)
1665 R......	1.33	−40.02	...	0.588	−1.121	1667 R......	2.21	−45.04	0.38	0.022	−0.023
	2.91	−40.61	0.46	0.549	−1.265		0.60	−47.82	0.26	0.963	−2.056
	25.07	−41.15	0.33	0.896	−0.221	1667 L......	0.73	−43.31	0.29	0.603	−1.998
	14.93	−41.56	0.88	0.615	−1.652		26.87	−44.43	0.44	0.477	−1.936
	17.30	−42.87	0.26	0.352	−1.608		1.15	−45.52	0.31	0.361	−1.101
	3.93	−43.34	0.37	0.383	−1.062		1.32	−46.28	0.57	−0.029	−0.251
	34.51	−44.17	0.41	0.261	−0.571		1.96	−47.77	0.32	0.942	−2.059
	200.54	−45.02	0.78	0.000	0.000	1612 R......	1.02	−41.48	0.30	0.840	−1.795
	20.42	−47.44	0.23	0.915	−0.093		6.21	−42.17	0.43	1.057	−1.852
	1.07	−48.39	...	0.949	0.234		3.78	−42.92	0.44	1.013	−1.836
	2.79	−48.90	0.28	0.879	0.310	1612 L......	0.25	−42.30	0.34	0.906	−1.877
1665 L......	1.42	−41.93	0.24	0.824	−1.840		1.68	−43.15	0.44	1.024	−1.309
	44.64	−44.67	0.66	0.573	−1.532		1.40	−43.81	0.40	1.034	−1.874
	54.01	−45.21	1.09	0.413	−1.801		0.90	−47.51	0.24	1.576	−1.650
	132.32	−46.29	0.51	−0.043	−0.225	1720 R......	4.47	−42.72	0.25	0.910	−0.052
	32.54	−47.45	0.22	0.883	−0.092		5.39	−43.12	0.27	0.760	−1.168
	0.83	−47.85	0.28	0.177	−0.093		8.32	−44.33	0.30	0.885	−0.066
	6.18	−48.56	0.41	0.917	0.193		7.72	−44.70	0.57	0.867	−0.086
	14.73	−48.94	0.28	0.918	0.259	1720 L......	2.69	−43.50	0.26	0.883	−0.302
1667 R......	21.36	−42.17	0.32	0.368	−1.955		5.72	−43.76	0.25	0.763	−1.051
	2.52	−42.90	0.21	0.851	−1.524		6.64	−45.23	0.45	0.859	−0.088
	2.02	−44.20	0.64	0.585	−1.829		10.40	−45.56	0.50	0.885	−0.073
	2.95	−44.69	0.36	0.115	−0.509						

TABLE 63

G173.481+2.445 (S231)

Trans.	S (Jy)	v_{LSR} (km s^{-1})	Δv (km s^{-1})	$\Delta\theta_x$ (arcsec)	$\Delta\theta_y$ (arcsec)	Trans.	S (Jy)	v_{LSR} (km s^{-1})	Δv (km s^{-1})	$\Delta\theta_x$ (arcsec)	$\Delta\theta_y$ (arcsec)
1665 L......	0.35	−9.17	0.26	0.004	−0.038	1665 L......	0.14	−12.53	0.44	0.037	−0.232
	1.72	−10.64	0.28	0.000	0.000		0.34	−12.88	0.36	−0.001	−0.216

TABLE 64

G188.946+0.886 (S252)

Trans.	S (Jy)	v_{LSR} (km s^{-1})	Δv (km s^{-1})	$\Delta\theta_x$ (arcsec)	$\Delta\theta_y$ (arcsec)	Trans.	S (Jy)	v_{LSR} (km s^{-1})	Δv (km s^{-1})	$\Delta\theta_x$ (arcsec)	$\Delta\theta_y$ (arcsec)
1665 R......	0.72	9.97	0.26	0.000	0.000	1665 R......	0.48	9.06	0.27	−0.013	−0.137
	0.37	9.45	0.43	−0.063	−0.053	1665 L......	0.60	8.54	0.27	−0.028	−0.093

TABLE 65

G196.454−1.677 (S269)

Trans.	S (Jy)	v_{LSR} (km s^{-1})	Δv (km s^{-1})	$\Delta\theta_x$ (arcsec)	$\Delta\theta_y$ (arcsec)	Trans.	S (Jy)	v_{LSR} (km s^{-1})	Δv (km s^{-1})	$\Delta\theta_x$ (arcsec)	$\Delta\theta_y$ (arcsec)
1665 R......	0.82	17.87	0.24	0.074	0.024	1665 R......	1.45	14.38	0.31	−0.261	−0.094
	0.35	16.80	0.25	0.057	−0.056	1665 L......	7.47	17.90	0.28	0.033	0.074
	1.53	16.03	0.36	0.010	0.068		2.34	16.85	0.26	−0.046	−0.085
	1.07	14.96	0.30	−0.337	−0.149		8.73	16.04	0.31	0.000	0.000

TABLE 66

G213.706−12.60 (Mon R2)

Trans.	S (Jy)	v_{LSR} (km s^{-1})	Δv (km s^{-1})	$\Delta\theta_x$ (arcsec)	$\Delta\theta_y$ (arcsec)	Trans.	S (Jy)	v_{LSR} (km s^{-1})	Δv (km s^{-1})	$\Delta\theta_x$ (arcsec)	$\Delta\theta_y$ (arcsec)
1665 R......	0.62	10.37	0.37	0.370	−0.050	1665 L......	1.92	8.29	0.21	−0.236	0.197
	19.01	9.70	0.44	0.000	0.000	1667 R......	2.14	9.77	0.55	0.000	0.003
	3.59	9.21	0.52	−0.165	0.086		0.20	8.75	0.42	−0.185	0.209
	2.06	8.34	0.24	−0.260	0.205		0.57	8.35	0.21	−0.189	0.236
1665 L......	7.54	11.48	0.25	−0.033	0.006	1667 L......	1.67	10.75	0.32	0.070	0.016
	2.21	11.15	0.42	−0.003	0.012		0.56	9.60	0.25	−0.085	−0.031
	1.51	9.67	0.49	−0.096	0.043		0.35	8.58	0.43	−0.178	0.186
	2.12	9.12	0.43	−0.229	0.137		0.41	8.39	0.33	−0.187	0.179

TABLE 67

G337.707−0.051

Trans.	S (Jy)	v_{LSR} (km s^{-1})	Δv (km s^{-1})	$\Delta\theta_x$ (arcsec)	$\Delta\theta_y$ (arcsec)	Trans.	S (Jy)	v_{LSR} (km s^{-1})	Δv (km s^{-1})	$\Delta\theta_x$ (arcsec)	$\Delta\theta_y$ (arcsec)
1665 R......	7.63	−49.46	0.73	0.077	−0.869	1665 L......	0.60	−53.39	0.80	−0.357	−0.133
	6.93	−49.88	0.57	0.010	−0.802		0.94	−54.10	0.38	0.033	−0.850
	9.19	−50.64	0.88	−0.158	−0.617	1667 R......	4.20	−49.83	0.44	1.914	−3.716
	9.27	−50.85	1.12	−0.140	−0.539		2.65	−50.50	0.65	1.805	−3.998
	3.20	−52.22	0.35	−0.154	−0.255		2.48	−51.20	0.71	1.681	−4.070
1665 L......	10.40	−48.68	0.81	0.044	−0.382		2.49	−51.35	0.66	1.630	−4.006
	15.35	−49.26	0.76	0.000	0.000	1667 L......	5.51	−49.27	0.47	1.955	−3.658
	2.63	−50.54	0.71	−0.063	−0.193		3.61	−49.57	0.65	1.929	−3.607
	2.22	−50.88	1.70	−0.081	−0.281		0.98	−50.27	0.44	1.789	−3.887
	0.82	−52.22	0.25	−0.106	−0.031		0.67	−50.55	0.60	1.755	−3.859
	0.68	−52.96	0.28	−0.177	−0.487		1.29	−51.17	0.33	1.677	−4.144

TABLE 68

G340.785−0.095

Trans.	S (Jy)	v_{LSR} (km s^{-1})	Δv (km s^{-1})	$\Delta\theta_x$ (arcsec)	$\Delta\theta_y$ (arcsec)	Trans.	S (Jy)	v_{LSR} (km s^{-1})	Δv (km s^{-1})	$\Delta\theta_x$ (arcsec)	$\Delta\theta_y$ (arcsec)
1665 R......	1.68	−99.21	0.35	−0.007	0.325	1665 L......	3.33	−103.71	0.42	−0.069	0.360
	1.12	−100.70	0.32	0.027	0.059		3.90	−104.01	0.56	−0.104	0.435
	9.87	−101.23	0.50	0.000	0.000		1.53	−105.18	0.42	0.019	0.315
	8.12	−101.73	0.32	−0.076	−0.133	1667 R......	4.08	−101.57	0.79	−0.007	0.192
	1.15	−102.82	0.43	−0.109	0.218		4.14	−101.79	0.33	−0.030	0.183
	1.38	−105.79	0.27	−0.185	0.413	1667 L......	0.38	−100.78	0.33	0.084	0.313
1665 L......	0.44	−101.45	0.33	0.004	0.193		1.17	−101.89	0.29	−0.030	0.230
	2.92	−102.24	0.35	−0.047	−0.051		2.94	−102.27	0.30	0.005	0.275
	5.74	−102.78	0.40	−0.017	0.078		0.96	−102.65	0.54	−0.037	0.206

TABLE 69

G341.219−0.212

Trans.	S (Jy)	v_{LSR} (km s^{-1})	Δv (km s^{-1})	$\Delta\theta_x$ (arcsec)	$\Delta\theta_y$ (arcsec)	Trans.	S (Jy)	v_{LSR} (km s^{-1})	Δv (km s^{-1})	$\Delta\theta_x$ (arcsec)	$\Delta\theta_y$ (arcsec)
1665 R......	1.94	−36.40	0.56	0.041	−0.108	1665 L......	0.28	−39.13	0.36	0.183	−0.220
	10.06	−37.39	0.34	0.000	0.000		3.74	−40.20	0.29	0.032	0.062
	0.35	−38.41	0.38	0.105	−0.114		3.50	−40.84	0.46	−0.001	−0.015
	0.86	−39.06	0.27	0.009	−0.055						

TABLE 70

G343.128−0.063

Trans.	S (Jy)	v_{LSR} (km s^{-1})	Δv (km s^{-1})	$\Delta\theta_x$ (arcsec)	$\Delta\theta_y$ (arcsec)	Trans.	S (Jy)	v_{LSR} (km s^{-1})	Δv (km s^{-1})	$\Delta\theta_x$ (arcsec)	$\Delta\theta_y$ (arcsec)
1665 R......	14.06	−30.69	0.32	−0.007	0.020	1665 L......	88.89	−31.74	0.36	0.000	0.000
	5.72	−31.70	0.48	0.026	0.083		3.90	−32.89	0.39	0.028	−0.112
	0.56	−32.76	0.63	0.153	0.380		14.70	−33.57	0.53	0.071	−0.193
	4.00	−33.75	0.38	0.020	−0.091		54.77	−33.93	0.36	−0.028	0.086
	0.52	−36.56	0.37	−1.559	0.605		0.27	−38.57	0.38	0.210	0.761
1665 L......	2.49	−30.84	0.42	−0.072	−0.040		0.25	−39.67	0.42	0.394	0.814

TABLE 71

G344.227−0.568

Trans.	S (Jy)	v_{LSR} (km s^{-1})	Δv (km s^{-1})	$\Delta\theta_x$ (arcsec)	$\Delta\theta_y$ (arcsec)	Trans.	S (Jy)	v_{LSR} (km s^{-1})	Δv (km s^{-1})	$\Delta\theta_x$ (arcsec)	$\Delta\theta_y$ (arcsec)
1665 R......	0.41	−29.73	0.26	−0.367	−0.963	1665 L......	2.14	−29.75	0.48	−0.348	−0.874
	4.89	−30.94	0.36	−0.338	−0.875	1667 R......	1.60	−30.67	0.44	−0.011	0.082
1665 L......	0.65	−23.52	0.28	−0.880	−0.063		6.87	−31.19	0.32	0.000	0.000
	0.38	−29.21	0.34	−0.327	−0.713	1667 L......	2.28	−29.88	0.61	0.010	0.090

TABLE 72

G344.581−0.022

Trans.	S (Jy)	v_{LSR} (km s^{-1})	Δv (km s^{-1})	$\Delta\theta_x$ (arcsec)	$\Delta\theta_y$ (arcsec)	Trans.	S (Jy)	v_{LSR} (km s^{-1})	Δv (km s^{-1})	$\Delta\theta_x$ (arcsec)	$\Delta\theta_y$ (arcsec)
1665 R......	0.89	1.35	0.31	0.393	−0.046	1667 R......	2.40	−2.51	0.42	0.221	−2.770
	0.57	−0.79	0.78	0.124	−0.058		2.06	−3.28	0.59	0.438	−2.767
	19.02	−2.30	0.54	0.000	0.000		3.58	−3.94	0.35	0.178	−3.044
	10.24	−2.71	0.54	0.131	−0.033		1.35	−4.39	0.48	0.156	−2.927
	3.14	−4.01	0.53	0.024	0.069		1.25	−5.18	0.58	0.301	−2.767
	3.58	−4.36	0.44	0.010	0.132		3.91	−5.61	0.28	0.214	−3.087
	3.45	−5.33	0.51	0.133	0.349		2.15	−6.59	0.36	0.356	−2.713
	1.80	−5.75	0.85	0.165	0.397		1.51	−7.40	0.34	0.338	−2.963
	1.47	−6.36	0.50	0.171	0.309		0.82	−7.68	0.67	0.269	−3.099
	1.68	−6.87	0.78	0.148	0.344		0.74	−8.16	0.38	0.317	−2.391
	1.67	−7.60	0.45	0.092	0.271		0.70	−8.85	0.54	0.315	−2.758
	0.84	−8.23	0.48	0.076	0.253		0.53	−9.63	0.35	0.398	−2.444
1665 L......	0.67	1.31	0.51	0.171	−0.283	1667 L......	0.30	0.70	0.29	0.447	−2.997
	0.81	0.90	0.62	0.129	−0.101		0.63	−1.49	0.58	0.400	−3.118
	1.31	−0.17	1.13	0.233	−0.102		3.94	−2.48	0.40	0.521	−2.901
	3.82	−1.18	0.88	0.289	−0.091		3.51	−3.09	0.45	0.387	−2.913
	14.22	−2.63	0.75	0.277	−0.057		7.32	−3.62	0.39	−0.003	−2.950
	2.33	−4.41	0.54	−0.005	0.056		1.29	−5.11	0.56	0.222	−2.732
	1.99	−4.66	1.07	−0.014	0.106		2.90	−5.57	0.45	0.379	−2.503
	4.66	−5.84	0.62	0.152	0.313		1.35	−6.07	0.69	0.237	−3.160
	15.48	−6.61	0.36	0.177	0.392		1.43	−7.02	0.46	0.393	−2.498
	2.14	−7.84	0.60	0.074	0.302		1.16	−8.19	0.53	0.296	−2.817
	1.83	−8.22	0.59	0.048	0.222		0.56	−9.01	0.96	0.345	−2.581
	2.21	−8.76	0.75	0.042	0.270		0.82	−9.60	0.74	0.353	−2.564
	1.53	−9.21	0.73	0.083	0.245		0.36	−10.25	0.45	0.379	−2.512
1667 R......	1.77	−2.29	0.40	0.247	−2.776						

TABLE 73

G345.003−0.224

Trans.	S (Jy)	v_{LSR} (km s^{-1})	Δv (km s^{-1})	$\Delta\theta_x$ (arcsec)	$\Delta\theta_y$ (arcsec)	Trans.	S (Jy)	v_{LSR} (km s^{-1})	Δv (km s^{-1})	$\Delta\theta_x$ (arcsec)	$\Delta\theta_y$ (arcsec)
1665 R......	0.44	−22.96	0.33	−4.360	0.930	1665 L......	6.42	−27.54	0.22	−0.089	−0.041
	0.86	−24.79	0.90	−0.639	−0.325		0.43	−28.19	0.57	−0.578	−0.332
	1.08	−25.14	0.46	−0.450	−0.337	1667 R......	1.01	−25.69	0.43	−0.282	−0.448
	1.23	−25.62	0.36	−0.474	−0.298		1.18	−26.08	0.20	−0.365	−0.247
	2.46	−27.35	0.45	−0.025	−0.011		3.47	−30.76	0.29	−0.335	−0.767
	0.19	−28.14	0.42	−0.373	−0.533	1667 L......	0.68	−27.73	0.24	0.038	−0.151
	1.77	−31.05	0.25	−0.694	−0.513	1720 R......	2.30	−28.83	0.50	−0.007	0.004
1665 L......	2.22	−26.98	0.32	−0.277	−0.095	1720 L......	51.62	−29.27	0.39	0.000	0.000

TABLE 74

G345.011+1.792

Trans.	S (Jy)	v_{LSR} (km s^{-1})	Δv (km s^{-1})	$\Delta\theta_x$ (arcsec)	$\Delta\theta_y$ (arcsec)	Trans.	S (Jy)	v_{LSR} (km s^{-1})	Δv (km s^{-1})	$\Delta\theta_x$ (arcsec)	$\Delta\theta_y$ (arcsec)
1665 R......	0.72	−17.21	0.35	−0.105	−0.509	1665 L......	2.90	−21.19	0.31	−0.086	0.077
	10.48	−19.72	0.25	−0.092	−0.075		3.36	−21.67	0.63	−0.027	−0.001
	20.36	−20.43	0.40	−0.188	−0.131		30.14	−22.75	0.40	0.000	0.000
	0.80	−22.87	0.24	0.028	0.035	1667 R......	1.71	−19.69	0.23	−0.345	−0.352
1665 L......	0.52	−15.75	0.32	−0.243	−0.140	1667 L......	0.50	−17.98	...	−0.704	−0.452
	1.13	−17.33	0.36	0.060	−0.159		1.30	−20.01	0.21	−0.369	−0.359
	0.70	−18.99	0.25	−0.164	−0.078		1.27	−20.89	0.30	−0.317	−0.329
	0.68	−19.79	0.21	−0.147	−0.025		0.61	−21.29	0.51	−0.361	−0.330

TABLE 75

G345.488+0.313

Trans.	S (Jy)	v_{LSR} (km s^{-1})	Δv (km s^{-1})	$\Delta\theta_x$ (arcsec)	$\Delta\theta_y$ (arcsec)	Trans.	S (Jy)	v_{LSR} (km s^{-1})	Δv (km s^{-1})	$\Delta\theta_x$ (arcsec)	$\Delta\theta_y$ (arcsec)
1665 L......	0.73	−22.81	0.23	0.000	0.000						

TABLE 76

G345.505+0.347

Trans.	S (Jy)	v_{LSR} (km s^{-1})	Δv (km s^{-1})	$\Delta\theta_x$ (arcsec)	$\Delta\theta_y$ (arcsec)	Trans.	S (Jy)	v_{LSR} (km s^{-1})	Δv (km s^{-1})	$\Delta\theta_x$ (arcsec)	$\Delta\theta_y$ (arcsec)
1665 R......	0.37	−13.79	0.46	−0.407	0.236	1667 R......	4.87	−12.69	0.34	−0.468	1.417
	0.68	−14.43	0.39	−0.269	0.110		1.30	−14.18	0.26	−0.204	1.127
	2.46	−15.30	0.27	−0.390	0.217		4.59	−17.51	0.57	0.025	0.989
	0.85	−17.47	0.39	−0.016	1.101		4.67	−19.45	0.95	−0.896	1.397
	4.38	−18.01	0.26	0.096	0.028		0.73	−20.12	0.96	−0.605	1.592
	1.26	−18.35	0.23	0.029	0.063		3.79	−21.24	0.32	−0.573	1.922
	8.85	−19.29	0.33	−0.925	0.520		0.44	−22.37	0.41	−0.813	1.766
	0.29	−23.64	0.45	1.162	1.024	1667 L......	2.37	−12.74	0.36	−0.461	1.398
1665 L......	0.34	−14.70	0.32	0.318	0.650		1.68	−13.30	0.29	−0.327	1.178
	0.49	−15.49	...	0.927	−0.054		0.38	−15.22	0.41	0.859	1.125
	0.44	−15.79	0.27	−0.250	0.548		0.76	−16.04	0.29	−0.089	1.104
	2.70	−16.92	0.46	0.011	−0.034		2.06	−16.83	0.41	0.005	1.058
	10.98	−17.33	0.35	0.000	0.000		1.50	−17.60	0.44	−0.076	1.018
	1.24	−18.00	0.25	0.010	0.160		5.11	−19.73	0.36	−0.627	0.797
	1.62	−18.43	0.40	−0.125	0.183		1.67	−21.58	0.37	−0.584	1.932
	3.92	−19.49	0.55	−0.468	−0.003		0.92	−23.08	0.26	−1.097	1.847
	0.56	−20.13	0.33	−0.478	0.452						

TABLE 77

G345.699−0.090

Trans.	S (Jy)	v_{LSR} (km s^{-1})	Δv (km s^{-1})	$\Delta\theta_x$ (arcsec)	$\Delta\theta_y$ (arcsec)	Trans.	S (Jy)	v_{LSR} (km s^{-1})	Δv (km s^{-1})	$\Delta\theta_x$ (arcsec)	$\Delta\theta_y$ (arcsec)
1665 R......	0.77	−3.15	0.26	−0.397	−1.017	1665 L......	0.65	−6.79	0.43	−0.253	−1.075
	0.43	−3.72	0.33	−0.357	−0.881		0.51	−8.47	0.28	0.105	−0.619
	1.03	−4.50	0.30	−0.486	−1.327	1667 R......	2.89	−5.79	0.26	−0.022	0.000
	3.37	−5.78	0.34	−0.014	−0.935		12.78	−6.45	0.29	0.000	0.000
	7.86	−6.33	0.37	0.009	−0.931		1.11	−6.97	0.43	0.018	0.107
	1.26	−6.82	0.63	−0.006	−0.915		0.85	−8.27	0.40	0.087	0.382
	2.62	−7.70	0.32	0.114	−0.760	1667 L......	1.09	−5.14	0.36	−0.046	0.048
	3.61	−8.22	0.23	0.165	−0.723		3.88	−5.82	0.70	0.024	0.004
	0.81	−8.55	0.25	0.283	−2.960		4.38	−6.15	0.46	0.012	0.026
1665 L......	0.94	−3.19	0.50	−0.360	−0.876		0.69	−6.79	0.45	−0.105	0.138
	6.43	−5.76	0.38	0.028	−0.956		0.63	−8.39	0.29	0.063	0.385
	6.39	−5.96	0.37	0.035	−0.961		0.33	−10.59	0.41	−0.069	0.882

TABLE 78

G347.628+0.149

Trans.	S (Jy)	v_{LSR} (km s^{-1})	Δv (km s^{-1})	$\Delta\theta_x$ (arcsec)	$\Delta\theta_y$ (arcsec)	Trans.	S (Jy)	v_{LSR} (km s^{-1})	Δv (km s^{-1})	$\Delta\theta_x$ (arcsec)	$\Delta\theta_y$ (arcsec)
1665 R......	3.58	−94.14	0.32	−0.011	0.034	1665 L......	18.43	−94.18	0.28	0.000	0.000
	1.77	−95.12	0.24	0.027	0.224		1.92	−95.79	0.26	0.059	0.033
	9.20	−95.79	0.25	0.002	0.057		0.75	−96.21	0.32	0.010	0.098
	6.45	−96.86	0.31	0.002	0.074		0.88	−96.89	0.28	−0.004	−0.032
	1.00	−97.92	...	0.017	0.040	1612 R......	5.86	−96.42	0.26	0.449	−2.163
1665 L......	0.72	−93.02	0.48	0.007	0.035	1612 L......	2.99	−97.16	0.26	0.456	−2.159
	4.24	−93.38	0.31	0.003	0.014						

TABLE 79

G348.549 − 0.978

Trans.	S (Jy)	v_{LSR} (km s^{-1})	Δv (km s^{-1})	$\Delta\theta_x$ (arcsec)	$\Delta\theta_y$ (arcsec)	Trans.	S (Jy)	v_{LSR} (km s^{-1})	Δv (km s^{-1})	$\Delta\theta_x$ (arcsec)	$\Delta\theta_y$ (arcsec)
1665 R......	0.79	−10.40	0.39	0.119	−0.061	1665 R......	2.63	−19.26	0.45	−0.013	−0.010
	0.67	−11.61	0.73	0.093	0.104		6.72	−19.84	0.40	0.000	0.000
	1.01	−12.19	0.77	0.082	0.085		3.32	−20.79	0.43	−0.058	0.049
	4.49	−13.13	0.46	0.106	−0.019	1665 L......	0.89	−11.98	0.30	0.265	0.059
	1.36	−13.72	0.45	0.156	0.015		0.80	−13.18	0.68	0.174	0.211
	2.69	−14.26	0.67	0.146	0.016		1.42	−18.47	0.37	0.041	−0.002
	2.68	−14.43	0.61	0.158	−0.006		3.08	−19.88	0.35	0.043	−0.001
	0.26	−15.57	0.76	0.130	0.034	1720 R......	4.57	−13.40	0.40	0.171	−0.014
	1.14	−16.43	0.25	0.623	−0.177	1720 L......	4.89	−12.77	0.35	0.167	0.032

TABLE 80

G348.698 − 1.027

Trans.	S (Jy)	v_{LSR} (km s^{-1})	Δv (km s^{-1})	$\Delta\theta_x$ (arcsec)	$\Delta\theta_y$ (arcsec)	Trans.	S (Jy)	v_{LSR} (km s^{-1})	Δv (km s^{-1})	$\Delta\theta_x$ (arcsec)	$\Delta\theta_y$ (arcsec)
1665 R......	1.19	−15.44	0.25	0.000	0.000						

TABLE 81

G350.011 − 1.341

Trans.	S (Jy)	v_{LSR} (km s^{-1})	Δv (km s^{-1})	$\Delta\theta_x$ (arcsec)	$\Delta\theta_y$ (arcsec)	Trans.	S (Jy)	v_{LSR} (km s^{-1})	Δv (km s^{-1})	$\Delta\theta_x$ (arcsec)	$\Delta\theta_y$ (arcsec)
1665 R......	2.09	−18.04	0.42	0.102	0.041	1665 L......	5.41	−19.74	0.29	0.000	0.000
	3.57	−19.32	0.23	−0.012	−0.035		1.31	−20.81	0.31	0.693	0.287
	1.10	−19.78	0.32	0.127	0.011		1.63	−23.76	0.29	0.774	0.113
	1.93	−23.08	0.27	0.753	0.140	1667 R......	0.31	−19.37	0.31	0.305	−0.257
	1.64	−23.74	0.29	0.794	0.144		0.37	−19.72	0.47	0.229	−0.280
	0.19	−26.25	0.35	0.509	0.213		2.58	−23.75	0.52	0.975	−0.179
1665 L......	3.85	−18.21	0.49	0.095	0.047	1667 L......	0.18	−19.32	0.51	0.314	−0.205
	0.74	−19.16	0.42	0.004	0.017		2.25	−23.74	0.53	0.981	−0.163

TABLE 82

G350.113 + 0.095

Trans.	S (Jy)	v_{LSR} (km s^{-1})	Δv (km s^{-1})	$\Delta\theta_x$ (arcsec)	$\Delta\theta_y$ (arcsec)	Trans.	S (Jy)	v_{LSR} (km s^{-1})	Δv (km s^{-1})	$\Delta\theta_x$ (arcsec)	$\Delta\theta_y$ (arcsec)
1665 R......	0.75	−65.27	0.31	0.155	−0.399	1665 L......	3.39	−68.66	0.29	−0.048	−0.091
	1.33	−67.72	0.35	0.200	−0.326		2.55	−69.05	0.40	−0.066	−0.117
	23.78	−71.16	0.36	0.000	0.000		15.38	−71.03	0.54	0.006	−0.109
	3.04	−72.36	0.50	−0.004	−0.001		11.06	−72.78	0.46	−0.106	−0.102
	2.76	−72.81	0.47	−0.087	0.014		3.28	−73.68	0.51	0.147	−0.191
	1.35	−73.78	0.93	0.046	−0.128		1.92	−74.53	0.56	−0.165	−0.084
	10.06	−74.79	0.64	−0.164	−0.303		1.13	−75.15	0.48	−0.151	−0.353
	1.22	−75.82	0.67	−0.239	−0.271		0.57	−75.61	0.57	−0.227	−0.317

TABLE 83

G351.161+0.697 (NGC 6334 B)

Trans.	S (Jy)	v_{LSR} (km s^{-1})	Δv (km s^{-1})	$\Delta\theta_x$ (arcsec)	$\Delta\theta_y$ (arcsec)	Trans.	S (Jy)	v_{LSR} (km s^{-1})	Δv (km s^{-1})	$\Delta\theta_x$ (arcsec)	$\Delta\theta_y$ (arcsec)
1665 R......	1.17	−5.79	0.59	1.594	1.550	1667 R......	1.02	−6.70	0.51	0.610	1.775
	3.91	−6.39	0.33	0.459	−0.554		21.17	−7.41	0.24	0.411	2.509
	2.97	−6.61	0.63	−0.172	−0.377		8.58	−8.94	0.37	1.045	1.600
	5.49	−7.69	0.89	−0.012	1.129		6.76	−9.26	0.37	0.929	1.642
	14.98	−8.51	0.34	−1.455	−1.641		78.82	−9.64	0.22	0.721	2.031
	1.70	−8.95	0.33	−0.528	−0.689		3.63	−10.17	0.23	0.477	1.572
	1.74	−10.23	0.27	−0.833	−0.965		1.68	−10.94	0.30	−0.034	2.172
	1.52	−10.57	0.29	−0.718	−1.049		1.85	−11.44	0.49	−0.133	1.539
	0.68	−11.32	0.39	−0.768	0.525		3.64	−12.15	0.40	−0.493	0.988
	0.85	−11.64	0.44	−0.594	0.351		11.39	−13.23	0.41	−0.247	0.258
	1.77	−12.18	0.40	−0.927	0.781		13.64	−14.10	1.63	−0.933	0.579
	0.62	−12.77	0.40	−1.202	0.879		4.64	−14.83	0.41	−1.181	0.216
	0.85	−13.15	0.33	−1.171	0.450		5.15	−15.23	0.30	−1.047	0.139
1665 L......	2.56	−3.95	0.21	1.600	−0.828	1667 L......	0.36	−4.49	0.27	1.990	−0.158
	1.67	−4.27	0.20	1.585	−0.714		0.38	−5.59	0.53	−0.077	1.993
	1.72	−5.76	0.27	1.477	2.259		1.10	−6.82	0.27	1.004	2.637
	2.34	−6.54	0.41	−0.112	−0.121		0.58	−7.47	0.37	0.790	2.157
	16.44	−8.84	0.70	−0.345	−0.589		4.82	−8.22	0.31	0.962	1.538
	2.99	−9.69	0.34	−1.297	−1.414		27.68	−9.04	0.60	0.004	−0.046
	11.76	−10.21	0.27	−0.788	−0.975		20.53	−9.72	0.30	0.733	2.060
	7.41	−10.48	0.40	−0.675	−1.007		7.32	−11.56	0.36	−0.215	0.227
	8.16	−11.62	0.35	−0.582	−0.369		96.65	−12.59	0.28	0.000	0.000
	4.48	−12.44	0.62	−1.144	0.936		8.63	−14.21	0.37	−1.030	0.530
	4.65	−12.67	0.57	−1.231	0.927		3.87	−14.68	0.48	−1.154	0.323
1667 R......	0.91	−5.72	0.29	0.136	1.115		7.59	−15.29	0.28	−1.064	0.140

TABLE 84

G351.232+0.682 (NGC 6334)

Trans.	S (Jy)	v_{LSR} (km s^{-1})	Δv (km s^{-1})	$\Delta\theta_x$ (arcsec)	$\Delta\theta_y$ (arcsec)	Trans.	S (Jy)	v_{LSR} (km s^{-1})	Δv (km s^{-1})	$\Delta\theta_x$ (arcsec)	$\Delta\theta_y$ (arcsec)
1667 R......	0.50	−7.39	...	0.341	2.383	1667 R......	0.38	−14.14	0.55	−0.978	0.542
	0.38	−8.82	0.44	1.027	1.434	1667 L......	0.87	−9.01	0.60	−0.127	0.215
	1.89	−9.65	0.23	0.730	1.861		0.58	−9.72	0.29	0.516	1.752
	0.38	−13.25	0.47	−0.288	0.279		2.41	−12.60	0.30	0.000	0.000

TABLE 85

G351.416+0.646 (NGC 6334 F)

Trans.	S (Jy)	v_{LSR} (km s^{-1})	Δv (km s^{-1})	$\Delta\theta_x$ (arcsec)	$\Delta\theta_y$ (arcsec)	Trans.	S (Jy)	v_{LSR} (km s^{-1})	Δv (km s^{-1})	$\Delta\theta_x$ (arcsec)	$\Delta\theta_y$ (arcsec)
1665 R......	5.35	−6.08	0.21	1.285	1.147	1667 R......	0.80	−6.61	0.20	1.113	0.627
	0.67	−6.86	0.30	0.716	−2.284		9.39	−8.97	0.29	0.846	0.278
	4.30	−7.77	0.41	0.403	0.629		6.63	−9.47	0.25	0.842	0.101
	3.13	−8.05	0.50	0.650	0.777		3.76	−9.88	0.22	0.349	−0.094
	20.64	−8.50	0.39	0.252	0.631		56.58	−11.11	0.26	0.134	0.065
	7.20	−9.56	0.38	0.719	−0.105		2.37	−12.33	0.47	0.001	−1.247
	6.91	−10.15	0.45	0.682	−0.081	1667 L......	0.92	−7.15	0.41	0.859	0.095
	7.47	−11.18	0.22	0.258	0.121		9.77	−7.87	0.37	0.429	0.154
	31.26	−11.98	0.59	−0.006	−0.040		5.45	−8.54	0.41	0.422	0.312
	40.43	−12.50	0.67	−0.020	−0.154		48.58	−9.25	0.27	0.137	0.075
1665 L......	1.01	−6.35	0.49	0.578	−0.812		37.71	−9.83	0.27	0.033	−0.291
	29.02	−7.41	0.46	0.313	0.041		23.74	−10.35	0.28	0.176	0.127
	182.49	−8.87	0.34	0.000	0.000		2.46	−11.09	0.53	0.009	−1.287
	4.59	−9.69	0.39	0.048	−0.002		0.64	−12.46	0.18	6.515	−1.542
	1.46	−10.32	0.22	0.342	0.096	1720 R......	0.59	−9.76	0.23	−1.104	−0.192
	3.91	−11.01	0.23	0.931	0.875		60.31	−10.59	0.39	−1.047	−0.519
	2.54	−11.89	0.56	0.441	0.770	1720 L......	83.88	−9.85	0.33	−1.045	−0.495

TABLE 86

G351.582−0.352

Trans.	S (Jy)	v_{LSR} (km s^{-1})	Δv (km s^{-1})	$\Delta\theta_x$ (arcsec)	$\Delta\theta_y$ (arcsec)	Trans.	S (Jy)	v_{LSR} (km s^{-1})	Δv (km s^{-1})	$\Delta\theta_x$ (arcsec)	$\Delta\theta_y$ (arcsec)
1665 R......	0.29	−91.91	0.33	−1.936	−1.929	1665 R......	0.52	−100.88	0.30	−3.261	−0.780
	0.45	−93.18	0.29	−0.082	−0.079	1665 L......	2.82	−90.97	0.29	−0.007	0.004
	6.19	−93.86	0.22	0.000	0.000		1.46	−94.80	0.48	−2.217	−1.966
	3.45	−94.81	0.27	−1.293	−1.032		1.05	−95.66	0.29	−1.257	−1.000
	1.13	−95.51	0.29	−1.630	−1.859		2.62	−96.12	0.21	−0.775	−1.672
	0.72	−96.25	0.77	−1.710	−2.021		0.47	−96.58	1.17	−2.077	−1.183
	3.15	−97.62	0.26	−2.066	−1.011		0.93	−97.60	0.34	−2.092	−1.758
	0.83	−98.61	0.60	−2.094	−1.309		1.06	−98.34	0.38	−1.302	−1.126
	1.12	−98.94	0.50	−1.992	−1.692		2.76	−99.02	0.23	−1.336	−1.382
	1.88	−100.08	0.34	−2.076	−0.718		2.04	−100.07	0.35	−2.075	−0.761

TABLE 87

G351.775−0.538

Trans.	S (Jy)	v_{LSR} (km s^{-1})	Δv (km s^{-1})	$\Delta\theta_x$ (arcsec)	$\Delta\theta_y$ (arcsec)	Trans.	S (Jy)	v_{LSR} (km s^{-1})	Δv (km s^{-1})	$\Delta\theta_x$ (arcsec)	$\Delta\theta_y$ (arcsec)
1665 R......	1.34	2.60	0.55	−0.156	−0.690	1665 L......	14.66	−7.55	0.31	0.299	0.682
	3.82	1.88	0.23	−0.377	0.035		4.24	−8.03	0.27	1.480	1.447
	11.84	1.21	0.42	−0.505	−0.548		39.15	−9.24	0.27	1.809	1.499
	3.70	−0.21	0.33	−1.478	−0.798		0.79	−13.55	0.37	−1.149	0.030
	117.68	−1.83	0.35	−0.012	−0.006		3.03	−25.59	0.39	1.195	−0.520
	1.05	−4.30	0.30	0.229	0.700	1667 R......	0.57	2.24	0.35	0.194	−0.696
	0.52	−5.55	0.44	1.210	1.283		1.12	0.25	0.70	−1.604	−0.773
	1.07	−6.06	0.35	0.903	1.327		1.59	−0.17	0.52	−1.605	−0.689
	3.06	−6.66	0.56	1.377	1.371		1.38	−1.84	0.32	−0.611	0.469
	22.25	−7.25	0.27	−0.231	1.553		1.86	−4.95	0.38	0.308	0.768
	6.91	−7.84	1.04	1.426	1.461		2.65	−5.83	0.27	0.481	2.256
	18.42	−9.23	0.28	1.780	1.500		0.93	−7.08	0.37	0.326	1.140
	4.42	−10.15	0.58	1.017	1.110		1.33	−7.89	0.62	0.410	2.845
	2.99	−10.72	0.39	0.968	1.140		6.74	−8.81	0.35	1.682	1.503
	0.40	−12.37	0.24	−1.037	0.026		5.82	−9.01	0.38	1.261	1.303
	0.83	−18.50	1.03	−0.405	0.569		0.70	−9.85	0.46	1.544	1.543
	0.70	−19.27	0.65	−0.384	0.524		0.38	−15.40	0.48	−0.459	0.563
	1.07	−20.28	0.37	−0.397	0.501		0.49	−16.61	0.52	−0.348	0.519
	0.77	−21.22	0.39	−0.355	0.390		0.31	−25.84	0.36	0.992	−0.392
	4.74	−27.85	0.41	1.171	−0.505		4.39	−27.43	0.39	1.217	−0.428
1665 L......	5.72	1.82	0.26	−1.031	0.462	1667 L......	0.34	2.31	0.27	0.138	−0.767
	11.80	1.21	0.49	−0.461	−0.458		1.53	0.37	0.42	−1.569	−0.719
	1.96	0.05	0.26	0.179	−0.672		3.03	−0.67	0.60	−1.713	−0.601
	7.07	−0.49	0.27	0.009	−0.142		9.70	−1.96	0.41	−0.039	0.088
	0.63	−1.09	0.39	−0.632	−0.559		10.38	−5.56	0.26	0.510	2.302
	776.53	−1.94	0.40	0.000	0.000		59.11	−6.96	0.30	0.342	0.787
	0.62	−3.97	0.60	−0.404	0.396		7.80	−7.67	0.32	1.102	1.232
	7.75	−4.72	0.30	0.912	1.193		7.45	−8.80	0.26	1.846	1.641
	11.07	−5.47	0.31	1.271	1.364		1.26	−9.18	0.35	1.785	1.679
	22.45	−6.07	0.29	0.799	1.284		1.92	−9.82	0.26	1.811	1.796
	17.42	−6.25	0.50	0.459	1.436		0.34	−13.24	0.46	−0.943	0.101
	56.07	−6.89	0.37	0.973	1.129		3.14	−26.12	0.36	1.226	−0.428

TABLE 88

G353.410−0.361

Trans.	S (Jy)	v_{LSR} (km s^{-1})	Δv (km s^{-1})	$\Delta\theta_x$ (arcsec)	$\Delta\theta_y$ (arcsec)	Trans.	S (Jy)	v_{LSR} (km s^{-1})	Δv (km s^{-1})	$\Delta\theta_x$ (arcsec)	$\Delta\theta_y$ (arcsec)
1665 R......	0.41	−18.73	0.86	−0.009	−0.003	1665 R......	0.29	−25.19	0.37	−0.070	0.219
	2.18	−19.24	0.89	−0.017	−0.034	1665 L......	0.74	−18.61	0.21	0.039	0.067
	3.30	−19.50	0.47	−0.023	0.001		19.65	−19.56	0.30	0.000	0.000
	2.93	−19.79	0.33	−0.089	0.091		3.55	−20.56	0.28	0.037	−0.021
	7.41	−20.53	0.27	0.088	−0.013						

TABLE 89

G355.345+0.146

Trans.	S (Jy)	v_{LSR} (km s^{-1})	Δv (km s^{-1})	$\Delta\theta_x$ (arcsec)	$\Delta\theta_y$ (arcsec)	Trans.	S (Jy)	v_{LSR} (km s^{-1})	Δv (km s^{-1})	$\Delta\theta_x$ (arcsec)	$\Delta\theta_y$ (arcsec)
1665 R......	0.51	22.78	0.35	−0.082	0.015	1665 L......	17.16	19.72	0.42	0.000	0.000
	0.99	17.70	0.53	0.015	0.031		15.39	18.94	0.73	−0.005	−0.004
	16.27	16.57	0.54	−0.005	−0.002		16.10	18.59	0.77	−0.005	−0.013
	3.00	14.99	0.37	0.025	0.018		6.76	18.01	0.40	0.009	0.008
1665 L......	2.94	20.46	0.55	0.005	0.019		0.32	16.18	0.37	0.155	0.141

TABLE 90

G358.235+0.116

Trans.	S (Jy)	v_{LSR} (km s^{-1})	Δv (km s^{-1})	$\Delta\theta_x$ (arcsec)	$\Delta\theta_y$ (arcsec)	Trans.	S (Jy)	v_{LSR} (km s^{-1})	Δv (km s^{-1})	$\Delta\theta_x$ (arcsec)	$\Delta\theta_y$ (arcsec)
1665 R	0.38	−23.65	1.13	−0.047	0.311	1667 R......	0.44	−24.37	1.07	−0.038	−0.032
	0.35	−25.40	0.54	0.011	0.353		0.43	−25.47	0.51	−0.096	0.026
	1.36	−27.07	0.85	−0.059	0.329		0.52	−26.69	0.67	−0.036	0.004
	1.46	−27.84	0.76	−0.061	0.344		0.50	−26.97	0.85	−0.012	0.028
	0.82	−28.74	0.89	−0.053	0.342		0.61	−28.34	0.54	−0.022	0.078
	0.39	−30.28	0.63	−0.039	0.253		0.62	−30.29	0.49	−0.012	0.068
	0.41	−32.15	0.50	−0.015	0.407		0.69	−30.59	0.49	0.036	0.074
1665 L	0.58	−21.90	0.47	−0.072	0.295		0.73	−31.20	0.56	0.001	0.019
	0.52	−22.45	0.44	−0.029	0.165		0.76	−32.16	0.54	−0.052	−0.003
	0.50	−22.72	0.65	−0.050	0.299		0.68	−32.40	0.51	−0.052	0.007
	1.03	−23.88	0.50	−0.054	0.318	1667 L......	1.12	−24.65	0.32	0.008	0.028
	1.93	−25.48	0.59	−0.030	0.332		1.33	−25.21	0.55	0.011	−0.019
	1.91	−26.20	1.40	−0.022	0.310		3.68	−26.40	0.89	0.000	0.000
	2.12	−26.85	0.80	−0.029	0.342		2.65	−26.92	1.15	−0.012	−0.008
	2.58	−27.64	1.15	−0.044	0.333		1.77	−28.00	0.69	−0.015	0.014
	2.90	−28.34	0.89	−0.045	0.332		1.32	−28.52	0.67	0.009	−0.055
	0.77	−30.02	0.86	−0.051	0.271		1.06	−29.26	0.37	−0.037	0.114
	0.99	−30.56	0.73	−0.022	0.332		1.21	−29.90	0.58	0.033	−0.030
	0.73	−32.12	0.37	−0.006	0.346		1.70	−30.36	0.42	−0.020	0.035
	0.25	−32.99	0.51	−0.073	0.425		1.15	−30.96	0.42	−0.003	−0.031
1667 R	0.34	−21.22	0.36	−0.090	0.194		1.13	−31.45	0.51	−0.044	0.088
	0.46	−22.68	0.46	−0.039	−0.083		1.45	−32.16	0.39	−0.002	0.057
	0.45	−23.34	0.60	−0.012	−0.042		0.92	−32.71	0.39	0.024	0.038

TABLE 91

G359.138+0.032

Trans.	S (Jy)	v_{LSR} (km s^{-1})	Δv (km s^{-1})	$\Delta\theta_x$ (arcsec)	$\Delta\theta_y$ (arcsec)	Trans.	S (Jy)	v_{LSR} (km s^{-1})	Δv (km s^{-1})	$\Delta\theta_x$ (arcsec)	$\Delta\theta_y$ (arcsec)
1665 R......	0.44	−0.08	0.42	−0.453	−0.724	1665 L......	4.72	−0.20	0.38	−0.142	−0.076
	3.18	−1.34	0.65	−0.172	−0.383		8.25	−1.33	0.47	0.000	0.000
	4.84	−2.11	0.49	−0.071	−0.280		0.84	−2.50	0.64	−0.303	−0.217
	2.86	−2.54	0.76	−0.043	−0.037		0.28	−3.43	0.73	−0.127	−0.600
	3.30	−2.99	0.75	−0.133	−0.065		0.28	−3.81	0.41	−0.066	−0.531
	0.44	−3.91	0.90	−0.052	−0.405		0.44	−5.19	1.06	−0.260	−0.280
	0.47	−4.26	0.41	−0.037	−0.644		0.48	−5.63	0.52	−0.207	−0.111
	0.73	−5.65	0.55	−0.221	−0.343		3.03	−6.19	0.31	−0.283	−0.128
	1.42	−6.09	0.29	−0.306	−0.088						

TABLE 92

G359.436−0.103

Trans.	S (Jy)	v_{LSR} (km s^{-1})	Δv (km s^{-1})	$\Delta\theta_x$ (arcsec)	$\Delta\theta_y$ (arcsec)	Trans.	S (Jy)	v_{LSR} (km s^{-1})	Δv (km s^{-1})	$\Delta\theta_x$ (arcsec)	$\Delta\theta_y$ (arcsec)
1665 R......	2.58	−52.12	0.69	0.004	0.027	1665 L......	0.81	−50.91	0.33	−0.013	−0.037
	0.65	−52.78	0.40	−0.015	0.114		4.80	−51.83	0.43	0.000	0.000
1665 L......	0.82	−48.02	...	−5.364	2.965						

TABLE 93

G359.969−0.457

Trans.	S (Jy)	v_{LSR} (km s^{-1})	Δv (km s^{-1})	$\Delta\theta_x$ (arcsec)	$\Delta\theta_y$ (arcsec)	Trans.	S (Jy)	v_{LSR} (km s^{-1})	Δv (km s^{-1})	$\Delta\theta_x$ (arcsec)	$\Delta\theta_y$ (arcsec)
1665 R......	3.84	17.13	0.22	−0.026	−0.159	1665 L......	0.28	17.05	0.33	−0.089	−0.002
	10.38	15.64	0.25	−0.011	−0.024		0.25	16.76	0.48	−0.063	−0.031
	2.58	14.35	0.32	0.021	0.025		4.66	15.68	0.22	−0.008	−0.008
1665 L......	2.21	17.67	0.30	−0.154	−0.323		13.53	14.59	0.32	0.000	0.000

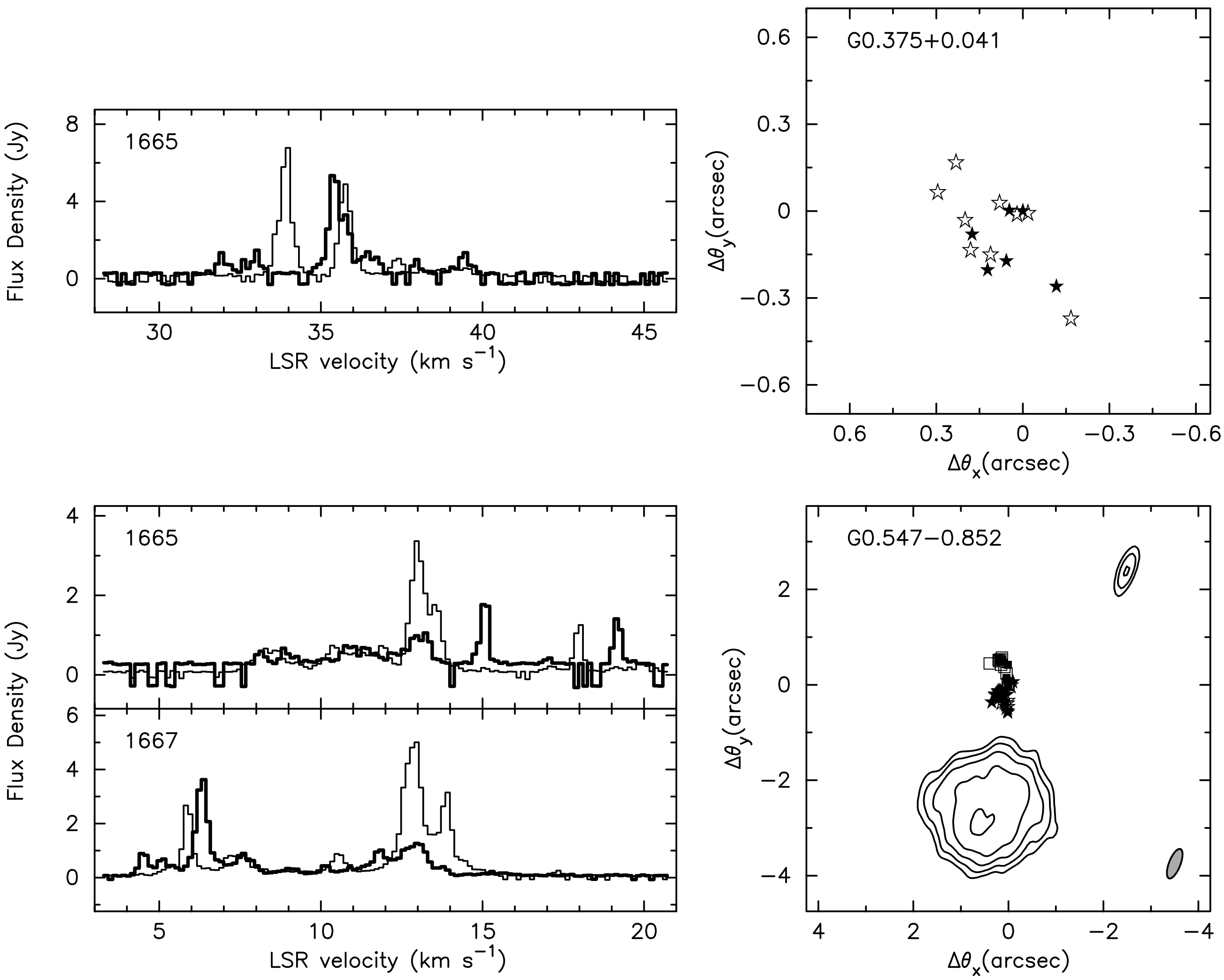

FIG. 2.—Spectra and maps of the sources G0.375+0.041 and G0.547−0.852. (*Left*) Spectra of the ground-state $^2\Pi_{3/2}\,J = 3/2$ OH hyperfine transitions labeled by the transition frequency in MHz. Heavy lines indicate right-circularly polarized (RCP) emission and light lines left-circularly polarized (LCP) emission. These spectra were constructed by assigning to each channel the maximum brightness (either positive or negative) in a region of the map, usually 10″ × 10″, containing the maser emission. The "noise" in these spectra is quantized at $\approx \pm 2.5\ \sigma$ and does not follow Gaussian random statistics. A few strong sources have spurious features, labeled "artifacts," which occur at the LSR velocity of strong features in neighboring sources within the primary beam of an individual VLA antenna. (*Right*) OH maser features superposed on 8.4 GHz continuum maps. The "stars" represent 1665, the "squares" 1667, the "triangles" 1612, and the "circles" 1720 MHz masers. Filled symbols are for LCP emission and unfilled symbols are for RCP emission. See Tables 3–93 for detailed positions, LSR velocities, and line widths for each maser feature. The 8.4 GHz continuum contours start at 4 times the rms noise levels (see Table 2) and increase by factors of 2. The maximum of the lower continuum plot is 10.1 mJy beam^{-1}. The restoring beam is shown as a shaded ellipse in the lower right hand corner. Maps are labeled with offsets from the position of the strongest OH maser feature, whose absolute position is given in Table 1.

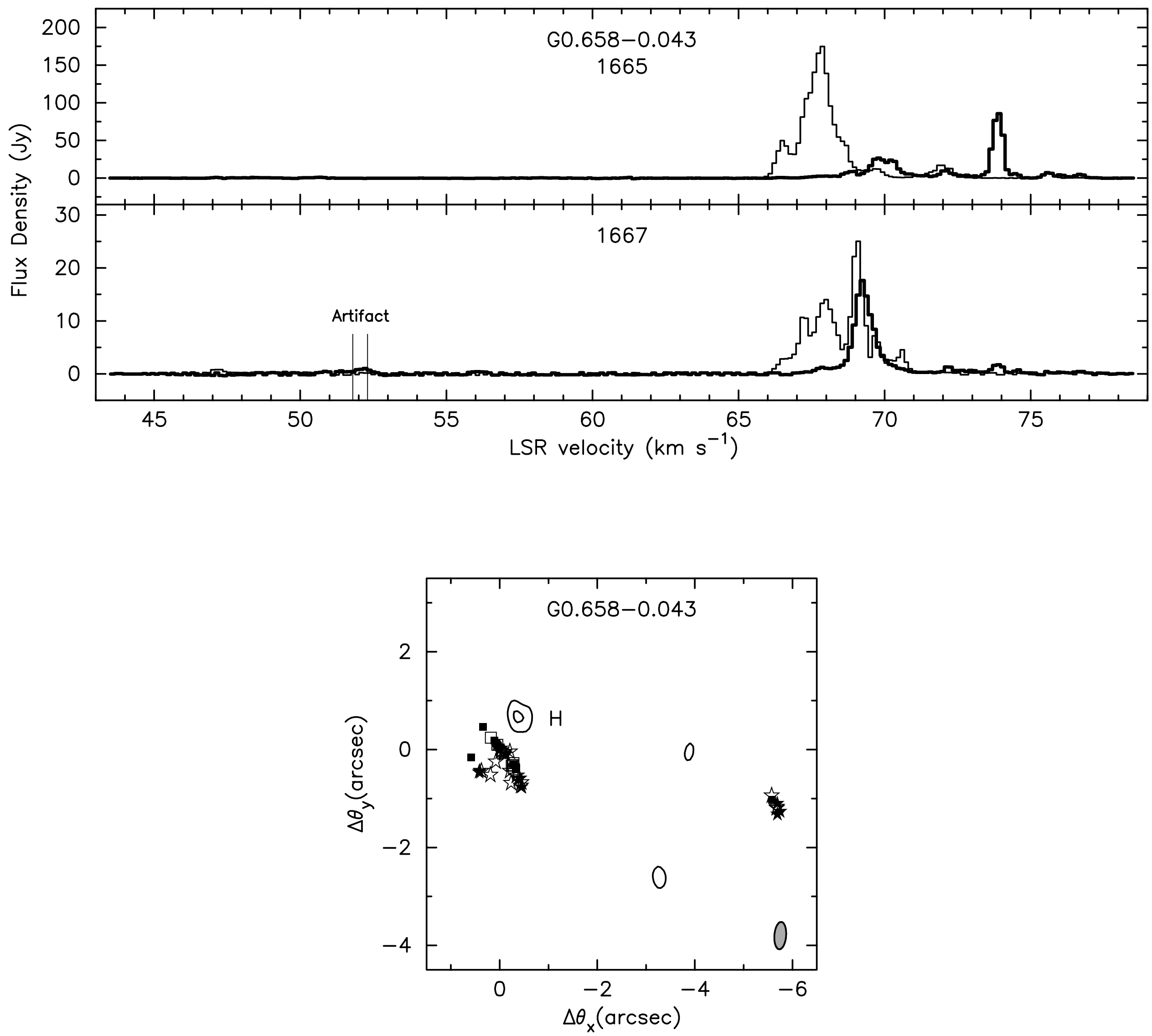

FIG. 3.—Spectrum and map of the source G0.658 − 0.043 (Sgr B2S). See Fig. 2 caption for details. Short (u, v)-spacings (< 50 kλ) were very poorly sampled and therefore omitted in the imaging of the continuum source. Component H was found to have a peak flux density of 18.0 mJy beam^{-1}. See also Benson & Johnston (1984). Note that twice the spectral range of the previous two sources is covered here.

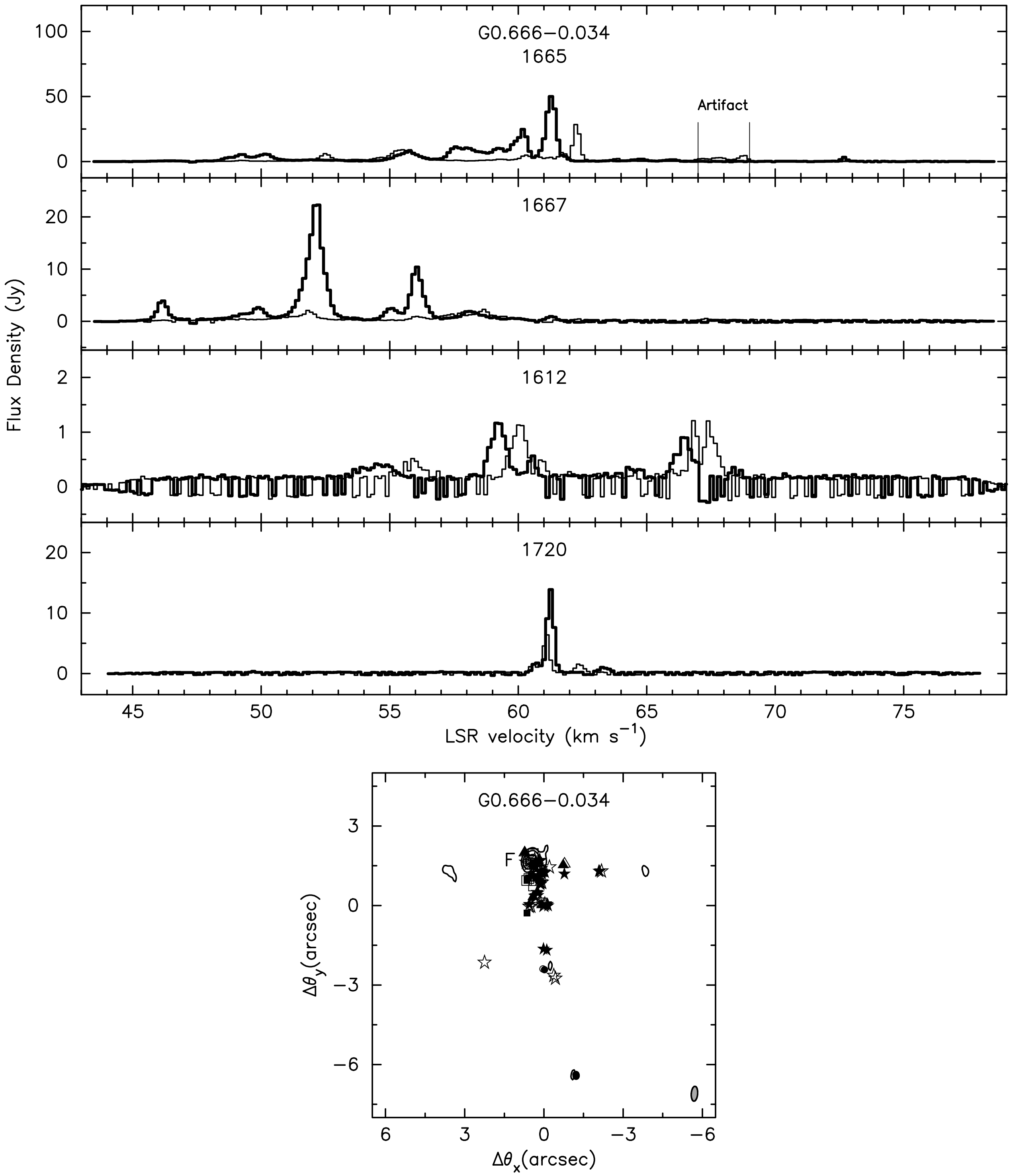

FIG. 4.—Spectrum and map of the source G0.666−0.034 (Sgr B2M). See Fig. 2 caption for details. Short (u, v)-spacings (<50 kλ) were very poorly sampled and therefore omitted in the imaging of the continuum source. Component F was found to have a peak flux density of 76.9 mJy beam^{-1}. See also Benson & Johnston (1984).

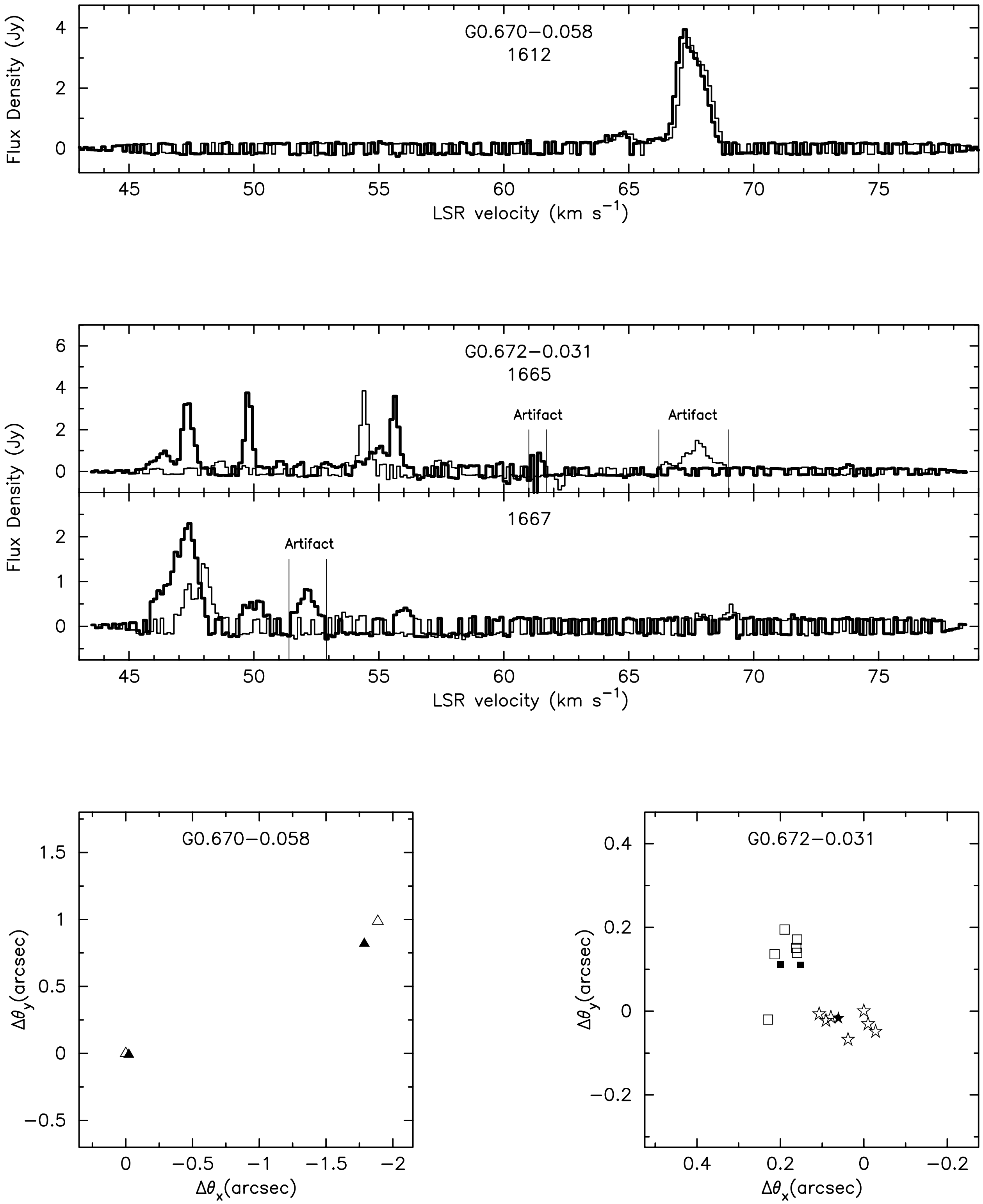

FIG. 5.—Spectra and maps of the sources G0.670 − 0.058 (Sgr B2) and G0.672 − 0.031 (Sgr B2N). See Fig. 2 caption for details. See also Gaume & Mutel (1987).

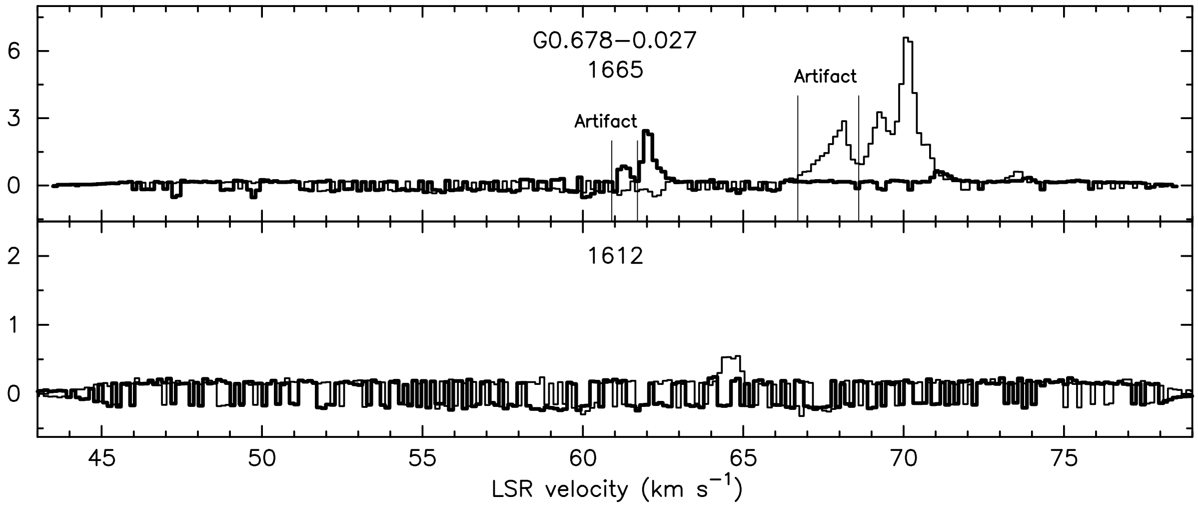

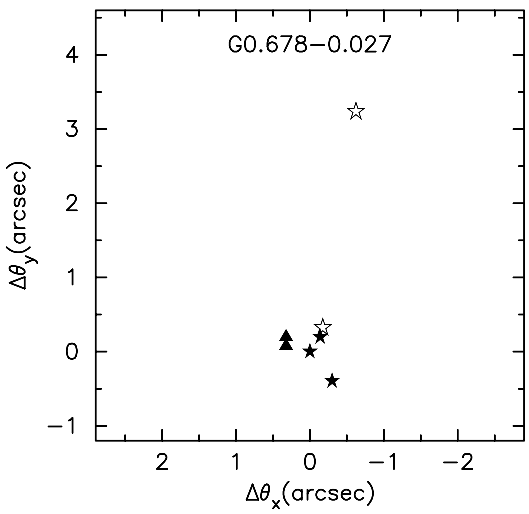

FIG. 6.—Spectrum and map of the source G0.678 − 0.027 (Sgr B2). See Fig. 2 caption for details.

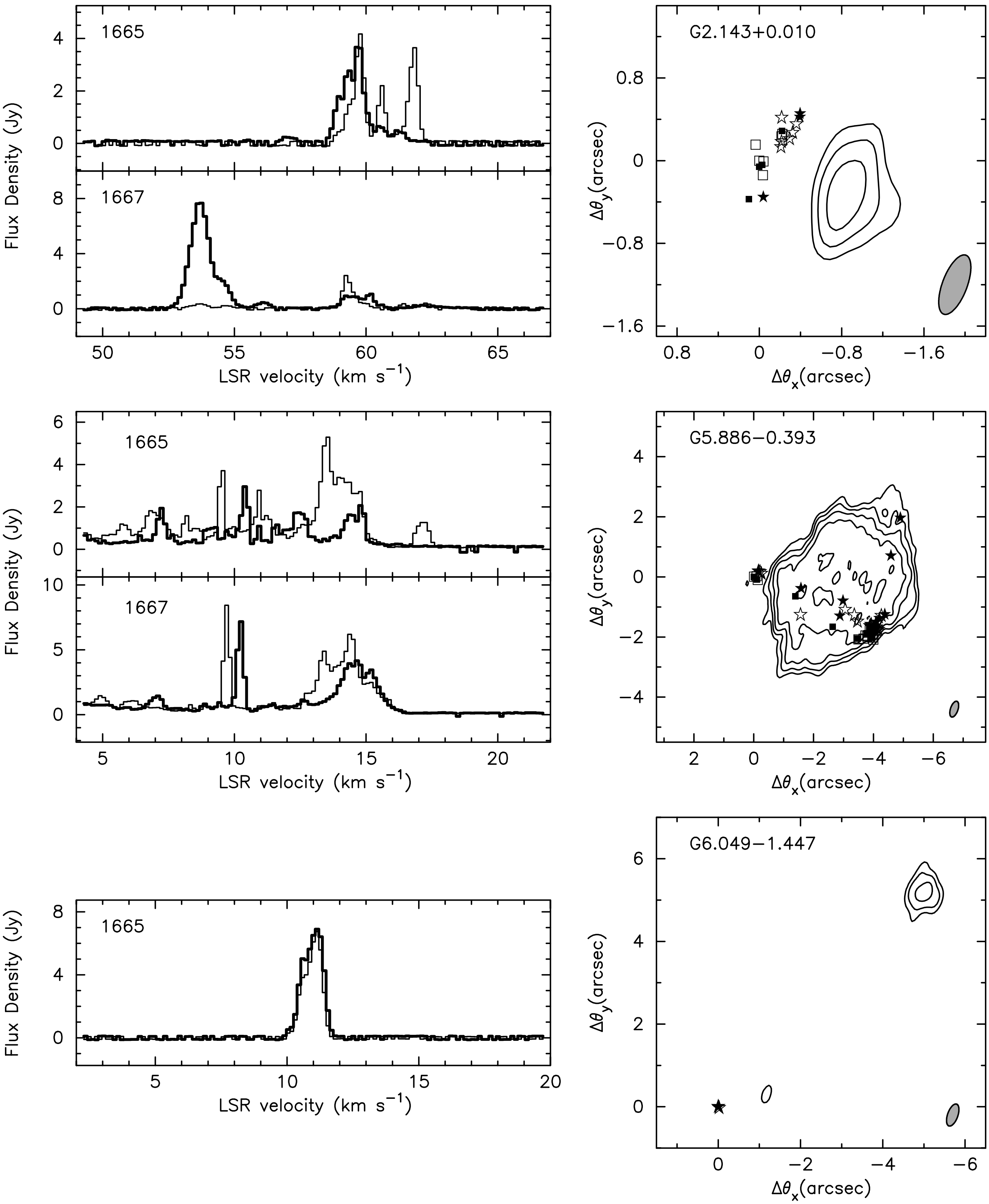

FIG. 7.—Spectra and maps of the sources G2.143 + 0.010, G5.886 − 0.393, and G6.049 − 1.447. See Fig. 2 caption for details. The maxima of the upper, middle, and lower continuum plots are 1.5, 74.9, and 1.9 mJy beam^{-1}, respectively.

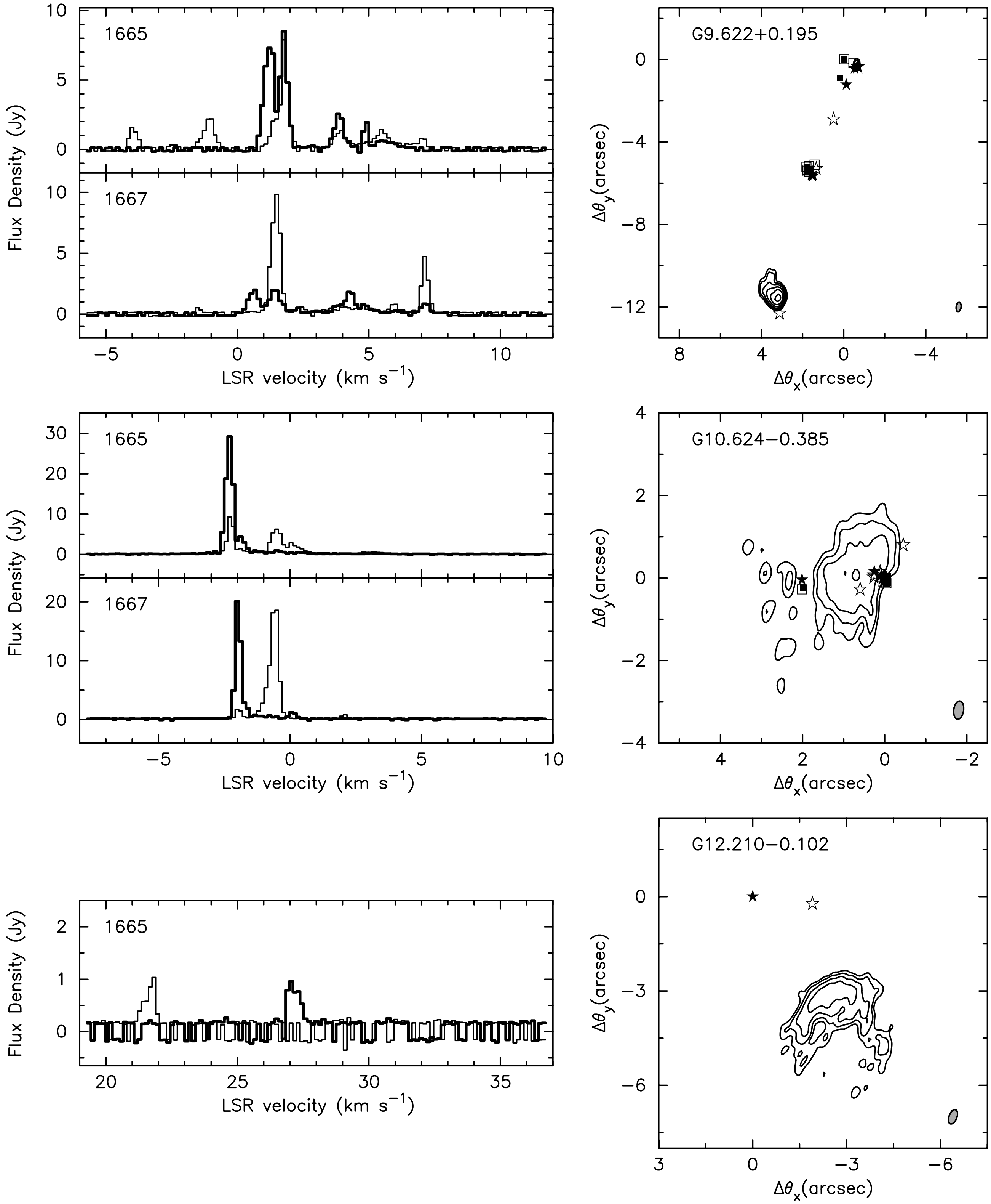

FIG. 8.—Spectra and maps of the sources G9.622 + 0.195, G10.624 − 0.385, and G12.210 − 0.102. See Fig. 2 caption for details. The maxima of the upper, middle, and lower continuum plots are 23.0, 58.3, and 5.9 mJy beam^{-1}, respectively.

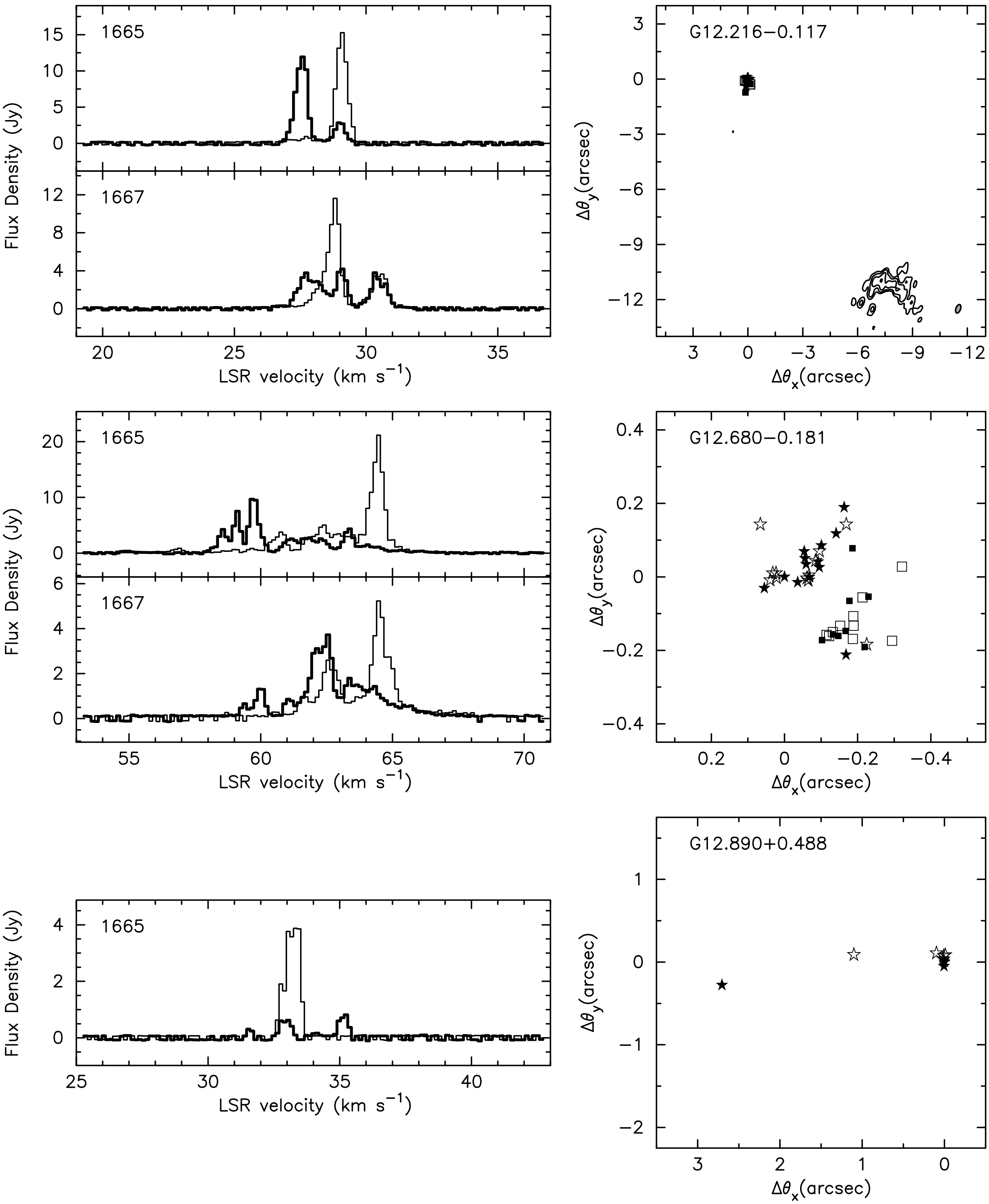

FIG. 9.—Spectra and maps of the sources G12.216 − 0.117, G12.680 − 0.181 (W33 B), and G12.890 + 0.488. See Fig. 2 caption for details. The maximum of the upper continuum plot is 3.8 mJy beam^{-1}.

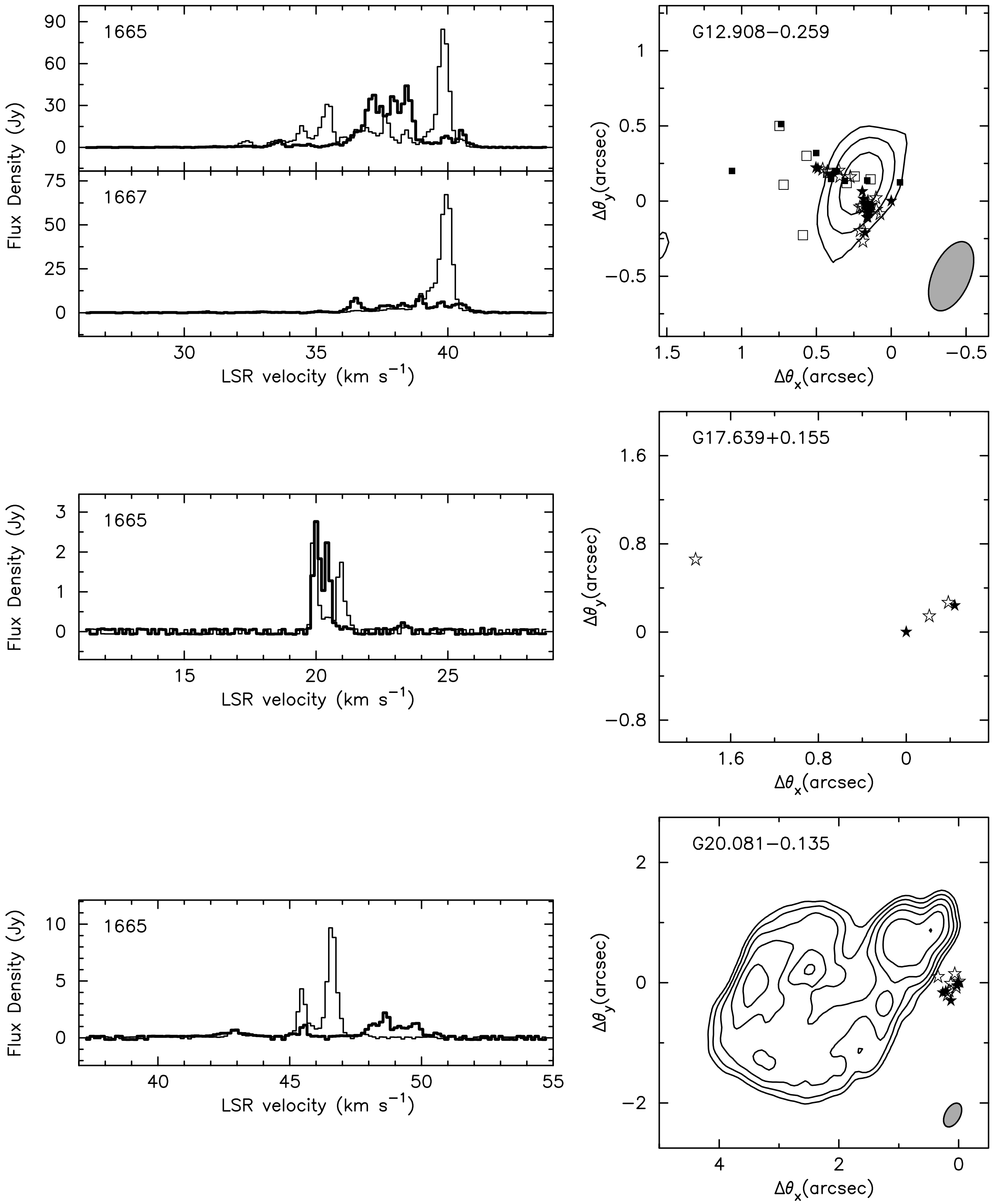

FIG. 10.—Spectra and maps of the sources G12.908 − 0.259 (W33 A), G17.639 + 0.155, and G20.081 − 0.135. See Fig. 2 caption for details. The maxima of upper and lower continuum plots are 0.7 and 33.7 mJy beam^{-1}, respectively. The W33 A continuum source was reimaged from one hour of VLA A array archive data (Ho, 1990 April 18).

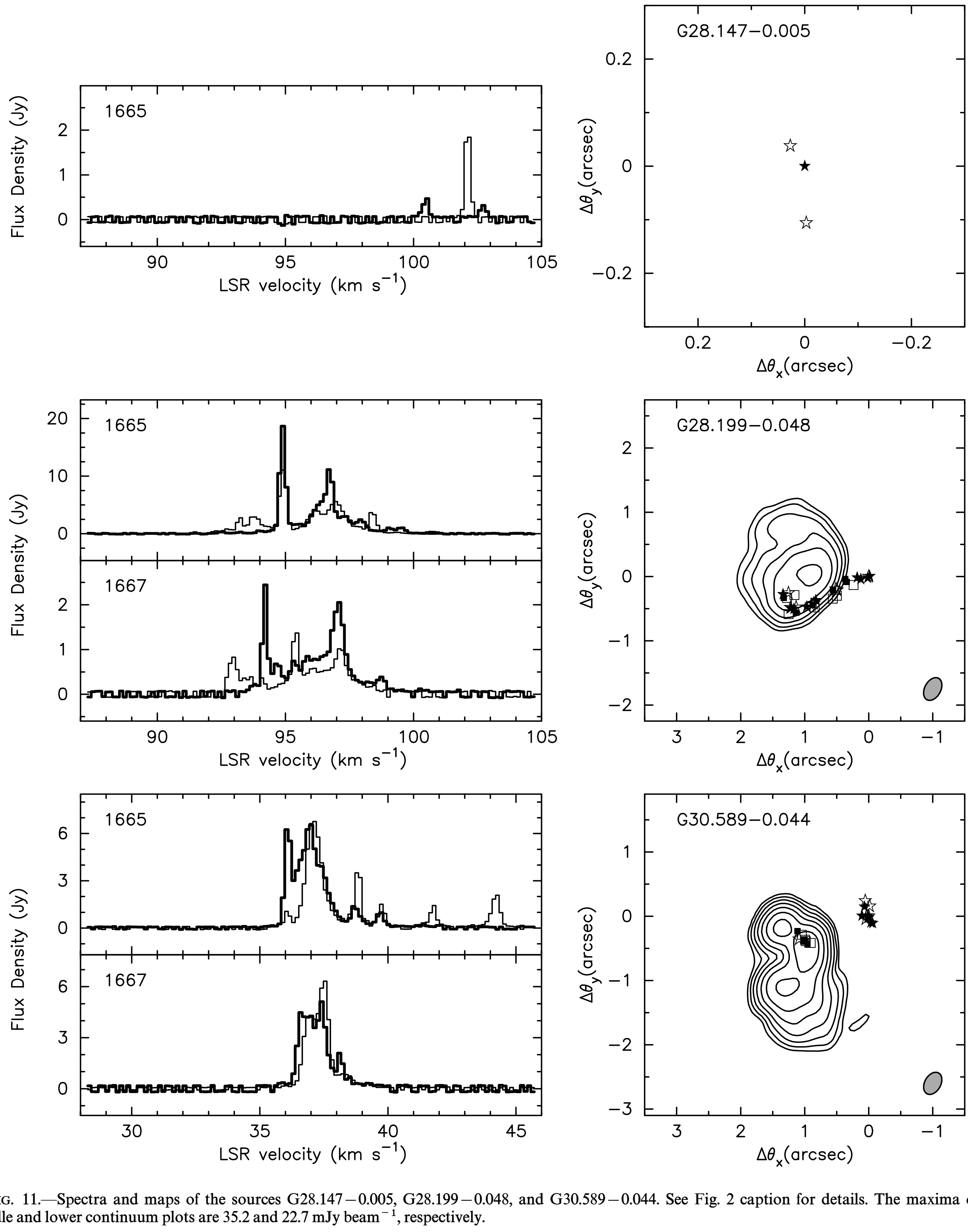

FIG. 11.—Spectra and maps of the sources G28.147 − 0.005, G28.199 − 0.048, and G30.589 − 0.044. See Fig. 2 caption for details. The maxima of the middle and lower continuum plots are 35.2 and 22.7 mJy beam^{-1}, respectively.

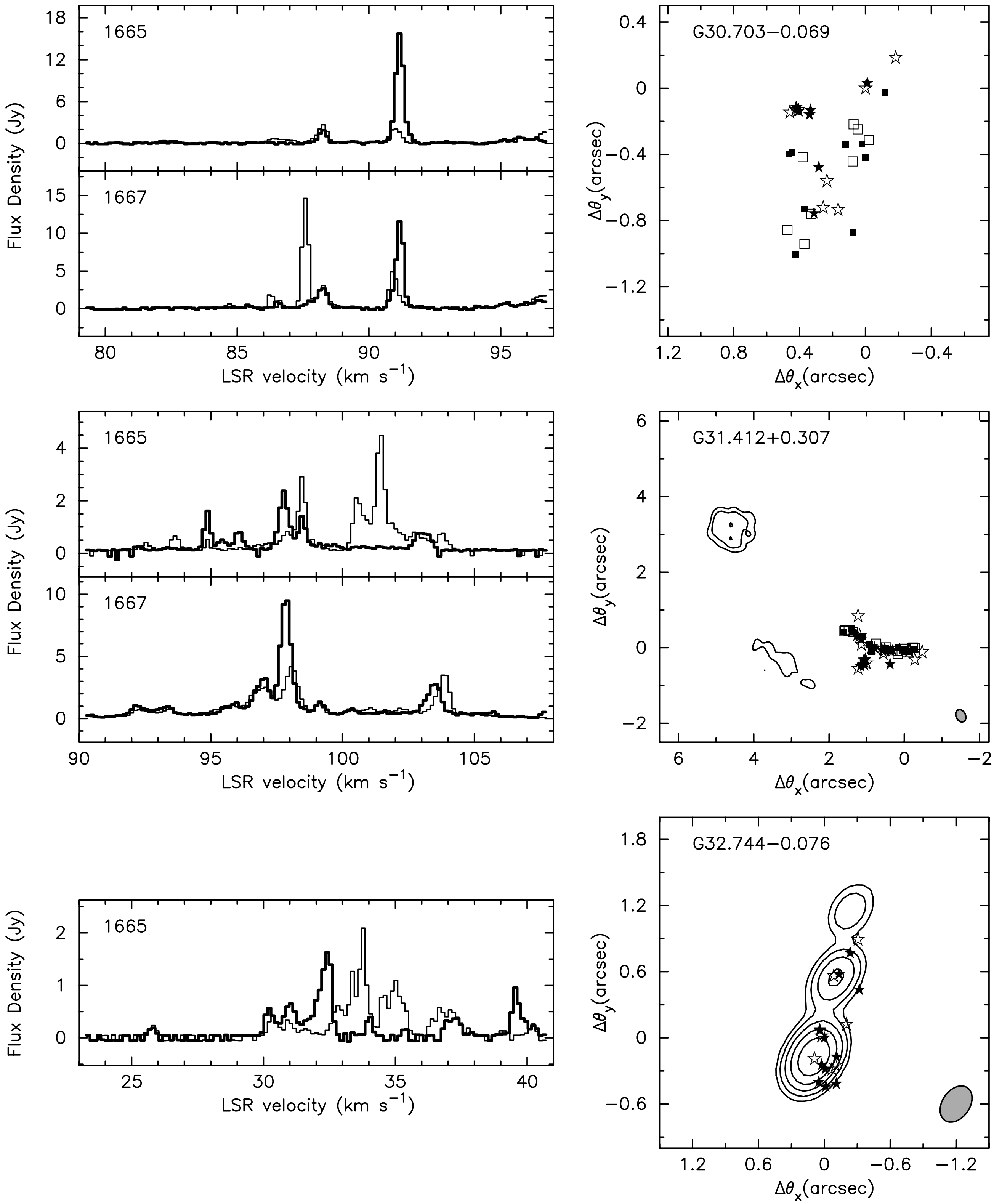

FIG. 12.—Spectra and maps of the sources G30.703 − 0.069, G31.412 + 0.307, and G32.744 − 0.076. See Fig. 2 caption for details. The maxima of the middle and lower continuum plots are 4.2 and 8.5 mJy beam^{-1}, respectively.

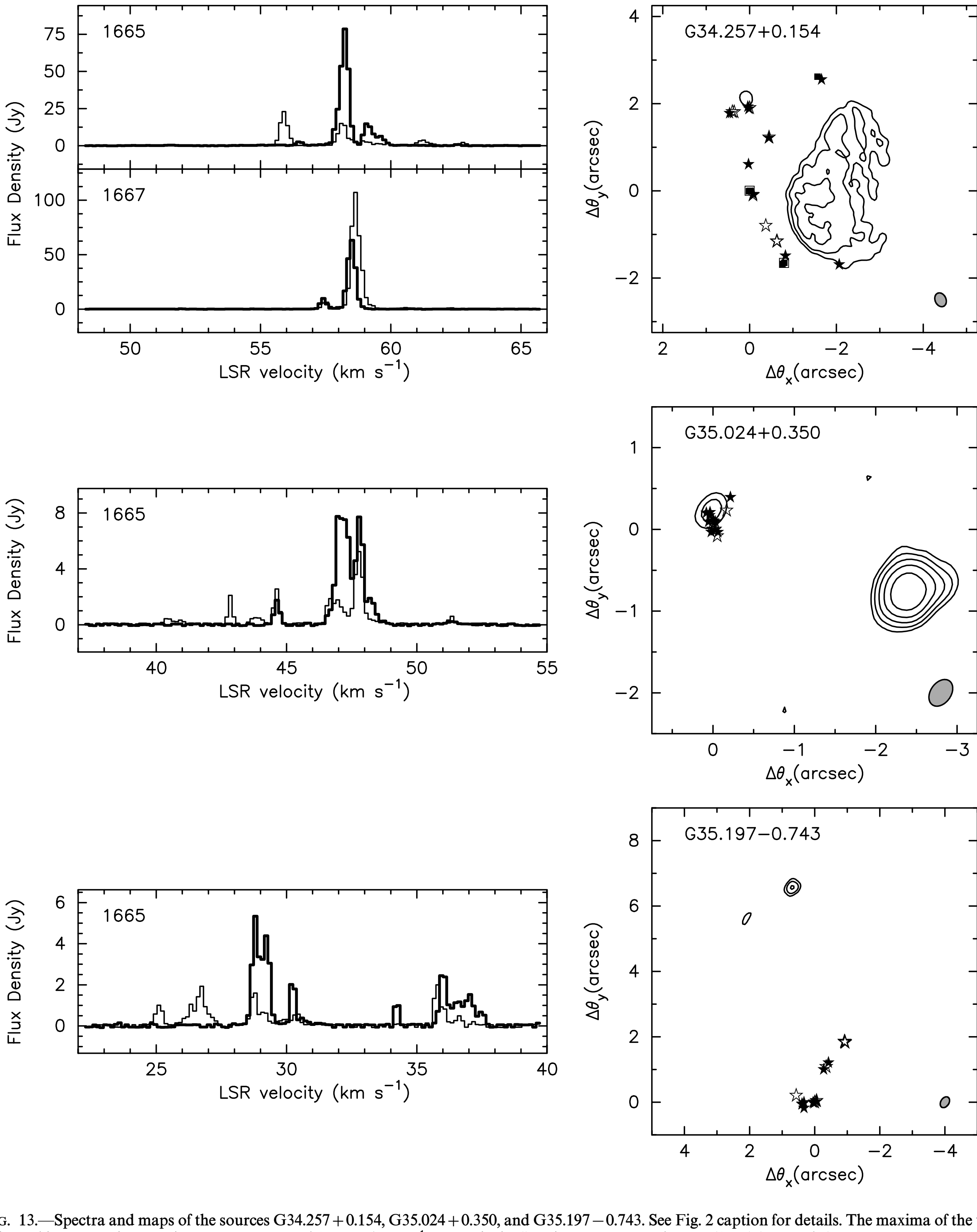

FIG. 13.—Spectra and maps of the sources G34.257 + 0.154, G35.024 + 0.350, and G35.197 − 0.743. See Fig. 2 caption for details. The maxima of the upper, middle, and lower continuum plots are 52.9, 5.8, and 1.2 mJy beam^{-1}, respectively. See also Benson & Johnston (1984) (*upper plot*).

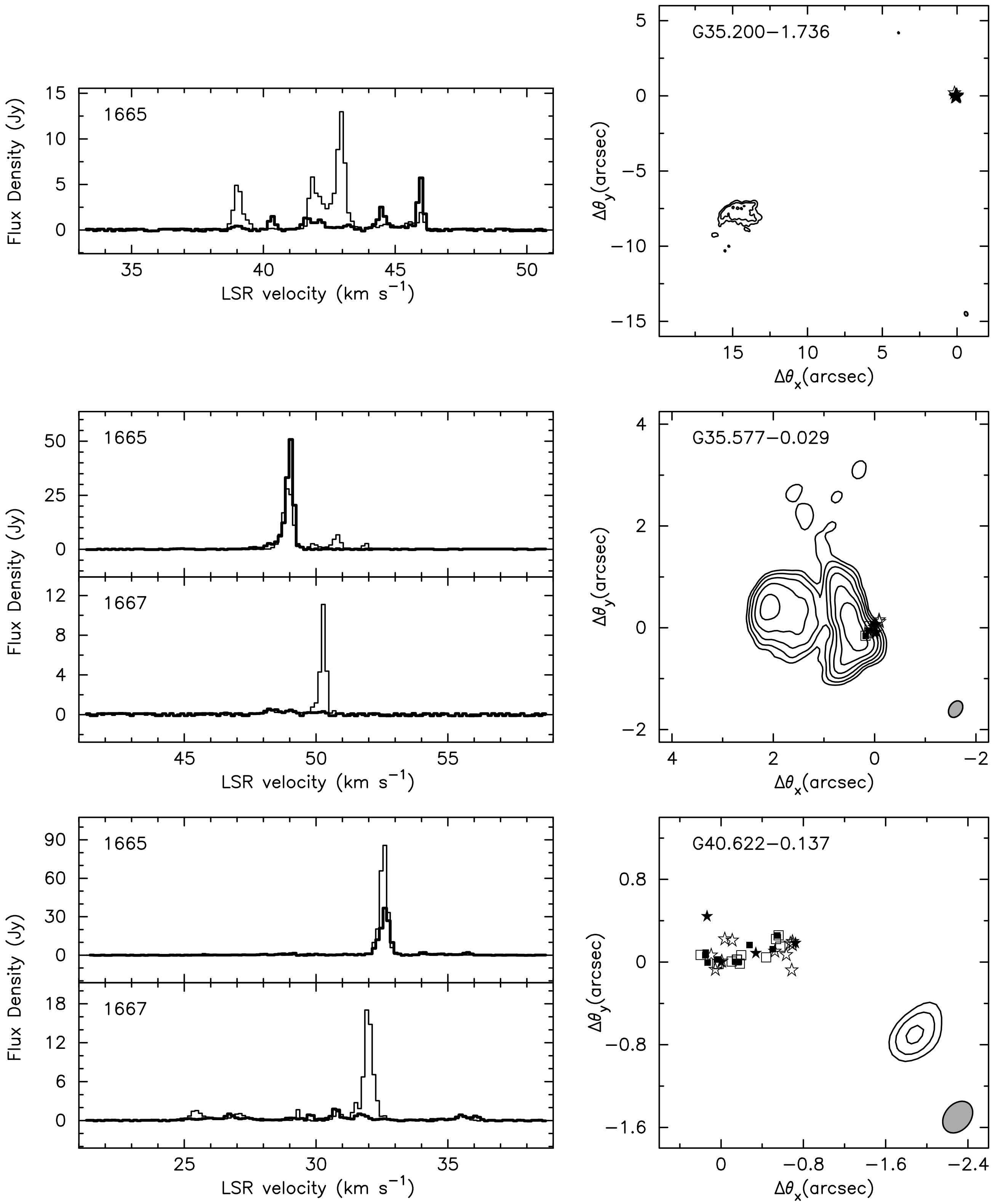

FIG. 14.—Spectra and maps of the sources G35.200 − 1.736, G35.577 − 0.029, and G40.622 − 0.137. See Fig. 2 caption for details. The maxima of the upper, middle, and lower continuum plots are 23.4, 24.6, and 1.4 mJy beam^{-1}, respectively.

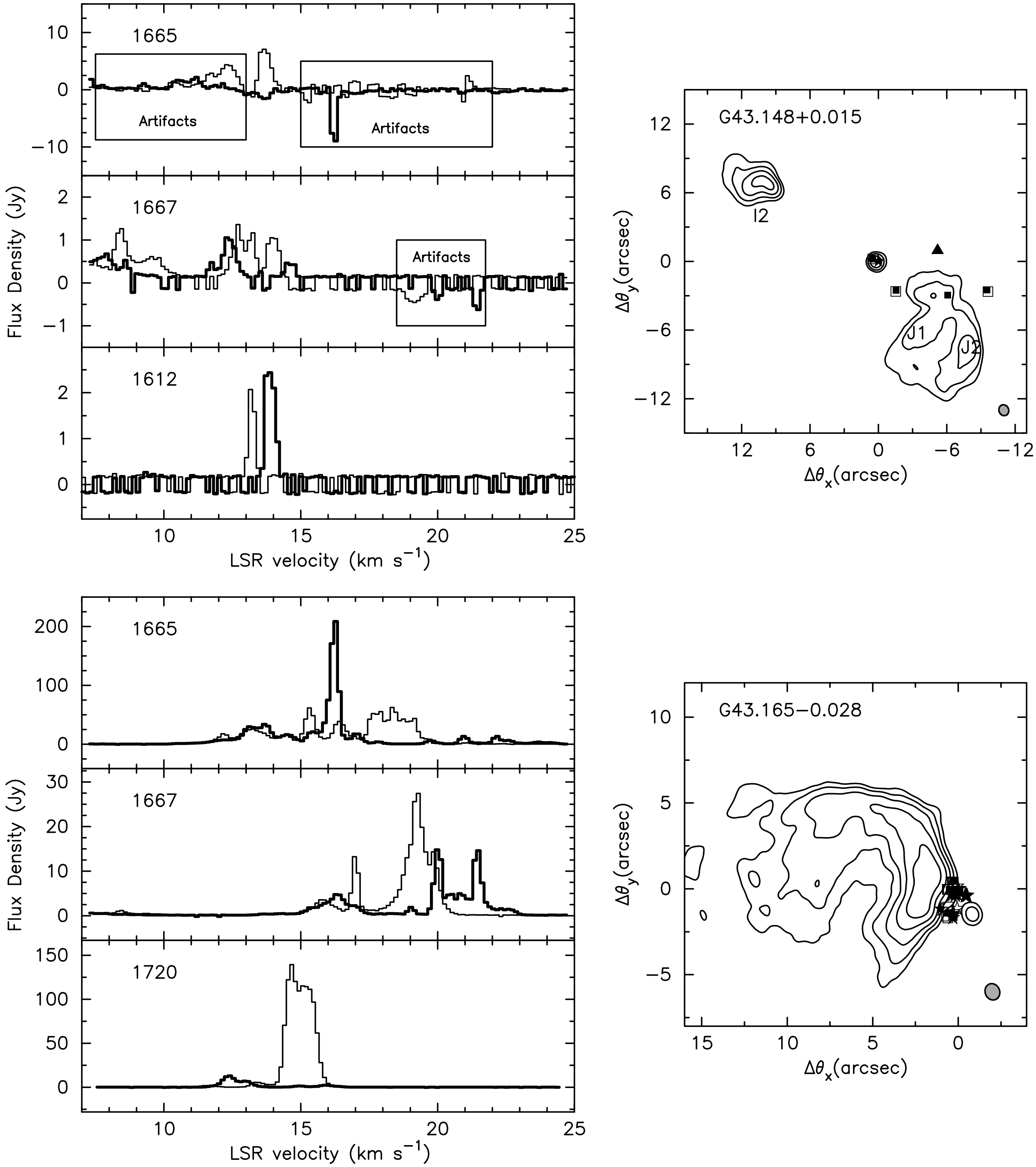

FIG. 15.—Spectra and maps of the sources G43.148 + 0.015 (W49) and G43.165 − 0.028 (W49 S). See Fig. 2 caption for details. The continuum sources were reimaged from 6.5 hr of VLA B array archive data (DePree, 1994 August 27) and the maxima of the upper and lower plots were found to be 116.2 and 196.3 mJy beam^{-1}, respectively. The Components I_2, J_1, and J_2 are labeled in the upper plot. See also Wink & Altenhoff (1975) (*upper plot*) and Gaume & Mutel (1987) (*lower plot*).

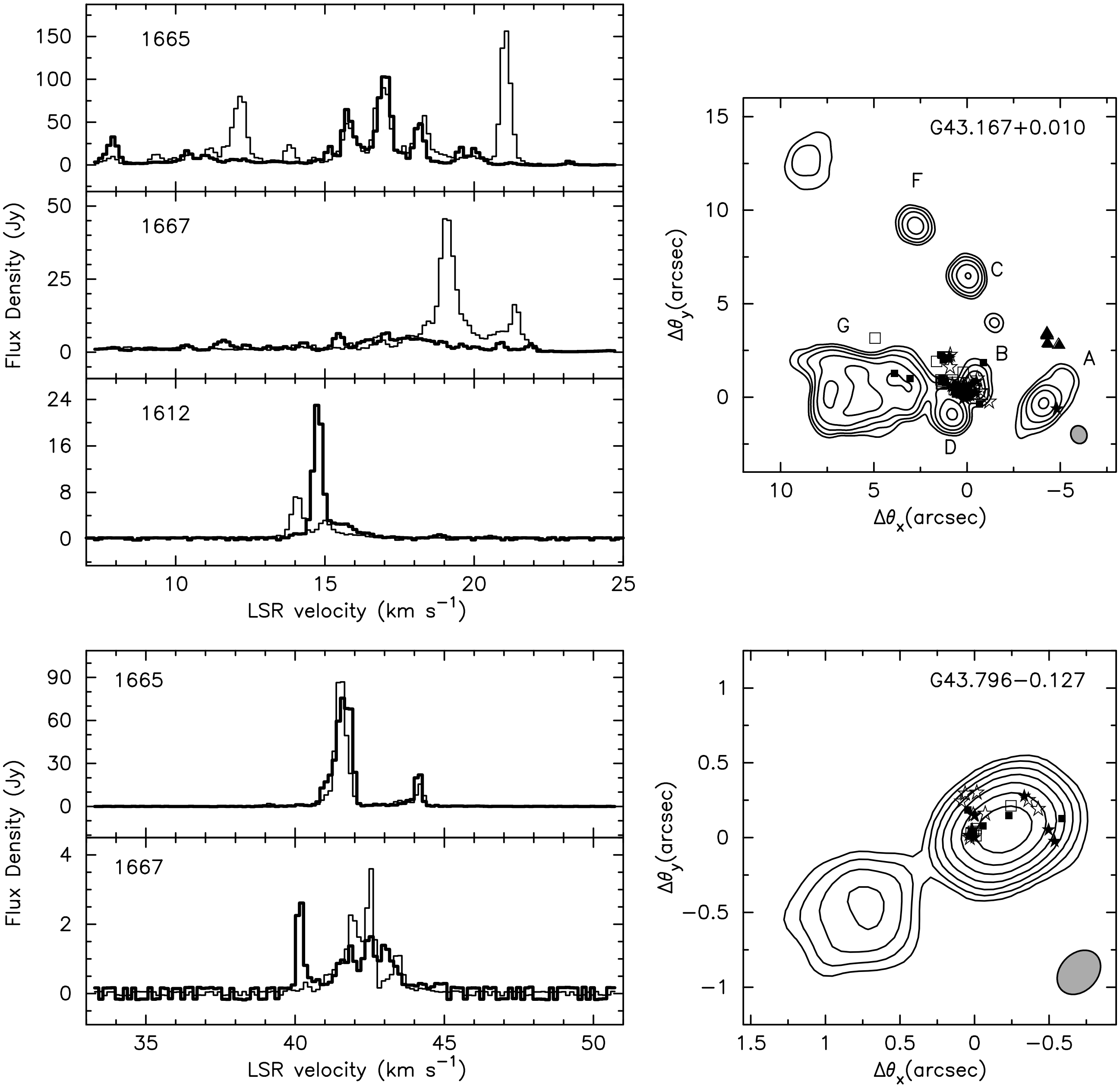

FIG. 16.—Spectra and maps of the sources G43.167 + 0.010 (W49 N) and G43.796 − 0.127. See Fig. 2 caption for details. The W49 N continuum source was reimaged from 6.5 hours of VLA B array archive data (DePree, 1994 August 27) and the maximum was found to be 298.6 mJy beam^{-1}. The components A, B, C, D, F, and G are labeled. See also Dreher et al. (1984). The maximum of the lower continuum plot is 28.7 mJy beam^{-1}.

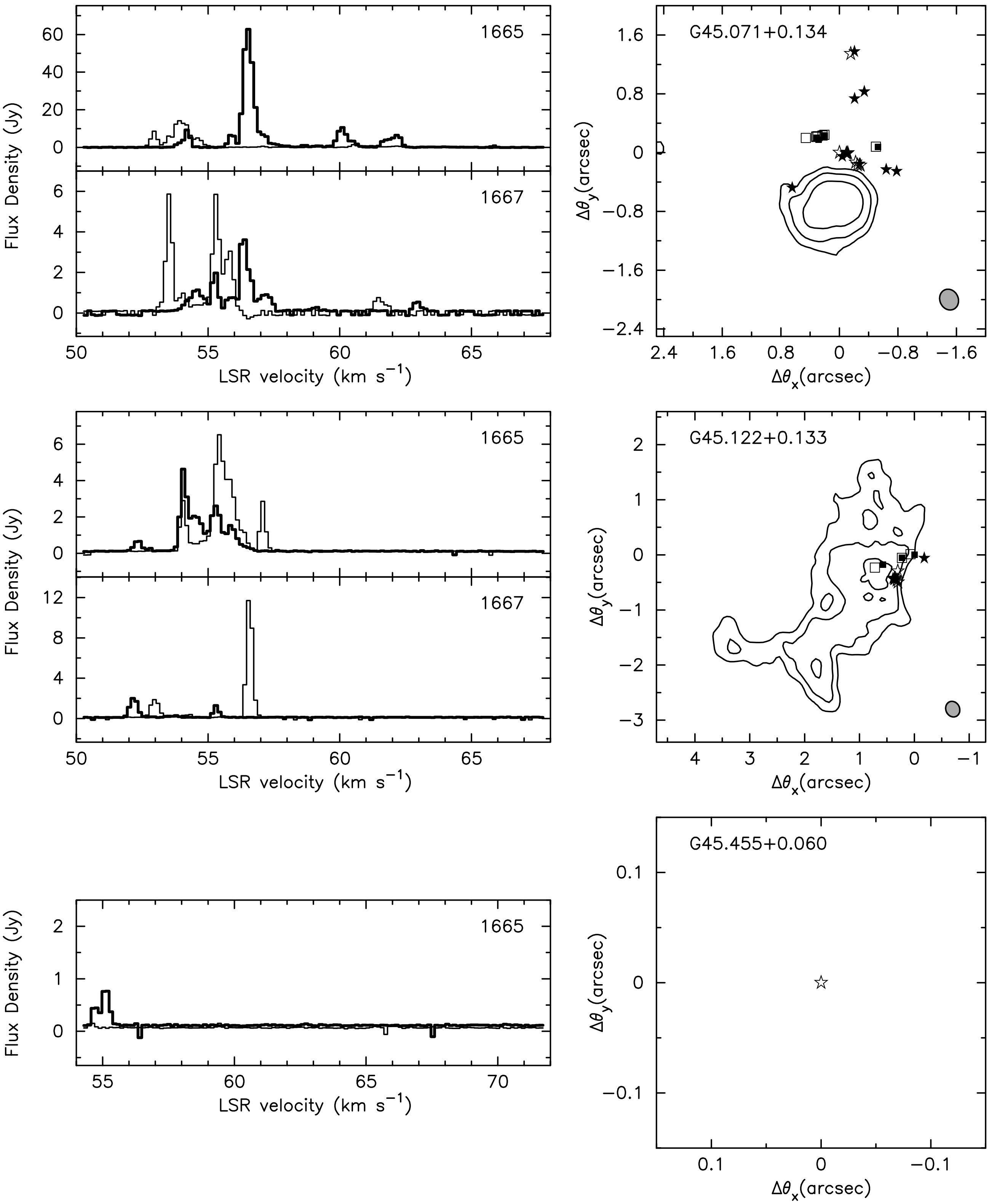

FIG. 17.—Spectra and maps of the sources G45.071 + 0.134, G45.122 + 0.133, and G45.455 + 0.060. See Fig. 2 caption for details. The maxima of the upper and middle continuum plots are 33.8 and 32.6 mJy beam^{-1}, respectively.

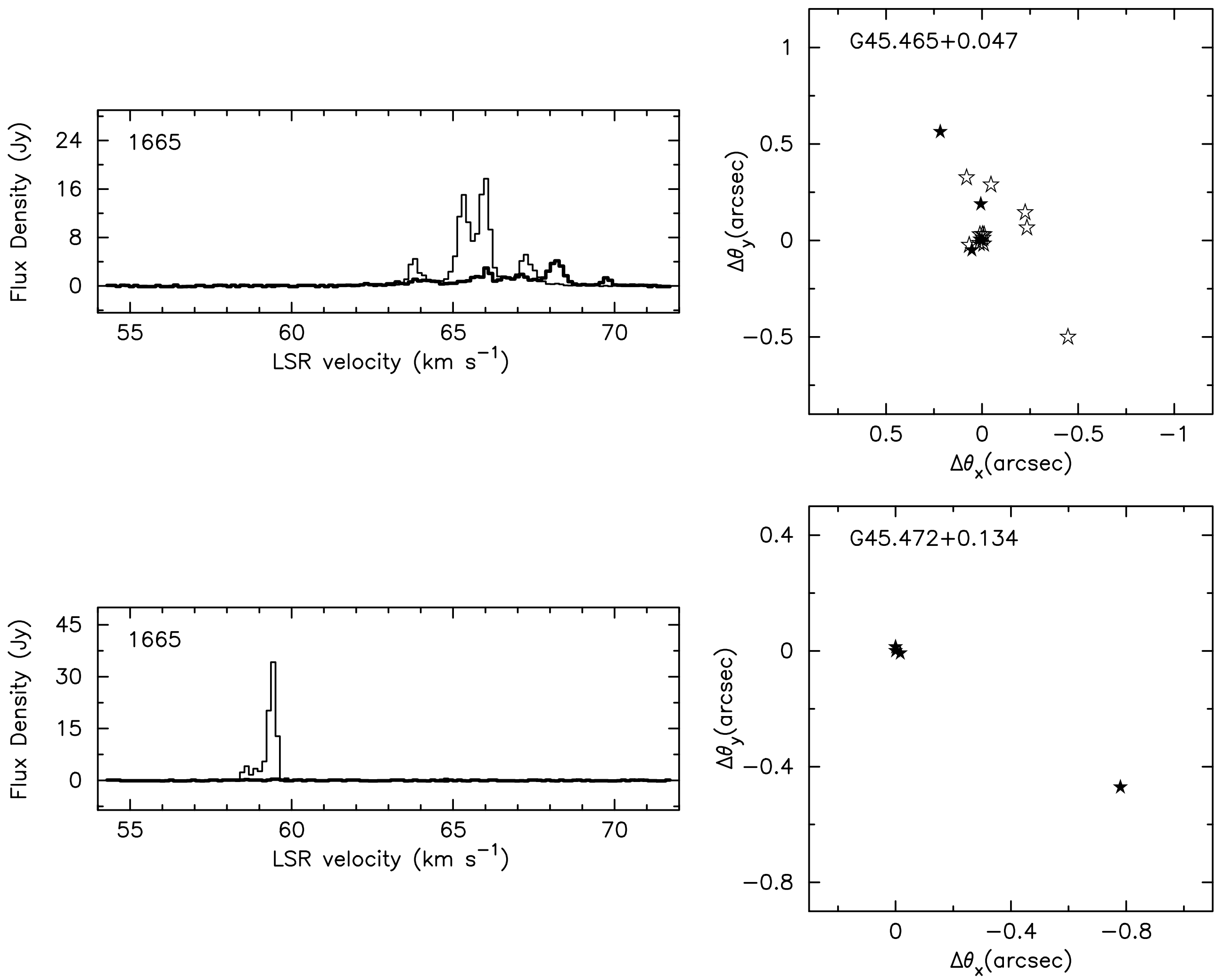

FIG. 18.—Spectra and maps of the sources G45.465 + 0.047 and G45.472 + 0.134. See Fig. 2 caption for details.

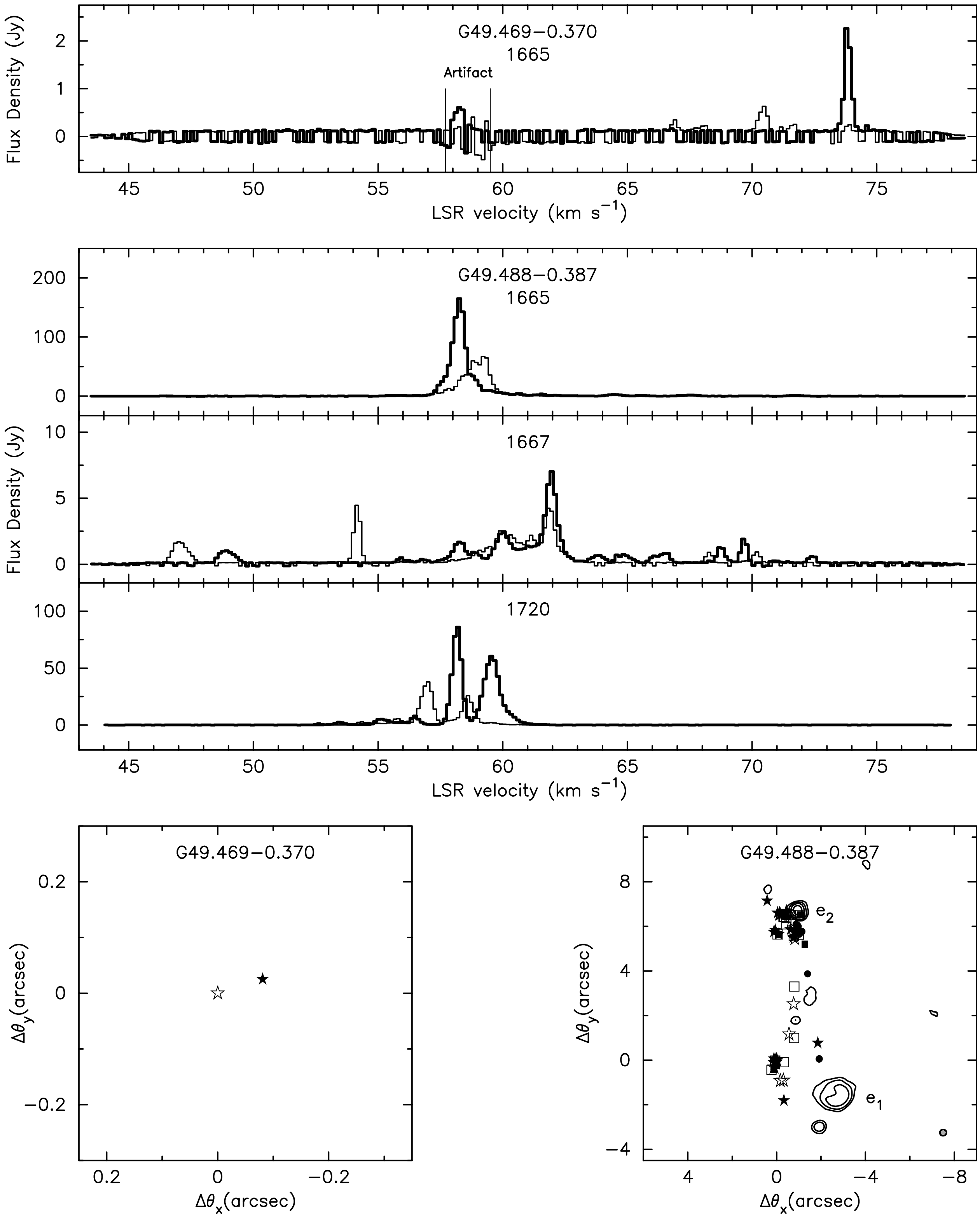

FIG. 19.—Spectra and maps of the sources G49.469−0.370 (W51) and G49.488−0.387 (W51 M, the region associated with "e_2" and W51 S, the region associated with "e_1"). See Fig. 2 caption for details. The G49.488−0.387 continuum source was reimaged from 2 hours of VLA A array archive data (Mehringer, 1992 October 25). Short (u, v)-spacings (<40 kλ) were very poorly sampled and therefore omitted in the imaging of this source. The maximum was found to be 16.7 mJy beam^{-1}. See also Gaume & Mutel (1987).

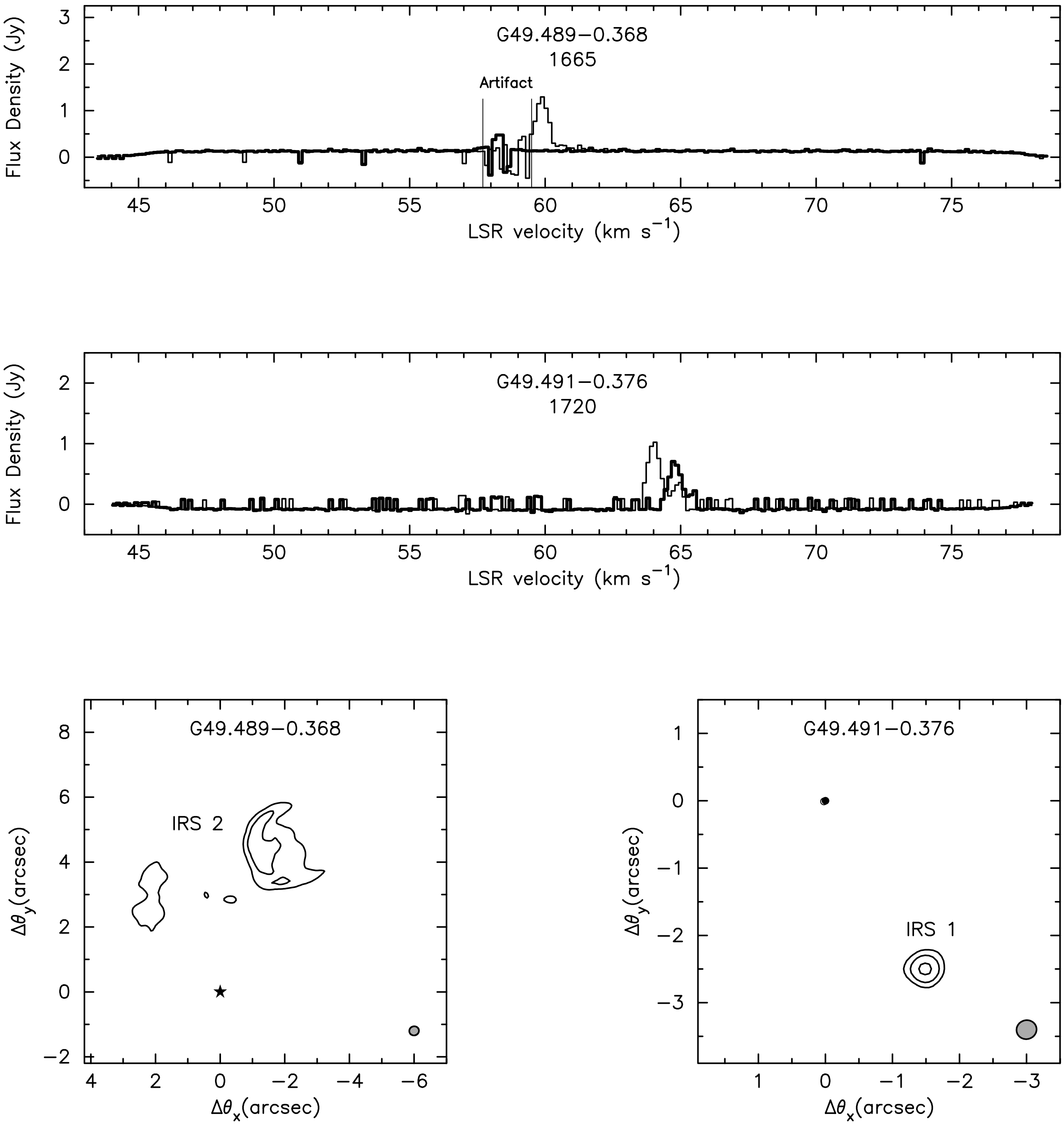

FIG. 20.—Spectra and maps of the sources G49.489−0.368 (W51 N) and G49.491−0.376 (W51). See Fig. 2 caption for details. The continuum sources were reimaged from 2 hr of VLA A array archive data (Mehringer, 1992 October 25). Short (u, v)-spacings (<40 kλ) were very poorly sampled and therefore omitted in the imaging of these continuum sources. The maxima for the left and right continuum plots were found to be 22.9 and 15.0 mJy beam^{-1}, respectively. The components IRS_2 and IRS_1 are labeled. See also Gaume & Mutel (1987).

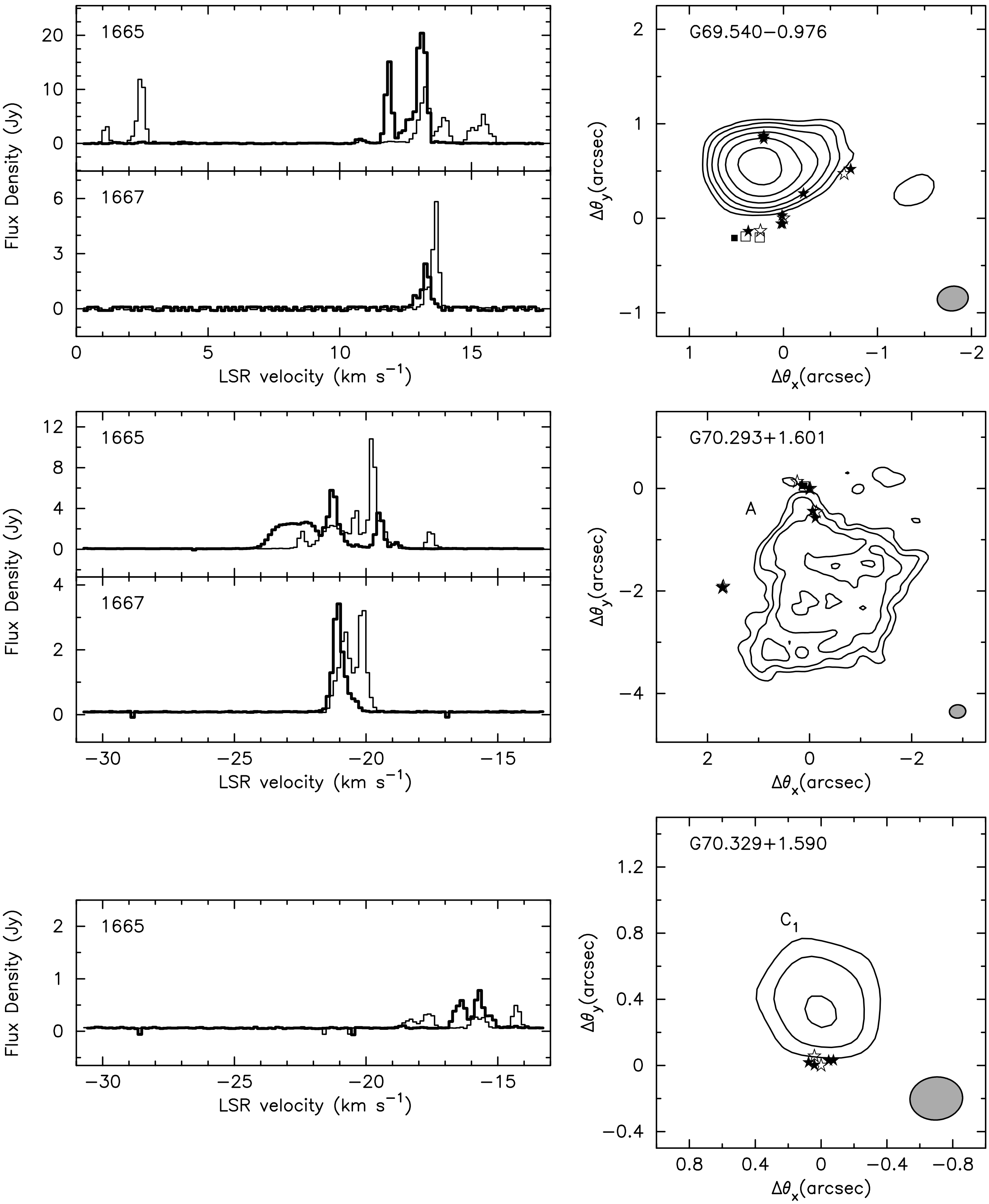

FIG. 21.—Spectra and maps of the sources G69.540 − 0.976 (ON 1), G70.293 + 1.601 (K3–50), and G70.329 + 1.590 (ON 3). See Fig. 2 caption for details. The maxima of the upper, middle, and lower continuum plots are 35.0, 49.7, and 24.3 mJy beam^{-1}, respectively. Components A and C_1 are labeled. See also Forster et al. (1978) (*upper plot*) and Winnberg et al. (1981) (*middle and lower plots*).

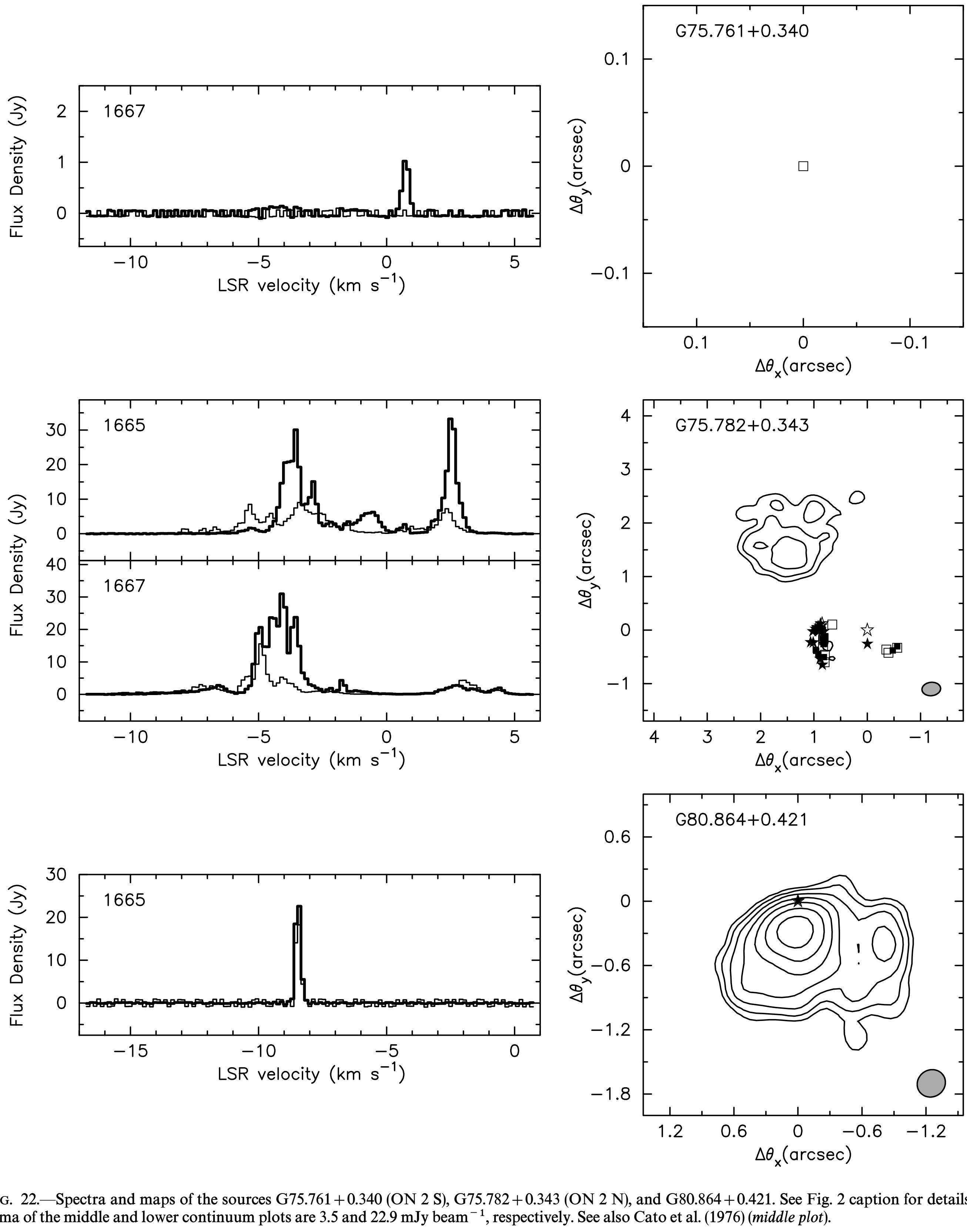

FIG. 22.—Spectra and maps of the sources G75.761+0.340 (ON 2 S), G75.782+0.343 (ON 2 N), and G80.864+0.421. See Fig. 2 caption for details. The maxima of the middle and lower continuum plots are 3.5 and 22.9 mJy beam^{-1}, respectively. See also Cato et al. (1976) (*middle plot*).

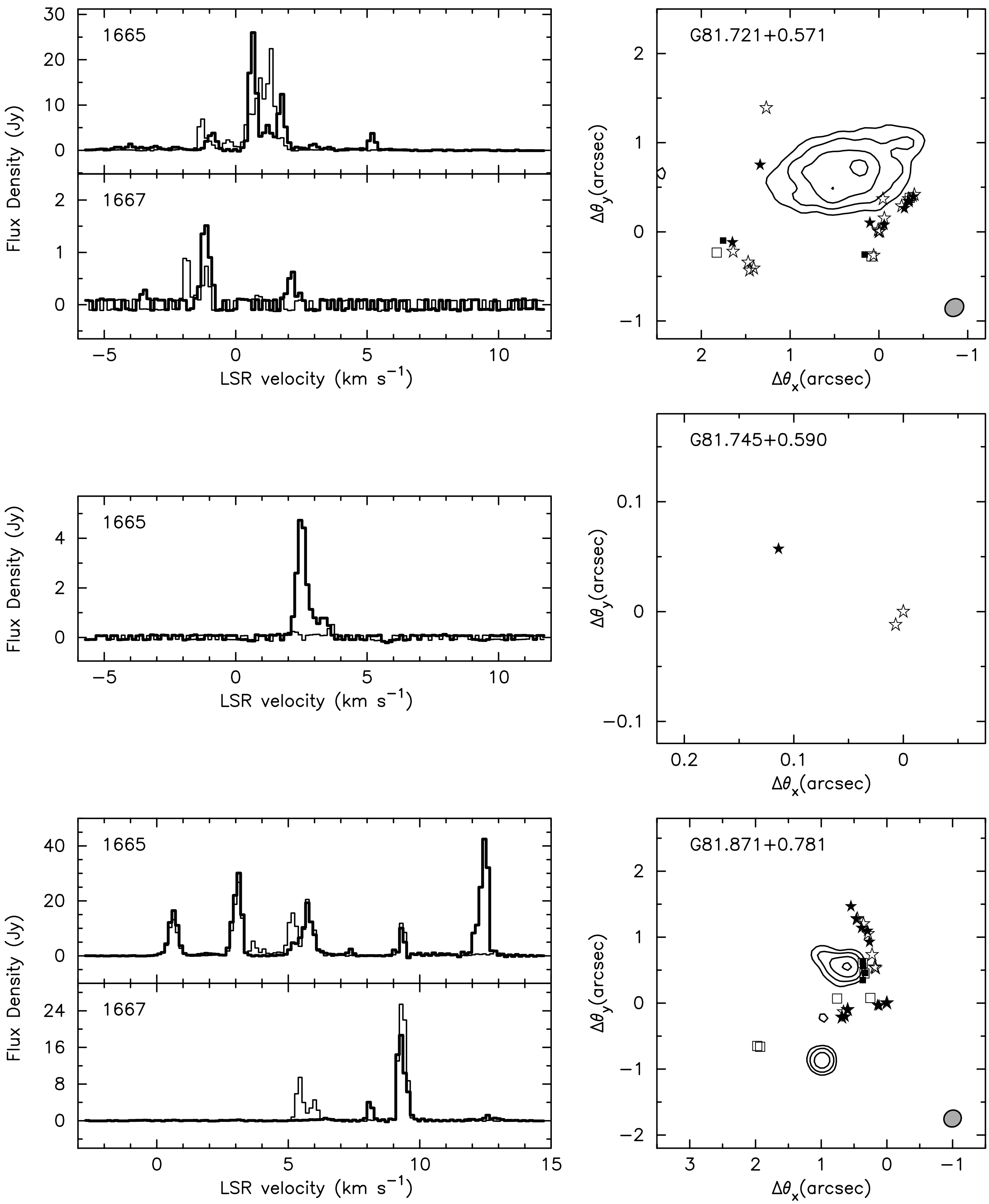

FIG. 23.—Spectra and maps of the sources G81.721 + 0.571 (W75 S), G81.745 + 0.590 (W75), and G81.871 + 0.781 (W75 N). See Fig. 2 caption for details. The W75 S continuum source was imaged from 2.8 hours of VLA A array archive data (Wootten, 1994 April 08), using only 18 antennas. In addition, short (*u*, *v*)-spacings (< 90 kλ) were very poorly sampled and therefore omitted in the imaging of the continuum source. The experiment was plagued with problems, but a compact component of 3.1 mJy beam^{-1} was found. The W75 N continuum source (our observations) was found to have a maximum of 1.7 mJy beam^{-1}.

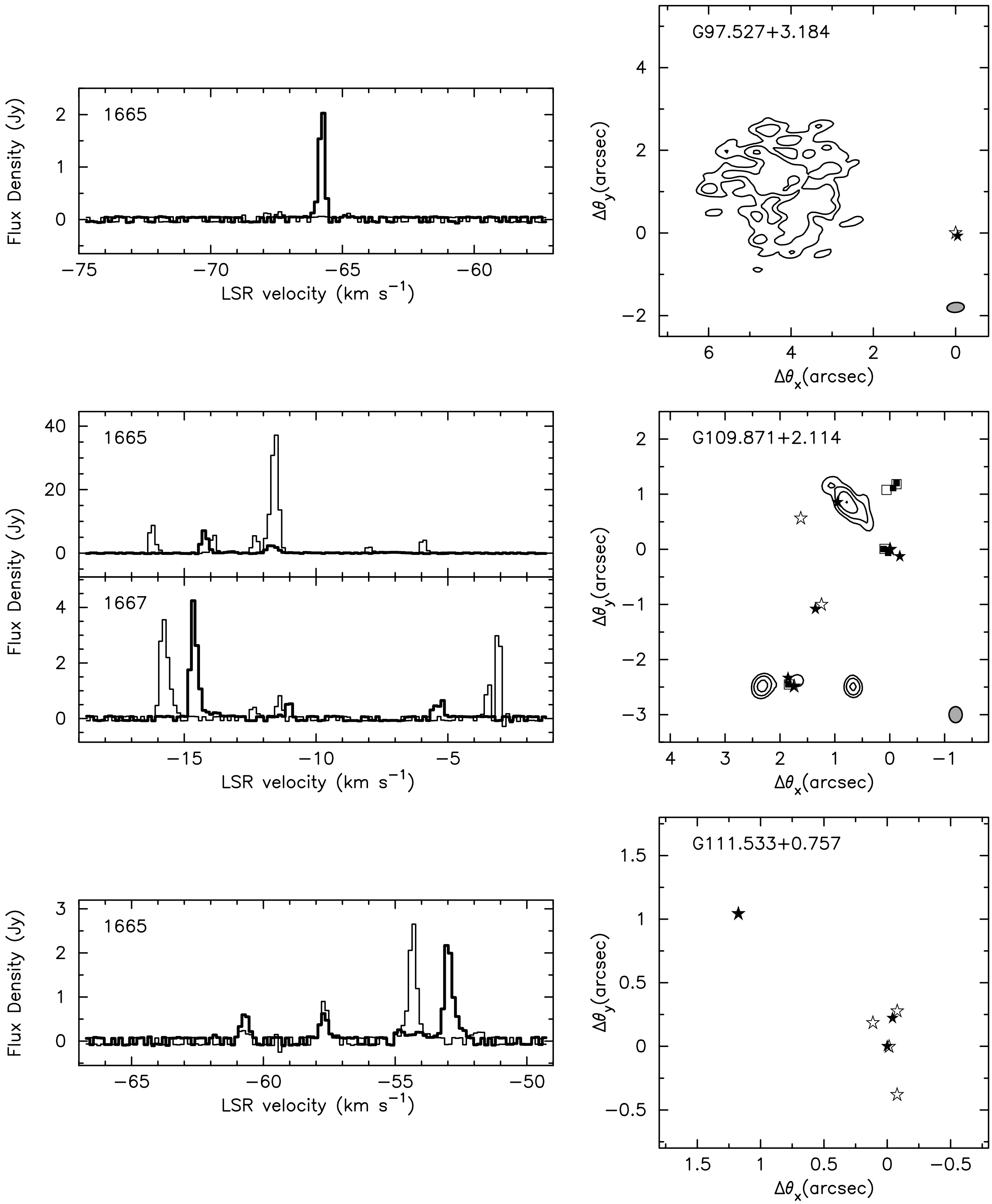

FIG. 24.—Spectra and maps of the sources G97.527 + 3.184, G109.871 + 2.114 (Cep A), and G111.533 + 0.757 (NGC 7538). See Fig. 2 caption for details. The maxima of the upper and middle continuum plots are 0.9 and 3.6 mJy beam^{-1}, respectively. See also Lada et al. (1981) (*middle plot*).

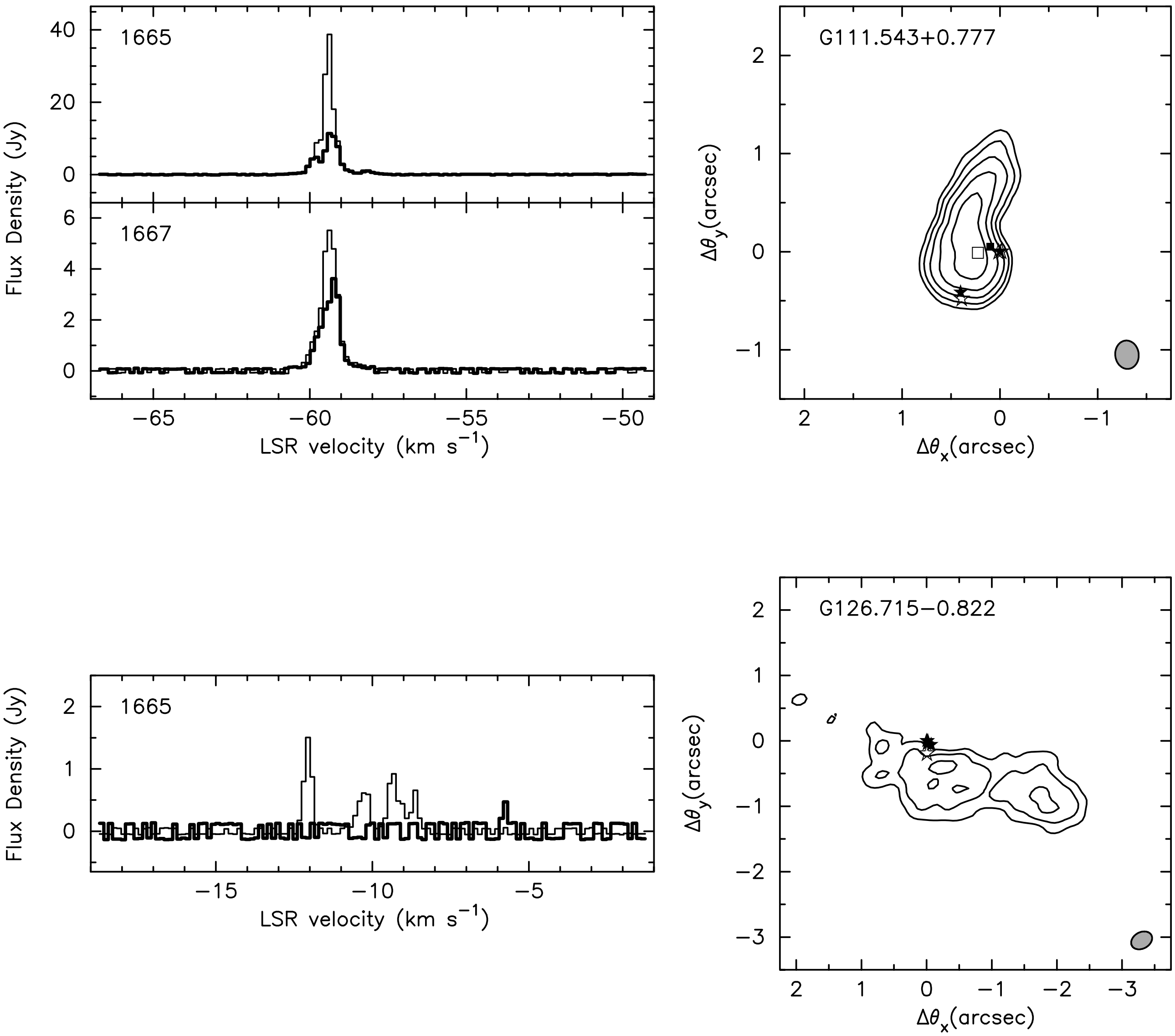

FIG. 25.—Spectra and maps of the sources G111.543 + 0.777 (NGC 7538) and G126.715 − 0.822. See Fig. 2 caption for details. The maxima of the upper and lower continuum plots are 29.2 and 1.5 mJy beam^{-1}, respectively. See also Cato et al. (1976) (*upper plot*).

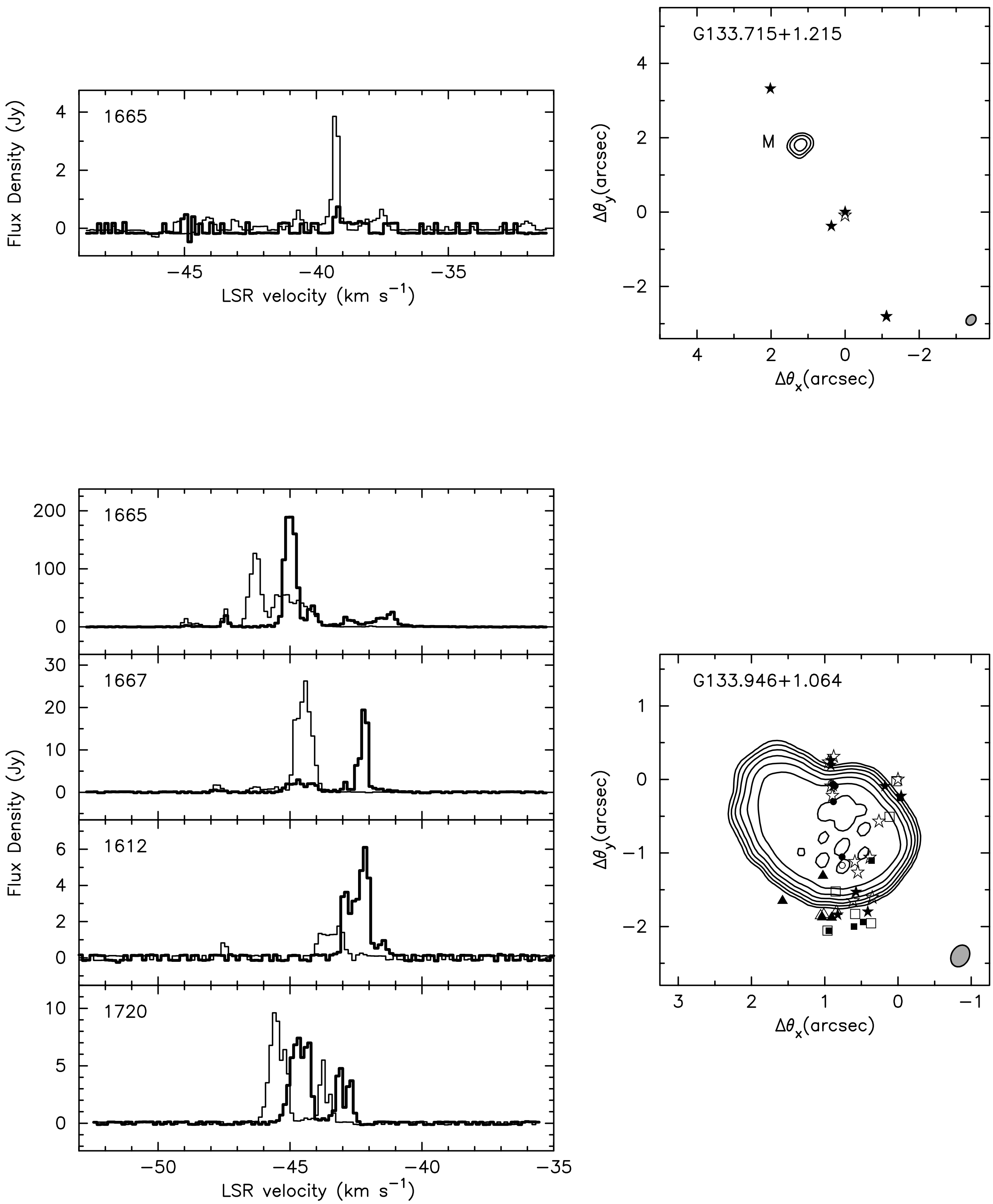

FIG. 26.—Spectra and maps of the sources G133.715+1.215 (W3) and G133.946+1.064 (W3 OH). See Fig. 2 caption for details. Short (u, v)-spacings (<125 kλ) were very poorly sampled for the W3 continuum source and were therefore omitted in the imaging of this source. The maxima of the upper and lower continuum plots are 5.7 and 56.9 mJy beam^{-1}, respectively. Component M is labeled. See also Colley (1980) (*upper plot*).

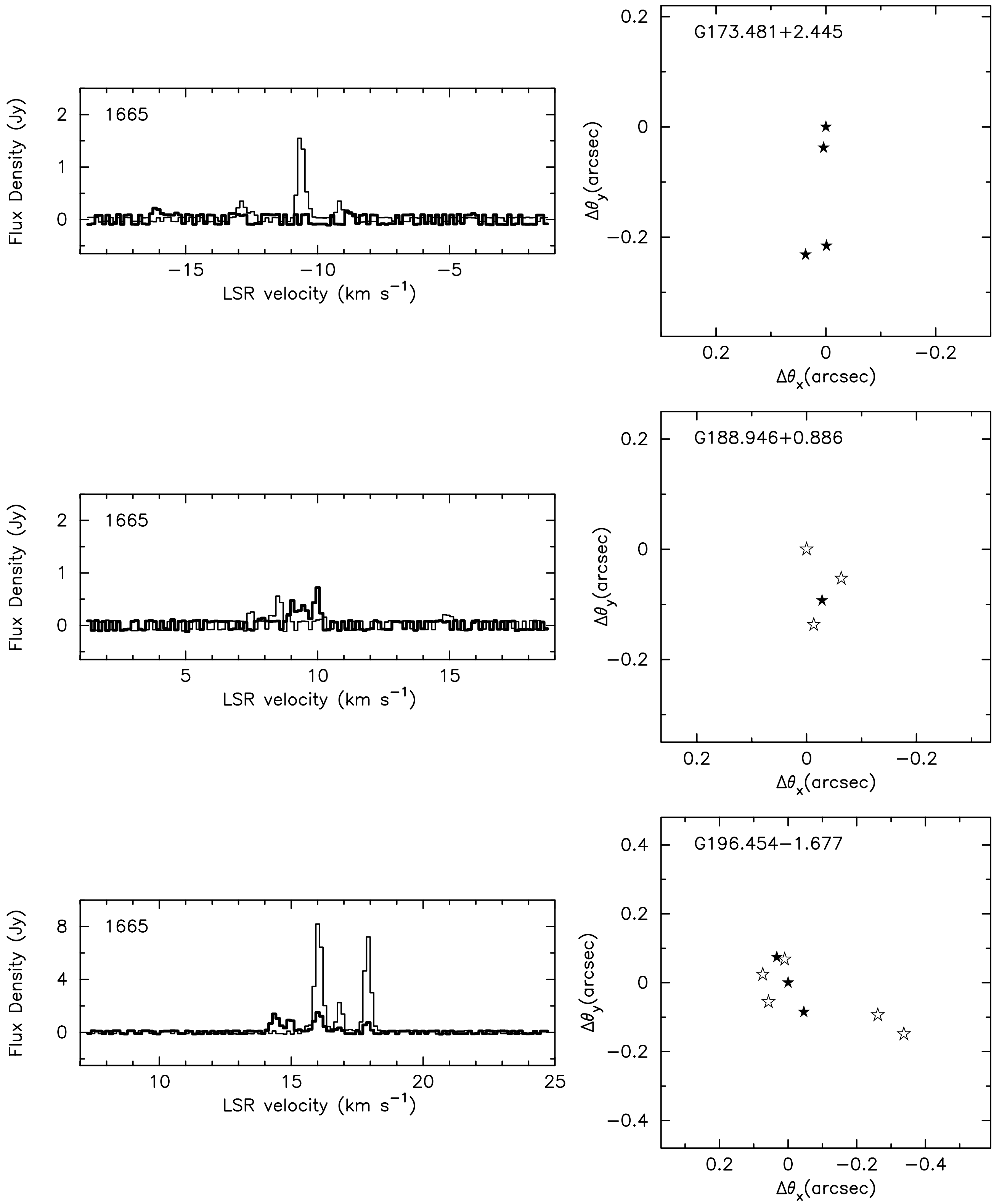

FIG. 27.—Spectra and maps of the sources G173.481 + 2.445 (S231), G188.946 + 0.886 (S252), and G196.454 − 1.677 (S269). See Fig. 2 caption for details.

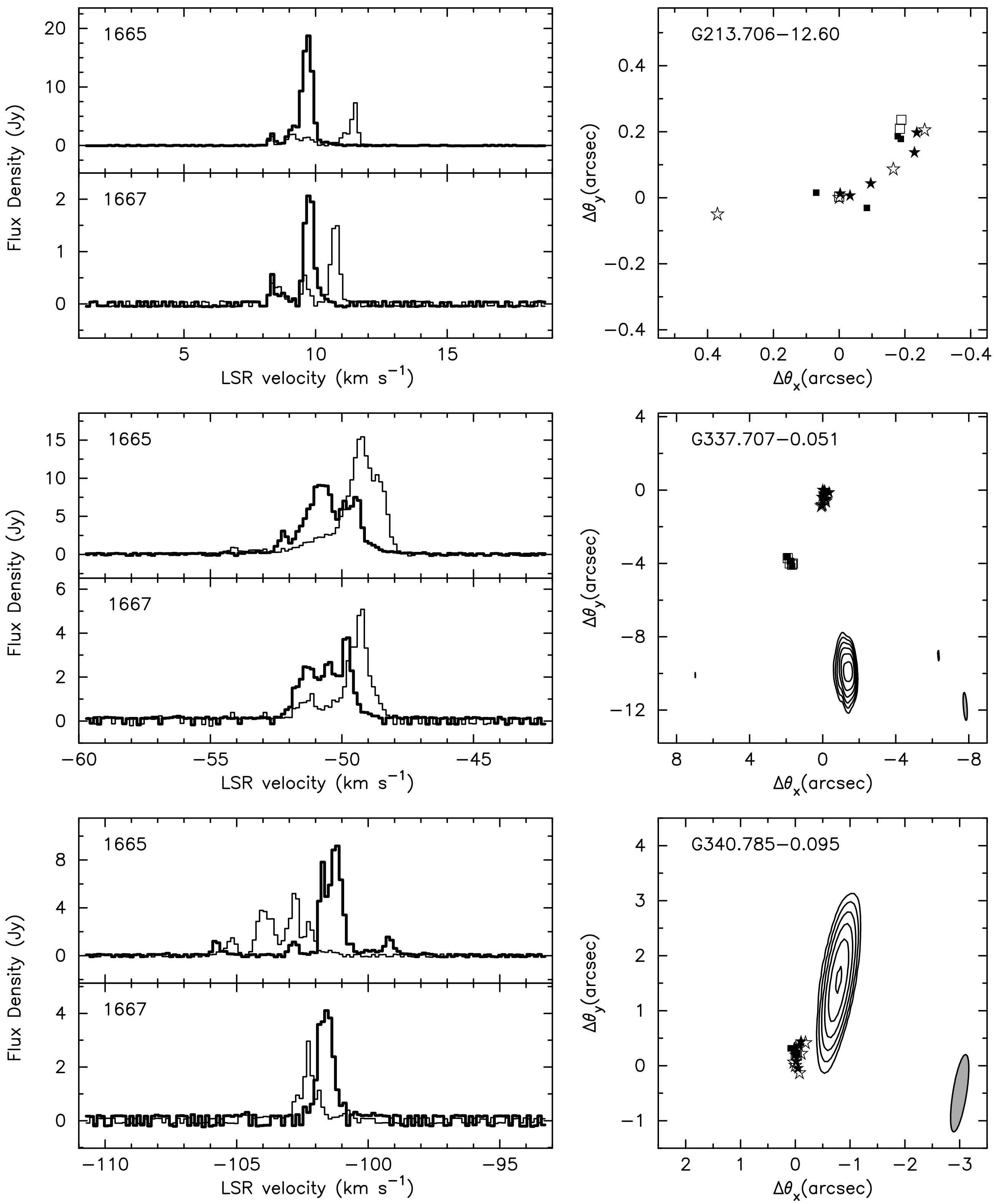

FIG. 28.—Spectra and maps of the sources G213.706−12.60 (Mon R2), G337.707−0.051, and G340.785−0.095. See Fig. 2 caption for details. The maxima of the middle and lower continuum plots are 54.3 and 12.2 mJy beam^{-1}, respectively. G337.707−0.051 is our southernmost source and can be expected to have a high declination error (see text). A comparison with Caswell's (1998) ATCA position reveals a probable declination error of 8″.

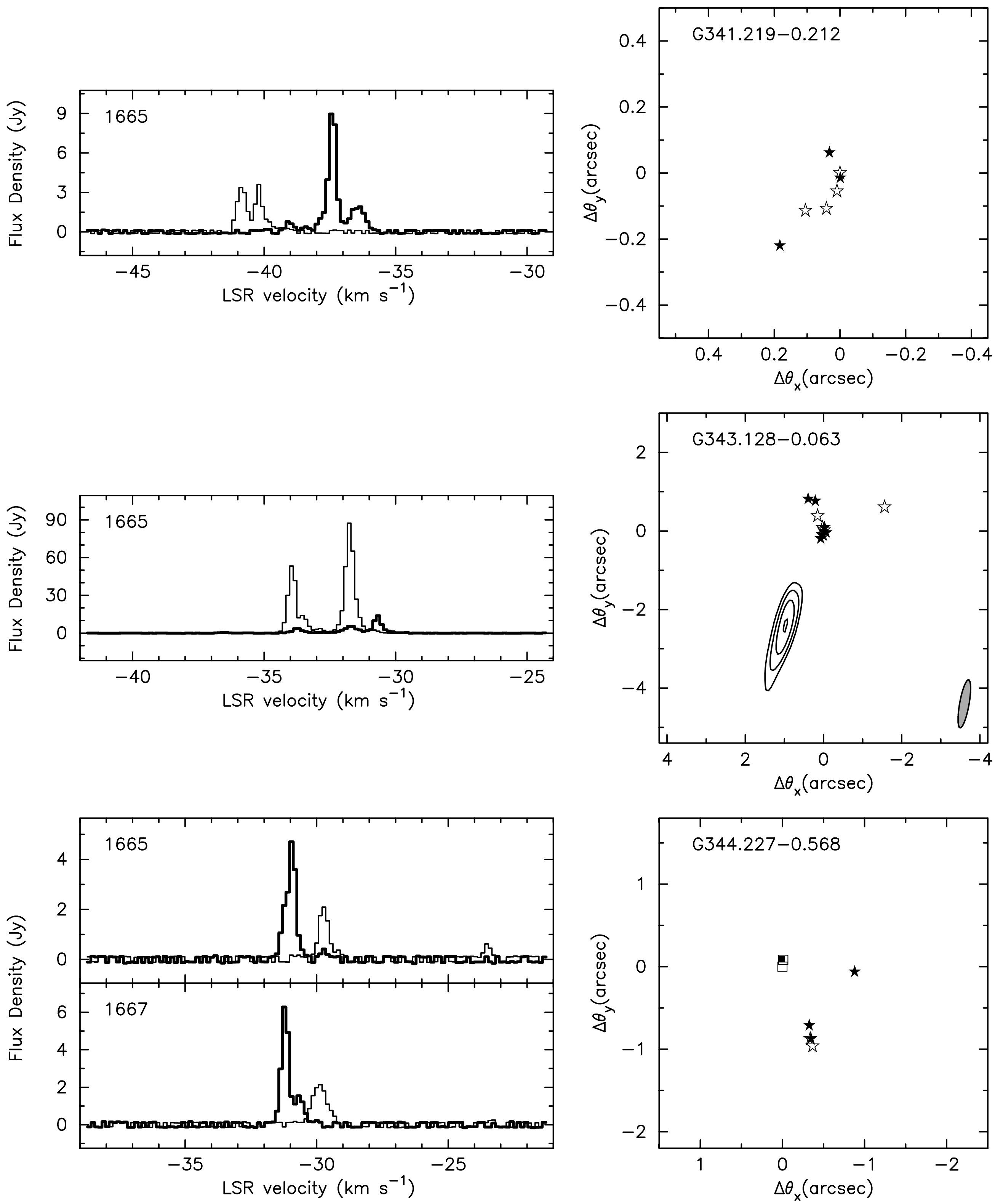

FIG. 29.—Spectra and maps of the sources G341.219 − 0.212, G343.128 − 0.063, and G344.227 − 0.568. See Fig. 2 caption for details. The maximum of the middle continuum plot is 3.5 mJy beam^{-1}.

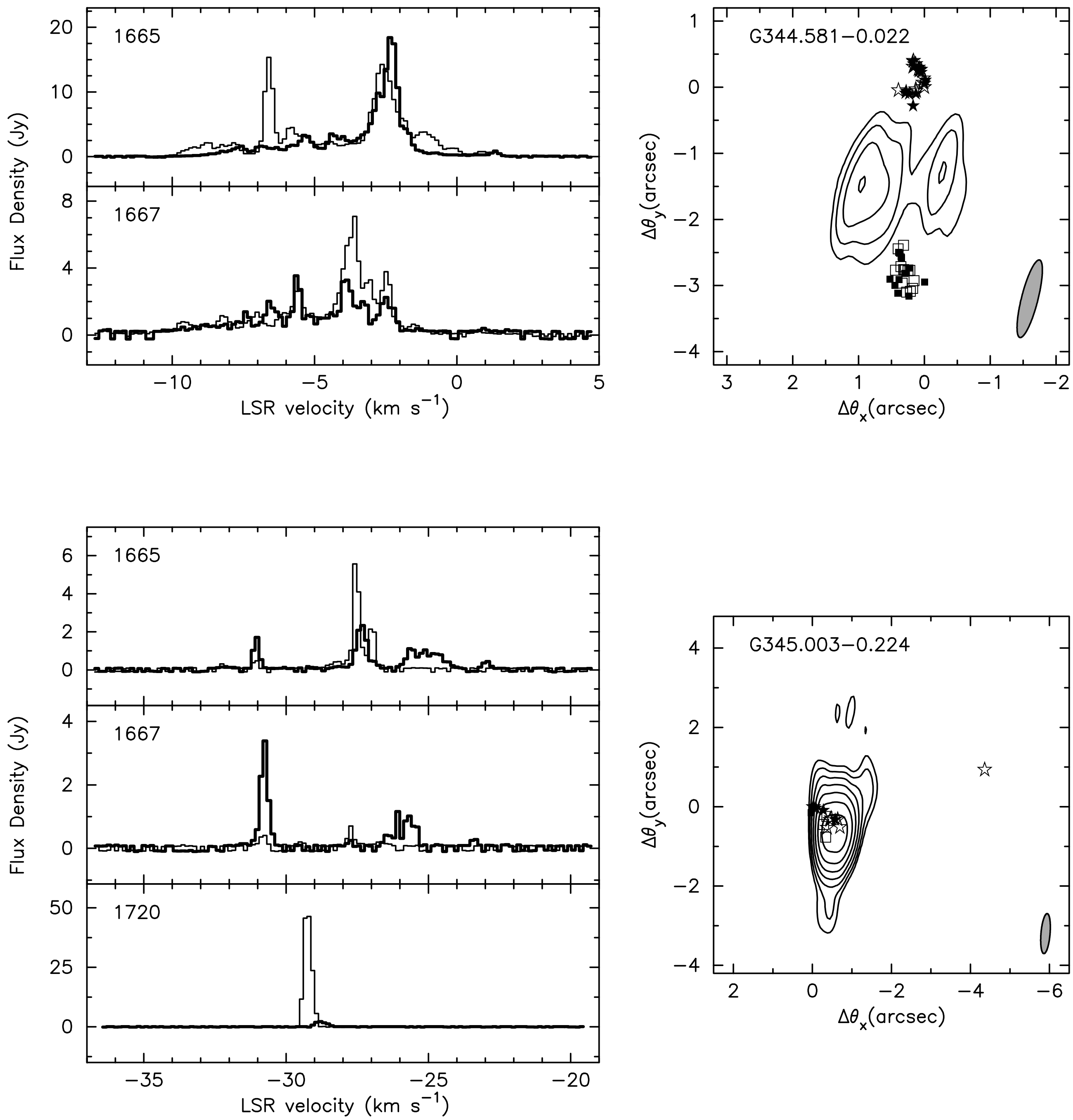

FIG. 30.—Spectra and maps of the sources G344.581 − 0.022 and G345.003 − 0.224. See Fig. 2 caption for details. The maxima of the upper and lower continuum plots are 2.6 and 64.5 mJy beam^{-1}, respectively. See also Gaume & Mutel (1987) (*lower plot*).

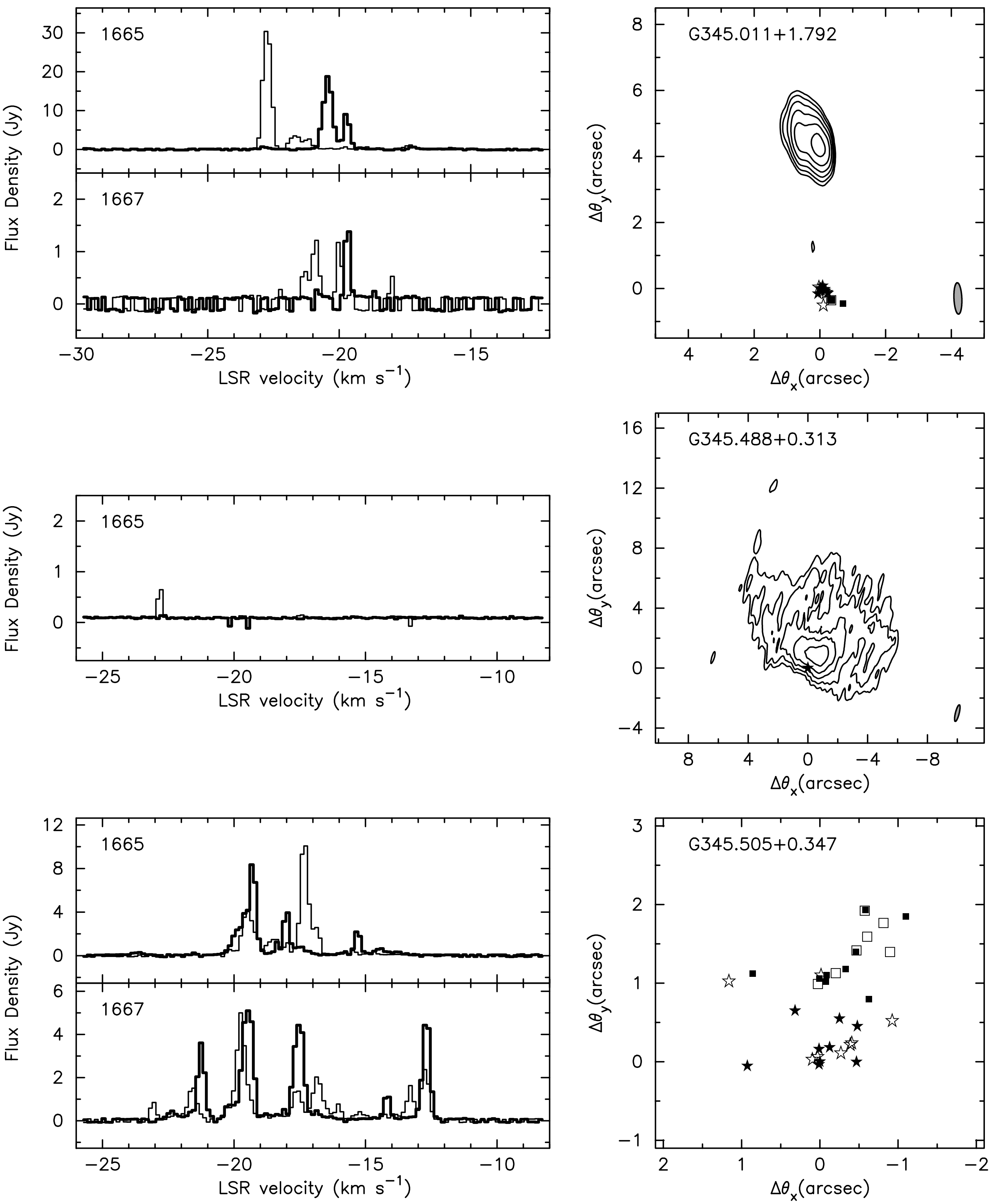

FIG. 31.—Spectra and maps of the sources G345.011 + 1.792, G345.488 + 0.313, and G345.505 + 0.347. See Fig. 2 caption for details. The maxima of the upper and middle continuum plots are 66.5 and 48.3 mJy beam^{-1}, respectively.

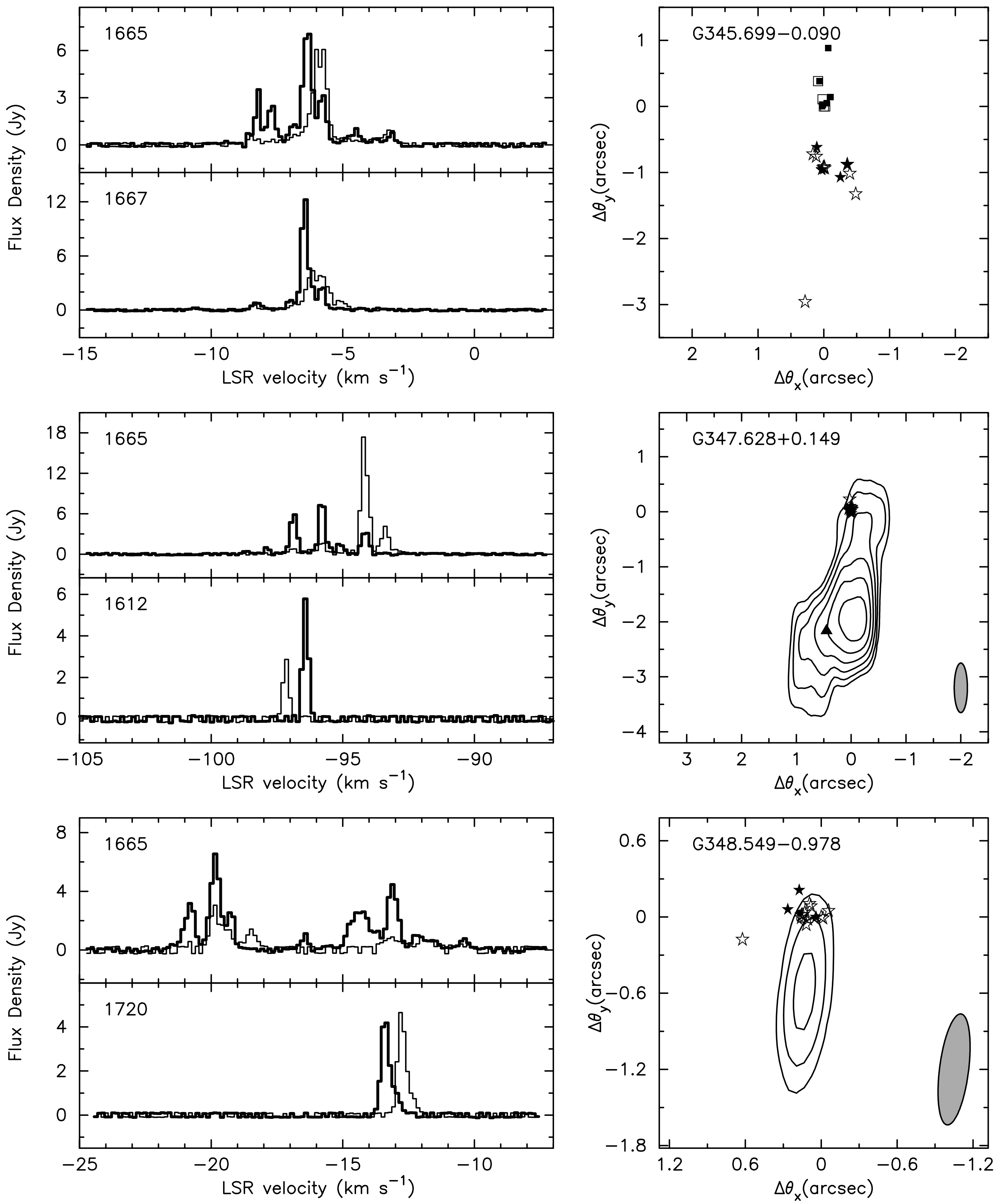

FIG. 32.—Spectra and maps of the sources G345.699 − 0.090, G347.628 + 0.149, and G348.549 − 0.978. See Fig. 2 caption for details. The maxima of the middle and lower continuum plots are 28.1 and 2.4 mJy beam^{-1}, respectively. See also Gaume & Mutel (1987) (*lower plot*).

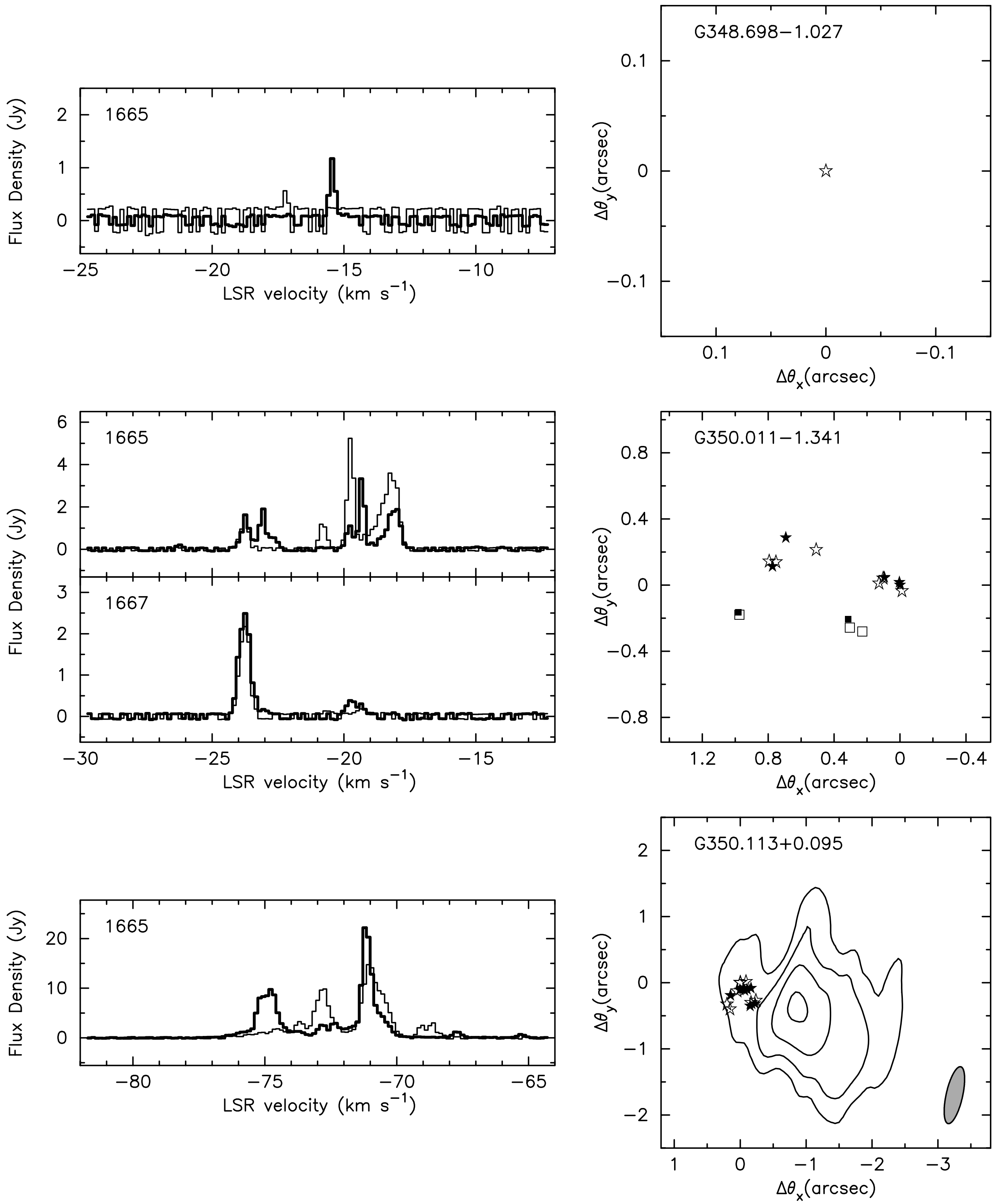

FIG. 33.—Spectra and maps of the sources G348.698 − 1.027, G350.011 − 1.341, and G350.113 + 0.095. See Fig. 2 caption for details. The maximum of the lower continuum plot is 36.7 mJy beam^{-1}.

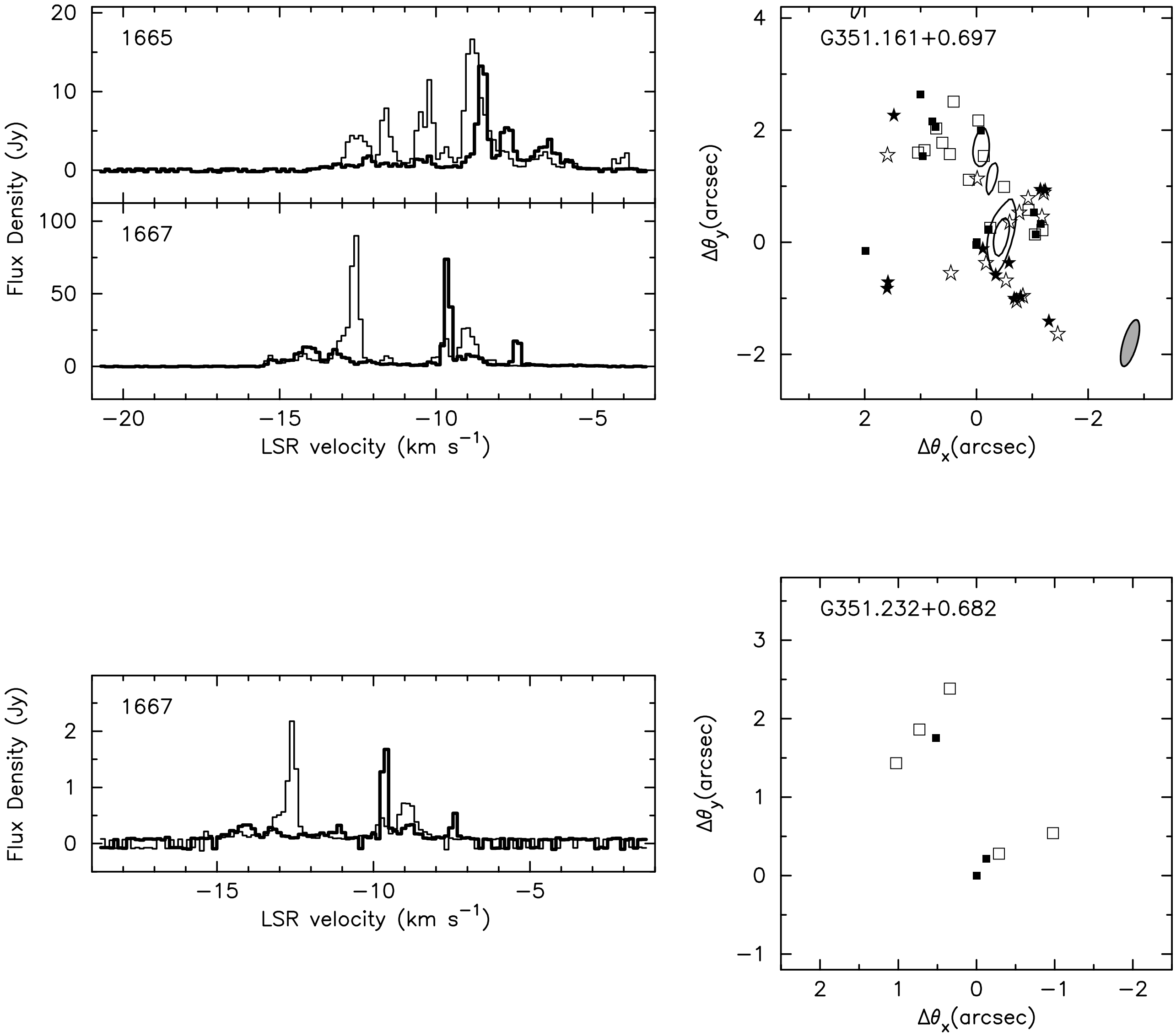

Fig. 34.—Spectra and maps of the sources G351.161+0.697 (NGC 6334 B) and G351.232+0.682 (NGC 6334). See Fig. 2 caption for details. The maximum of the upper continuum plot is 1.3 mJy beam^{-1}.

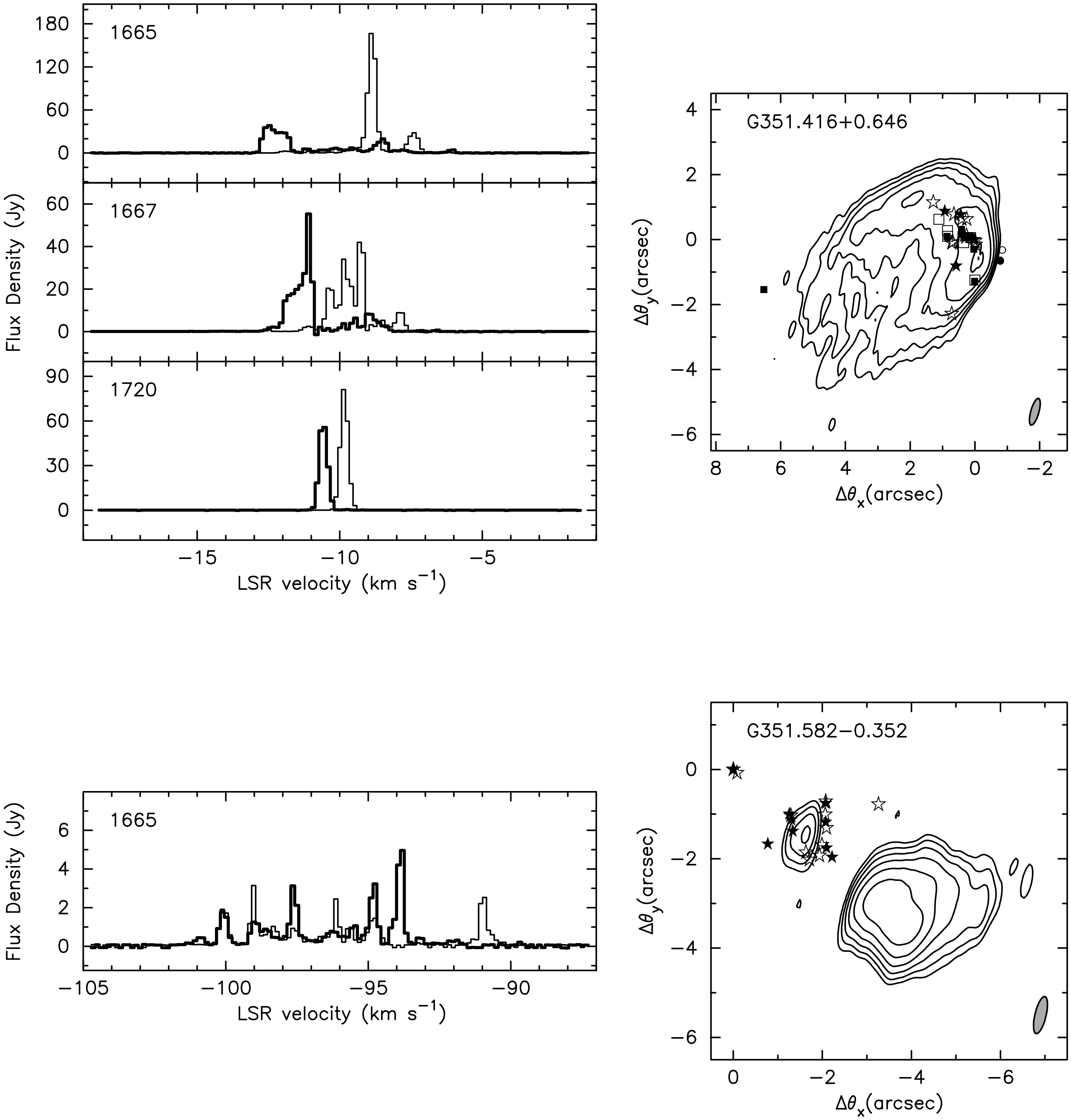

FIG. 35.—Spectra and maps of the sources G351.416 + 0.646 (NGC 6334 F) and G351.582 − 0.352. See Fig. 2 caption for details. The maxima of the upper and lower continuum plots are 98.2 and 73.4 mJy beam^{-1}, respectively.

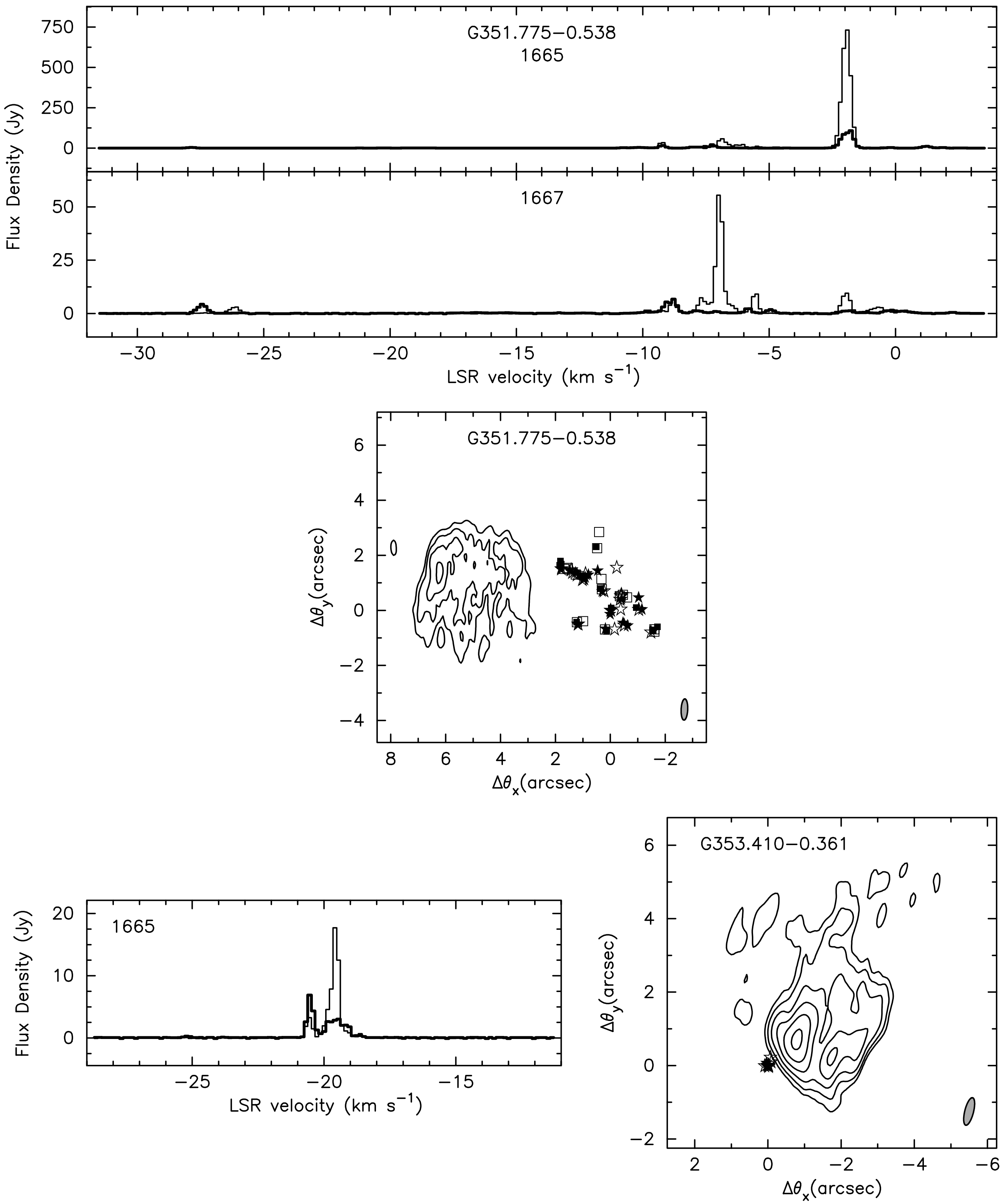

FIG. 36.—Spectra and maps of the sources G351.775−0.538 and G353.410−0.361. See Fig. 2 caption for details. The maxima of the middle and lower continuum plots are 11.5 and 49.3 mJy beam^{-1}, respectively.

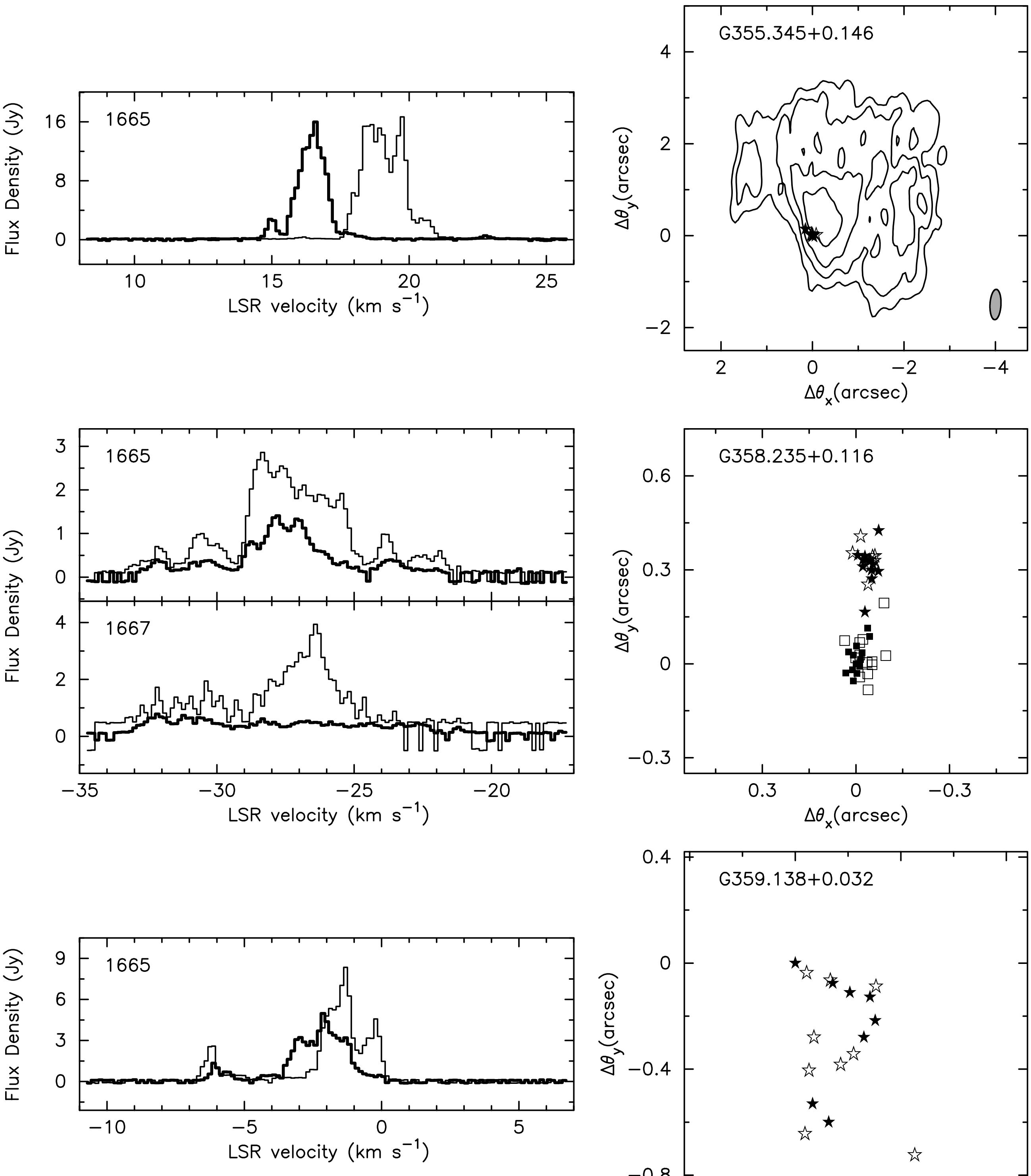

FIG. 37.—Spectra and maps of the sources G355.345 + 0.146, G358.235 + 0.116, and G359.138 + 0.032. See Fig. 2 caption for details. The maximum of the upper continuum plot is 17.5 mJy beam^{-1}.

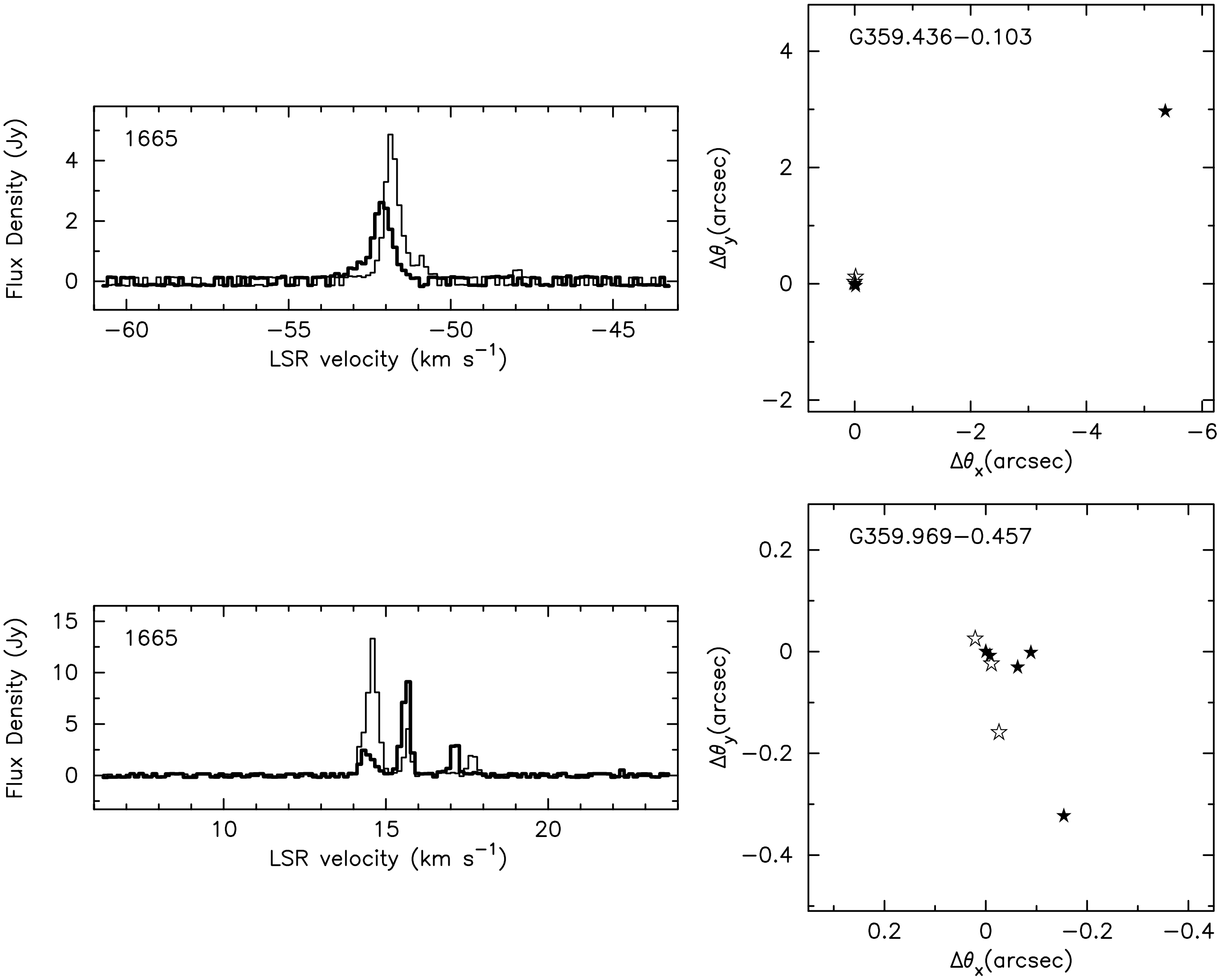

FIG. 38.—Spectra and maps of the sources G359.436 − 0.103 and G359.969 − 0.457. See Fig. 2 caption for details.

REFERENCES

Baart, E. E., & Cohen, R. J. 1985, MNRAS, 213, 641
Baart, E. E., Cohen, R. J., Davies, R. D., Norris, R. P., & Rowland, P. R. 1986, MNRAS, 219, 145
Benson, J. M., & Johnston, K. J. 1984, ApJ, 277, 181
Benson, J. M., Mutel, R. L., & Gaume, R. A. 1984, AJ, 89, 1391
Braz, M. A., & Epchtein, N. 1983, A&AS, 54, 167
Caswell, J. L. 1998, MNRAS, 297, 215
Caswell, J. L., & Haynes, R. F. 1983a, Australian J. Phys., 36, 361 (CH83)
———. 1983b, Australian J. Phys., 36, 417 (CH83)
Cato, B. T., Rönnäng, B. O., Rydbeck, O. E. H., Lewin, P. T., Yngvesson, K. S., Cardiasmenos, A. G., & Shanley, J. F. 1976, ApJ, 208, 87
Cesaroni, R., Palagi, F., Felli, M., Catarzi, M., Comoretto, G., Di Franco, S., Giovanardi, C., & Palla, F. 1988, A&AS, 76, 445
Colley, D. 1980, MNRAS, 193, 495
Dreher, J. W., Johnston, K. J., Welch, W. J., & Walker, R. C. 1984, ApJ, 283, 632
Fix, J. D., Mutel, R. L., Gaume, R. A., & Claussen, M. J. 1982, ApJ, 259, 657
Forster, J. R., & Caswell, J. L. 1989, A&A, 213, 339
———. 1999, A&AS, 137, 43
Forster, J. R., Welch, W. J., Wright, M. C. H., & Baudry, A. 1978, ApJ, 221, 137
Gaume, R. A., & Mutel, R. L. 1987, ApJS, 65, 193
Haschick, A. D., Reid, M. J., Burke, B. F., Moran, J. M., & Miller, G. 1981, ApJ, 244, 76
Kent, S. R., & Mutel, R. L. 1982, ApJ, 263, 145
Lada, C. J., Blitz, L., Reid, M. J., & Moran, J. M. 1981, ApJ, 243, 769
Masheder, M. R. W., Field, D., Gray, M. D., Migenes, V., Cohen, R. J., & Booth, R. S. 1994, A&A, 281, 871
Norris, R. P., Booth, R. S., & Diamond, P. J. 1982a, MNRAS, 201, 209
Norris, R. P., Booth, R. S., Diamond, P. J., & Porter, N. D. 1982b, MNRAS, 201, 191
Reid, M. J., Haschick, A. D., Burke, B. F., Moran, J. M., Johnston, K. J., & Swenson, G. W., Jr. 1980, ApJ, 239, 89
Reid, M. J., Schneps, M. H., Moran, J. M., Gwinn, C. R., Genzel, R., Downes, D., & Rönnäng, B. 1988, ApJ, 330, 809
Wink, J. E., & Altenhoff, W. J. 1975, A&A, 38, 109
Winnberg, A., Terzides, Ch., & Matthews, H. E. 1981, AJ, 86, 410
Zheng, X. 1989, Chinese Astron. Astrophys., 13, 336
———. 1997, Chinese Astron. Astrophys., 21, 182